ARMY RESEARCH LABORATORY

Indirect Vision Driving With Fixed Flat Panel Displays for Near-Unity, Wide, and Extended Fields of Camera View

Christopher C. Smyth
James W. Gombash
Patricia M. Burcham

ARL-TR-2511 JUNE 2001

Flock of Birds® is a registered trademark of Ascension Technology Corporation.

OmniView™ is a trademark of Dolch Computer Systems, Inc.

Polar Vantage XL® is a registered trademark of Polar Electro Oy.

The findings in this report are not to be construed as an official Department of the Army position unless so designated by other authorized documents.

Citation of manufacturer's or trade names does not constitute an official endorsement or approval of the use thereof.

Destroy this report when it is no longer needed. Do not return it to the originator.

ERRATA SHEET

RE: ARL-TR-2511, "Indirect Vision Driving With Fixed Flat Panel Displays for Near-Unity, Wide, and Extended Fields of Camera View," by Christopher Smyth of the Human Research & Engineering Directorate, U.S. Army Research Laboratory

Page 44 of this document should be replaced with the attached page 44.

A nonparametric RM Friedman test by ranks is significant for the component ($p < .004$, chi-square = 13.105, df = 3, N = 8).

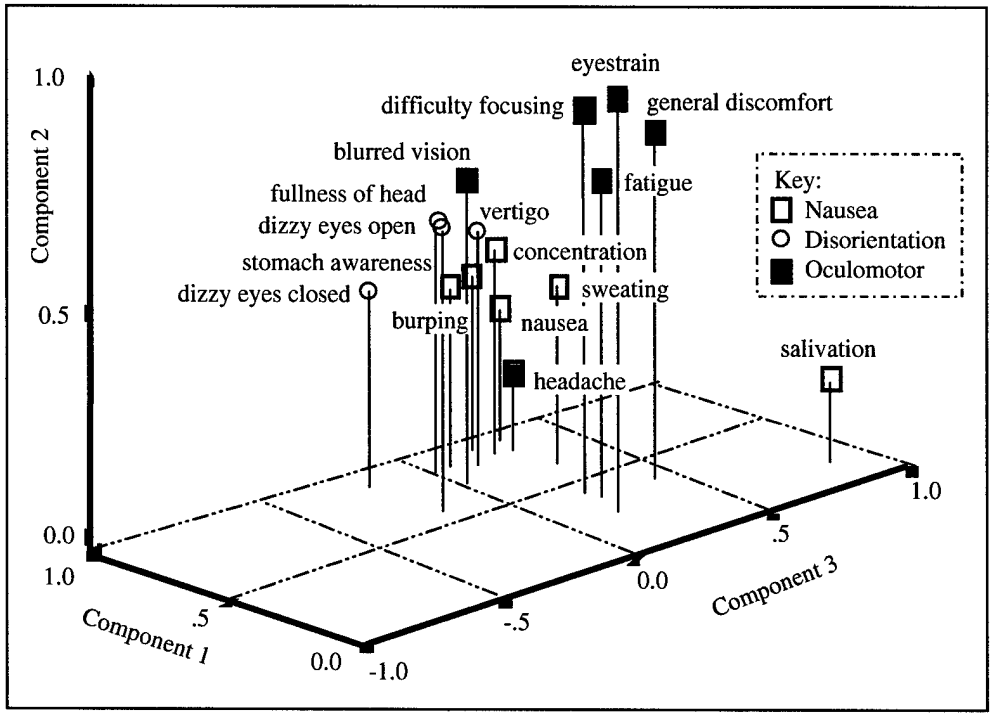

Figure 27. Motion Sickness Factorial Component Plot in Rotated Space.

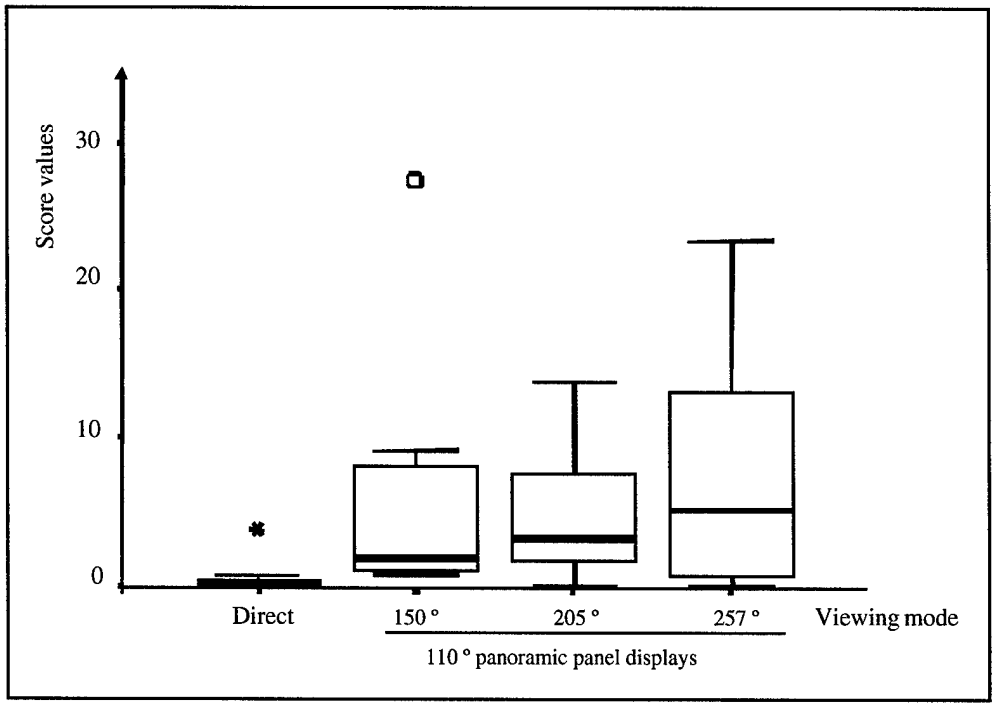

Figure 28. Motion Sickness First Factorial Component Box Plots.

Army Research Laboratory
Aberdeen Proving Ground, MD 21005-5425

ARL-TR-2511 June 2001

Indirect Vision Driving With Fixed Flat Panel Displays for Near-Unity, Wide, and Extended Fields of Camera View

Christopher C. Smyth
James W. Gombash
Patricia M. Burcham
Human Research & Engineering Directorate

Abstract

The effect of indirect vision on vehicle driving is of interest to designers of future combat vehicles, particularly the effect of the camera lens field of view (FOV). In a field study with eight participants negotiating a road course in a military vehicle, the driving performance was measured for natural and indirect vision. The indirect vision system was driven with fixed panoramic flat panel, liquid crystal displays in the cab and a forward viewing monocular camera array mounted on the front roof of the vehicle and tilted slightly downward.

The results are that for benign driving conditions (a well-marked course, good visibility, and essentially flat terrain), the participants successfully drove the vehicle with indirect vision for the different camera FOVs: near unity, wide, and extended. However, with natural vision, they drove the course 26.5% faster and made 0.5% fewer lane-marker strikes than they did with the indirect vision systems. Further, the course speed significantly decreased with increased camera FOV, while the number of lane marker strikes increased slightly. While the course speed decreased with increasing FOV, the speed of travel was perceived as increased because of the scene compression. Although the heart rate increased significantly with course speed because of the increased exertion, the estimated metabolic work output was least for the natural vision and increased with the indirect FOV because of the longer course times.

Workload ratings show a significant increase in perceived workload with indirect vision, while an investigation of situational awareness shows an increase in the demand component. Most participants reported discomfort associated with motion sickness while in the moving vehicle with the displays. The estimated subjective stress rating of the drivers was least for natural vision and increased with indirect FOV.

When the camera's FOVs were compared, the driving performance was fastest with the near unity FOV. However, cognitive processing experiments show a trend for improved spatial rotation and map planning after the wide FOV trial. The wide FOV was intentionally selected by the researchers to provide a balance of the resolution needed for obstacle avoidance and scene perspective for course following. Finally, the participants rated the near unity as more useful for steering; however, the wider FOVs were preferred for navigation since they allow the driver to see farther for path selection.

ACKNOWLEDGMENTS

The authors would like to express appreciation for the support and interest in this experiment by Mr. Bruce Brendle and Ms. Melissa J. Karjala of the U.S. Army Tank Automotive Development and Engineering Center at Warren, Michigan. We would like to thank Mr. Christopher Stachowiak, our team leader, for guidance in computer integration and driving course methodology and safety. We would like to thank Ms. Linda Fatkin of the U.S. Army Research Laboratory's Human Research and Engineering Directorate Soldier Stress and Performance Research Team for providing copies of and guidance in the application of the Comprehensive Psychological Stress Assessment Battery and cognitive battery tests for our use in this study. Further, Ms. Linda Mullins and Ms. Debbie Patton were kind enough to provide support and guidance in the data reduction of the assessment and cognitive experiments and interpretation of the data. This experiment would not have been possible without the support of our technical personnel, Nicky Keenan for fixture construction and hardware integration, Dave Kuhn for electrical integration, and Tom Hoerr, Daniel Brown, and Dave Ostrowski for data collection. We would also like to thank Army CPT Dennis Gaare and the personnel of the Air Force 1/351st Training Detachment and the Marine Training Detachment at Aberdeen Proving Ground, Maryland, who volunteered to participate in this experiment as vehicle drivers. Finally, we would like to thank our Branch Chief, David Harrah, and team leader, Christopher Stachowiak, for their guidance in and close scrutiny of purpose and detail in the preparation of this report.

The authors further thank Nancy Nicholas of the Computational and Information Sciences Directorate of ARL for technically editing this document.

INTENTIONALLY LEFT BLANK

Contents

Appendices

Figures

Tables

INTENTIONALLY LEFT BLANK

INDIRECT VISION DRIVING WITH FIXED FLAT PANEL DISPLAYS FOR NEAR UNITY, WIDE, AND EXTENDED FIELDS OF CAMERA VIEW

1. Introduction

In this section of the report, we describe the background rationale for the experiment, comment on vehicle design and the effects of camera and display selection on performance, suggest criteria for optimal crew performance, including workload and situational awareness (SA), and discuss the potential effects on motion sickness and cognitive functions.

1.1 Background

To support a rapidly deployable force, the Army needs combat vehicles that are smaller, lighter, more lethal, survivable, and more mobile. Combined with the need to assimilate and distribute more information to, from, and within the vehicle as the Army moves toward a digital battlefield, there is the need for an increase in vehicle and command, control, communications, computers, and intelligence (C4I) systems integration and performance. Consequently, the Army will need sophisticated, highly integrated crew stations for these future combat vehicles. In support of this effort, the U.S. Army Tank Automotive Development and Engineering Center (TARDEC) is developing the crew integration and automation test bed (CAT) advanced technology demonstrator (ATD). The purpose of the CAT ATD is to demonstrate crew interfaces, automation, and integration technologies required to operate and support future combat vehicles. The Human Research and Engineering Directorate of the U.S. Army Research Laboratory (ARL) is providing human factors expertise in determining the effect of these new crew station technologies with a continuing series of studies and investigations. The results can dramatically increase the operational effectiveness and capabilities with fewer crew members, thereby contributing to smaller and lighter weapons systems. Because of the need to determine design parameters for their concept vehicle, TARDEC asked ARL to investigate the effects of the use of cameras upon driving performance. In this study, ARL conducted an experiment to determine the driving performance of vehicle crews, using flat panel displays with optical systems as a function of the camera's field of view (FOV).

1.2 Vehicle Design

To satisfy Army requirements for reduced gross weight and lower silhouette, as well as the need for increased crew protection against ballistic and directed energy threats, designers of future armored combat vehicles will place the crew stations deep within the hull of the vehicle. For protection against direct and indirect fire as well as chemical and biological agents, the crews will operate with their hatches closed and sealed. High intensity combat lasers that can penetrate

direct vision blocks may force the crew to operate on the battlefield with indirect vision systems for driving, target search, and engagement. In these vision systems, the conventional optics, which consist of periscopic vision blocks and optical sights, will be replaced by displays at each crew station and externally mounted camera arrays on the vehicle. These vision systems will show computerized digitized images acquired by the camera arrays. The crew member will see a selected portion of the computerized display buffer that depends upon his or her role and viewing direction. No doubt, future vision systems will appear to the user as "see-through armor" by incorporating virtual reality components for the seemingly direct viewing of the external scene.

Before indirect vision systems can be considered for future vehicle designs, combat and materiel developers will need to know the potential impact upon the crew's combat performance. During night operations, replacing the vision blocks with infrared thermal viewers improves crew performance by enhancing visibility at low light levels (McCarley & Krebs, 2000). In daylight conditions, however, several factors may affect performance, and the use of indirect vision may reduce visual performance and SA. This is because of the decrease in visual resolution and FOV of the current sensors and displays as compared to vision with the human eye through vision blocks. This reduction in visual performance may reduce overall combat performance. Furthermore, the choice of camera configuration and placement on the vehicle can negatively influence performance. For example, the use of a single camera for driving instead of a convergent dual camera array will deprive the driver of the near depth perception that is needed to avoid obstacles. This is true since the scene will appear to be biocular instead of the binocular needed for stereopsis (i.e., stereoscopic vision). However, distant depth perception is still apparent from stereoscopic vision induced by motion and terrain features.

1.3 Camera Field of View

One area of interest is the effect of the choice of camera FOV upon driving performance for panoramic panel displays. This would be the case for a driver operating an armored vehicle with a video display and camera array in place of direct vision from an open hatch or through vision blocks. The choice of camera FOV may depend on the task being performed. The driver may prefer a unity view[1] for driving along a known route to increase his or her perception of potential road hazards. On the other hand, the driver may prefer a compressed image at road turns for route selection because of the wider scene. Some prefer to see the sky and the front of the vehicle's hood in the scene. Of course, the increase in camera FOV without a commensurate increase in display FOV will compress the camera scene as seen at the displays and will result in a concomitant loss of detail.

[1]A unity camera FOV is defined as one equal to the display FOV.

While the FOV of the camera may be varied with either a mechanical or electronic switching of the lens, the panoramic displays are presumably fixed in size. In a camera array, the angular spacing between adjacent cameras must be adjusted accordingly to prevent scene overlap or separation. The effect is to compress the scene on the display as the camera FOV is enlarged, thereby reducing the size and resolution of objects' images. In addition, the scene is distorted when depth perception is reduced because the camera image is flattened. When the camera is moving, the velocity field of the scene appears reduced in intensity and distorted. This distortion is especially noticeable in a turn since the center of curvature, acting as a "sink point" (visually a fixed point about which the vehicle turns) for the velocity field, has been brought forward in the scene.

1.4 Display Selection

The display selection will influence the vehicle design. The design may use a set of panel-mounted displays, either cathode ray tube (CRT) or flat panel liquid crystal displays (LCDs), which are fixed in a panoramic arrangement about the crew member's station. In addition to LCDs, plasma and electro-luminescence are suitable candidates for flat panel displays because of their rugged sturdiness. Another option is the use of a miniature head-mounted display (HMD) attached to the crew member's helmet. The display scene of the HMD can be "slaved" to head movements with a head tracker, and for that reason, the display scene may appear more natural although with a limited FOV. Compared to the CRT and LCD panel displays, the use of an HMD significantly reduces the size, weight, and power requirements for the crew station. However, the miniature displays that are currently available cannot match the brightness and resolution of the larger panel systems and may result in degraded crew performance.

The display selection will also have an impact on the crew size needed to operate future armored vehicles. We can expect future crews to consist of two or three people. The form of computerized aiding used with the crew member's electronic associate[2] for the armored crew station may be influenced by the display design. A panoramic design of panel displays for a two-person crew seated together may facilitate team interaction and performance. In contrast, the use of HMDs may tend to isolate the crew members while requiring increased electronic communication between them.

1.5 Optimal Crew Performance

From the human factors viewpoint, there are three criteria for optimal driving performance:

1. Proper design choice for the camera and display system,

[2] crew member's associate program

2. A well-designed vehicle control system, and
3. A supportive ambient environment in the cab area.

Human operators can, however, perform well with less than optimal systems by increasing their efforts to meet the more demanding workload. The problem is that over time, excessive workload can lead to fatigue and increased errors. Furthermore, the increased flow of information and tasks may result in a loss of SA; this is because the ability of humans to process information is innately limited. As noted by Endsley (1993), SA is a precursor to optimal performance, since a loss in awareness impacts decision making and leads to a risk of performance error. For this reason, a fourth criterion is that the system design reduce excessive workload and increase SA as well as demonstrate improved performance.

1.6 Motion Sickness

Another issue influencing crew performance is the possibility of motion sickness, which can occur in an enclosed cab area with spatial disorientation. As noted by Yardley (1992), motion sickness is provoked by sensory conflict between the visual and sensorimotor activities, which involve the vestibular system via head movements. Associated with motion sickness is a constellation of mainly autonomic symptoms such as pallor, drowsiness, salivation, sweating, nausea, and finally, vomiting in the more severe cases. Although some individuals may eventually adapt to situations that initially provoke sickness (Yardley, 1992), the occurrence may be severe enough to stop task performance until the symptoms subside.

1.7 Cognitive Functions and Emotional Stress

Another research issue of interest is the effect of the system design on the cognitive functioning and the emotional stress state of the operator. This is important because the commander in the two-person armored vehicle design may have the additional role of being the driver. The commander may be expected to cognitively process information acquired visually from data displays for decision making, such as for target engagement, and to select routes of approach from digital map displays. These cognitive functions may be composed of such basic elements as mathematical, semantic, logical, and spatial reasoning, as well as higher level functions such as planning. In addition, the ability and desire to acquire and process information may be influenced by the stress state of the commander.

2. Objective

We conducted a field experiment on the ability of soldiers to drive a vehicle with an external vehicle-mounted camera array and panel-mounted video displays, as a function of the camera's FOV. In addition to task load performance, we investigated the effects of the indirect vision driving on the soldiers' metabolic work effort, mental workload measures, and cognitive abilities. The mental workload measures include perceived workload and attention allocation, SA, induced motion sickness, subjective stress, and emotional state. The results are compared to those of direct vision driving as representative of a "see-through armor" vision system.

3. Experimental Methodology

Reported here are the experimental apparatus, indirect vision configuration, camera FOV, display characteristics, driving task, road course, participants, experimental design, questionnaires, control of Type I (false positive) error, and training and research procedures.

3.1 Apparatus

The experimental apparatus was a high mobility, multipurpose, wheeled vehicle (HMMWV), which was equipped with a forward viewing camera array attached to the front roof of the vehicle (see Figure 1). The HMMWV is a fairly conventional vehicle from the driving standpoint, featuring power steering, an automatic transmission, and a diesel engine; however, at 85 inches in width, it is wider than most civilian passenger vehicles. The HMMWV was fitted with a passenger-side safety brake. Table 1 lists the experimental apparatus and equipment used in this study. During operations with the indirect vision system, the driver's cab was modified by the addition of flat panel displays, an inside canvas screen, and covers over the windshield and side window (see Figure 2). In the direct vision mode, the displays, covers, and canvas screen were removed so that the subjects could drive by viewing the scene directly through the windshield.

The roof-mounted camera array consisted of three monocular Panasonic charge coupled device (CCD) color cameras mounted side by side on a holding plate (see Figure 3). The central camera was tilted downward 13 degrees, while the side cameras were turned outward and aligned as closely as possible for a consistent scene across the cameras. In the indirect vision mode, the camera output was seen as monoscopic images on the three fixed flat panel displays that

were mounted in the cab area in front of the driver (see Figure 4). These displays were Dolch Computer Systems' "OmniView™" LCD active matrix displays with 640- by 480-pixel graphics, three-color sub-pixels (red, green, and blue), and a 60-Hertz vertical synchronization refresh rate. A bank of video converters converted the NTSC-170 signals from the cameras to the video graphics adapter (VGA) signals for the displays. Changing the camera lens provided different camera FOVs.

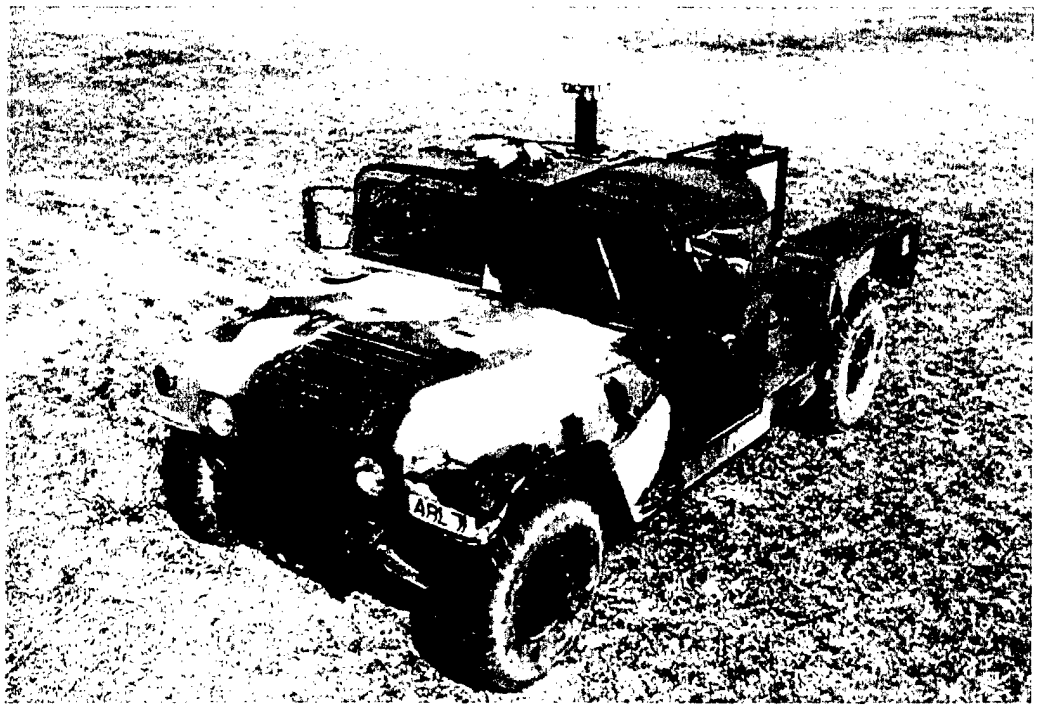

Figure 1. Experimental Vehicle.

The driver could see the central display without head movement; however, eye movements toward objects beyond 15 degrees are usually performed with head movements (Sanders & McCormich, 1993). Since the near edges of the side displays are close to the limit for tracking objects without head movements, a head tracker was used to collect head movement data during driving. The head tracker was an Ascension FOB with a pulse-driven magnetic field source, mounted in the vehicle behind the driver. A safety helmet worn by the driver had an FOB magnetic field sensor mounted on top (see Figure 5). A PC read the sensor-determined position and orientation via an RS-232 connection by program control and computed the head's pitch and bearing. These values were stored in the on-board computer during the experimental runs for post-processing analysis. Figure 6 shows the FOB source, the PC, the video converters, and the DC-to-AC power converter mounted on the bed of the vehicle.

Table 1. Experimental Apparatus and Equipment

1. HMMWV with addition of passenger-side safety brake system and DC-to-AC power converter.
2. Panasonic CCD color cameras, Model WV-GL-352.
3. Camera lens with focal lengths of 7.5 mm, 6.0 mm, and 4.8 mm.
4. NEC[3] video signal converters NTSC-170 to VGA.
5. Dolch "OmniView™" Model OV142C LCD flat panel displays.
6. Canvas light shield enclosures for the cab area.
7. Ascension "flock-of-birds®" (FOB) magnetic field head-tracking source and sensor.
8. Industrial Systems x-586 personal computer (PC).
9. Polar Vantage XL® heart rate monitor (Model 8799) with wrist recorder and chest band-mounted sensor and transmitter.
10. Safety helmet with mounting for FOB receiver.

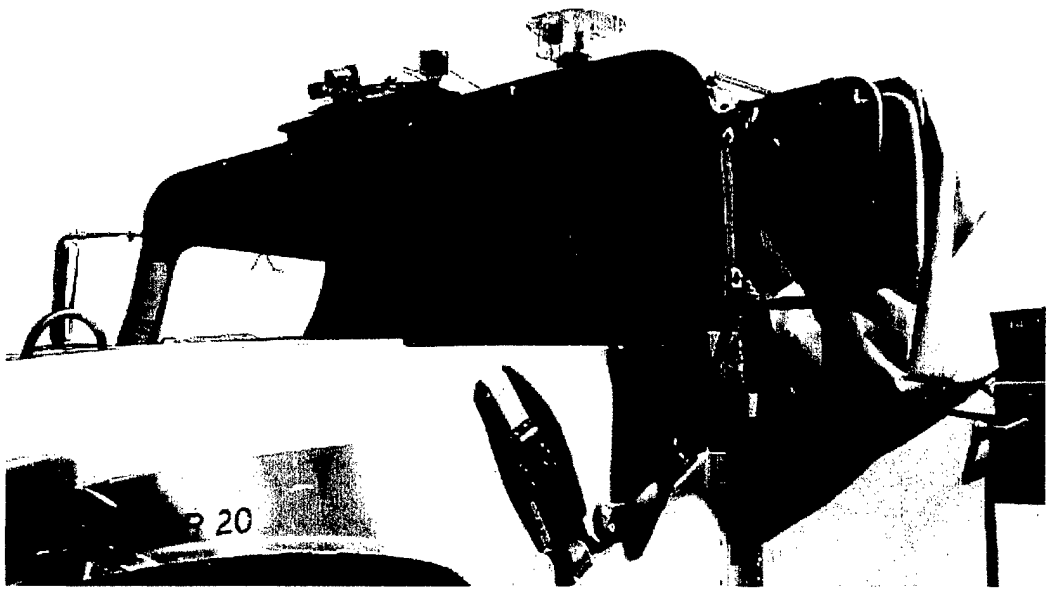

Figure 2. Cab Enclosures.

[3] not an acronym

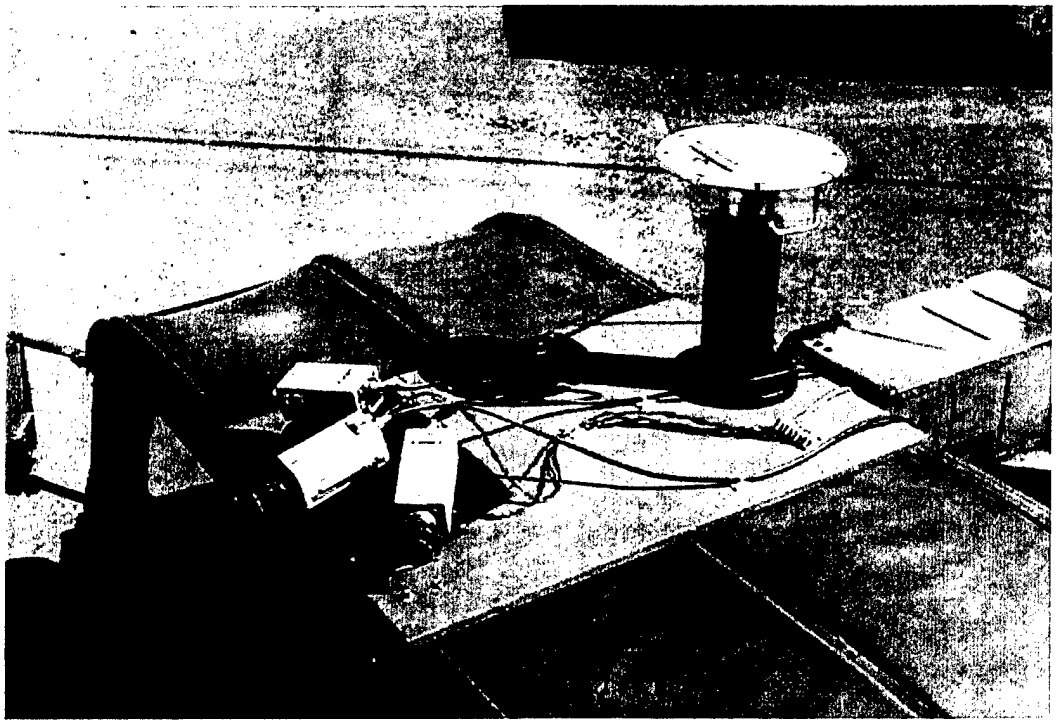

Figure 3. Camera Configuration and Global Positioning System (GPS) Antenna (not used).

Figure 4. Flat Panel Display Configuration.

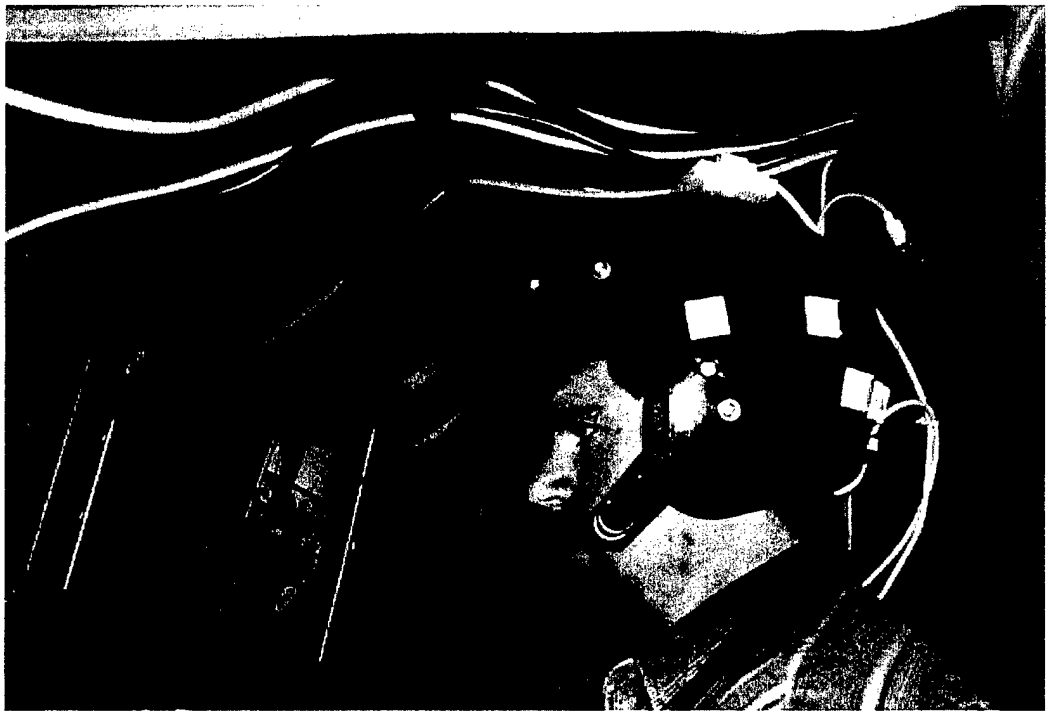

Figure 5. Driver Wearing Safety Helmet With FOB Receiver.

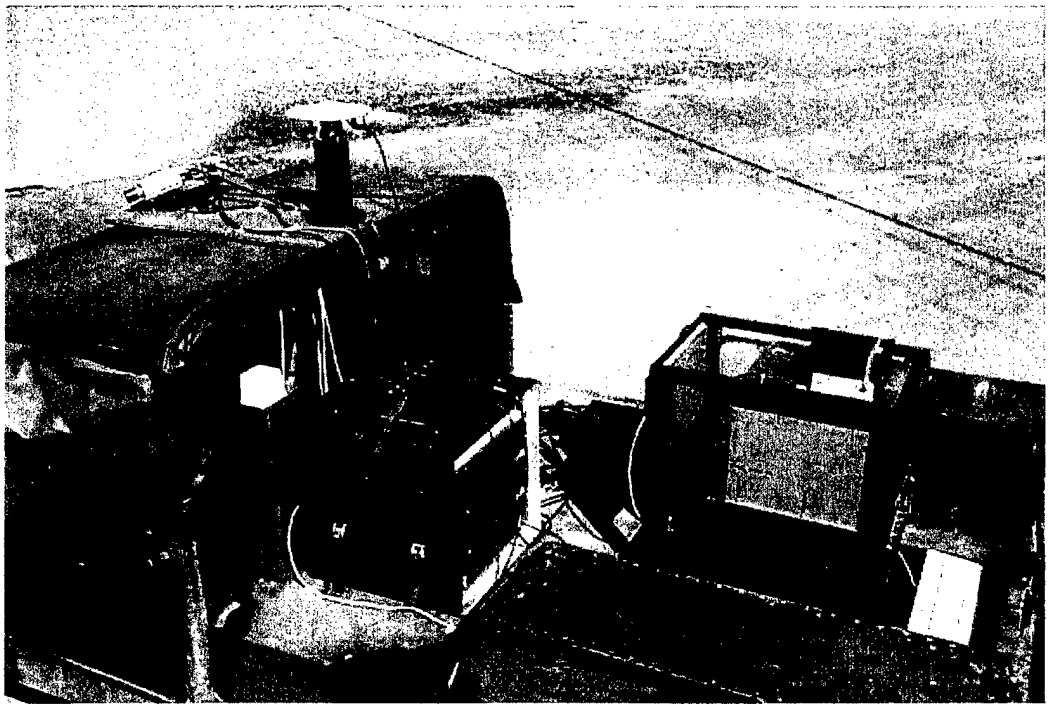

Figure 6. Cargo Bay With Video Converters, FOB Field Source, GPS Receiver, and Computer.

3.2 Indirect Vision Configuration

In the indirect mode, the three LCD flat panel displays were mounted in front of the windshield, and the driver's portion of the cab was completely enclosed to prevent direct viewing. This was done to simulate an armored combat vehicle operating in a "buttoned up" mode. The displays were arranged with a central display directly in front of the driver and with left and right side displays (see Figure 4). The central camera fed a video signal through the video converters to the central display, and the two side cameras fed the corresponding side displays. The side edges of the mounting frame that holds the displays produced a visual "dead" space between adjacent displays, and the side cameras were adjusted to accommodate this space. Prior studies had shown that participants preferred to see the scene naturally as they would through a window, allowing the frame edges to obscure the view beyond, and the cameras were adjusted accordingly.

The displays were mounted against the windshield on the far side of the steering wheel for safety reasons, and in this position, the central display is about 22 inches from the eye position of the driver. The driver could not turn the steering wheel in one continuous arm movement unless the display was positioned high against the windshield. At this distance, the 11.5- by 8.6-inch display subtended horizontally about 30 degrees (see Figure 7). The display, including the 2.375-inch side of the mounting frame, subtended about 40 degrees. The side displays were pivoted inward horizontally by 40 degrees so as to be normal to the viewing direction at the display center, which resulted in a slight outward torsion of the visual space. Considering the 4.75-inch dead space between adjacent displays, the frontal camera field was compressed into a panoramic 110-degree FOV (55 degrees left and right of center) across displays and the intermediate mounting frame.

Depending on the camera lens, the participants drove with the three camera FOVs to see a near-unity (150 degrees), a wide (205 degrees), and an extended (257 degrees) horizontal visual front compressed in image by the displays to a 110-degree scene with the same aspect ratio. Here, the near-unity camera FOV is slightly larger than that of the display. Since the camera array was mounted on the roof and tilted downward 13 degrees, the central point of the scene did not vary, while the extent of coverage and resolution varied with the lens. While the near-unity FOV showed just the immediate road ahead, the wide FOV showed the road as far as the horizon, and the extended FOV showed the right side views as well. The near-unity FOV showed the scene ahead just above the hood and below the skyline in normal resolution. The wide FOV showed the frontal hood and the lower sky ahead of the vehicle. Finally, the extended FOV showed most of the hood and more sky while on a level roadway. As analyzed in Appendix A, the wide and extended FOVs satisfy the amount of sky and hood in the scene and the near ground vision distance, which is preferred for driving according to

prior investigations. Furthermore, while little sky and no hood is in view for the near-unity FOV, the near ground vision distance is satisfactory by this analysis.

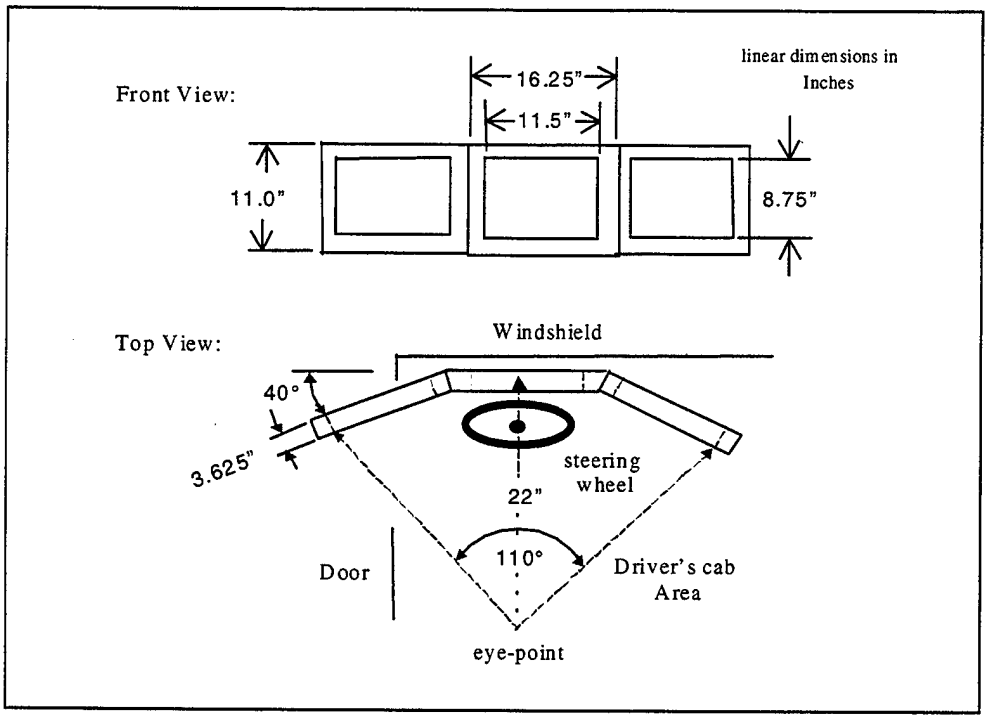

Figure 7. Top and Front Views of Flat Panel Display Frame.

3.3 Choice of Cameras' FOV

The cameras' FOVs were selected by the researchers to study a full range of resolution and scene view. In particular, the near-unity FOV was chosen to provide the full resolution of a natural scene as closely as possible via a camera lens with a focal length of 7.5 mm—the largest available for this study. Here, a unity FOV would match the real world in scene resolution. In contrast, the wide FOV (6.0-mm lens) was intentionally selected by the researchers to provide a balance of scene resolution and course perspective. The FOV was judged to show both sufficient resolution for driving and enough of the course and skyline ahead to allow adequate route selection and navigation. This FOV was judged to be most practical for the conflicting tasks of obstacle avoidance and selection of the driving course. Finally, the extended FOV (4.8-mm lens) was selected to show as much of the road scene as possible over a full front without concern for degradation in scene resolution. Using a Snellen chart (American Optical Corporation, Chart No. 1930) placed 20 feet in front of the central camera, a single observer judged the visual acuity of the central display as roughly 20/30 for the near unity, 20/40 for the wide, and 20/60 for the extended FOV.

3.4 Display Compression Ratio

The display compression ratio is a measure of the compression of the camera's scene by the display and is calculated as the ratio of the camera's horizontal FOV to the FOV of the display's 110 degrees. Here, the compression ratios for the near-unity, wide, and extended camera FOVs are 1.364, 1.864, and 2.336, respectively. Note that these values are relatively close to the inverse of the corresponding visual acuity reported previously. While the compression ratio is unity for direct viewing, the scene is drastically different with natural depth perception and resolution and free head movement over the entire viewing front. In contrast, indirect viewing is limited to the panoramic displays with relatively limited resolution, no depth perception, and visual dead spaces between displays. Furthermore, there are minor differences among the indirect vision displays such as the amount of hood and sky in the scene. For this reason, the direct and indirect vision systems are properly considered as different treatments for statistical analysis. However, much of the data variation in this experiment is explained by the display compression ratio, and for this reason, the ratio is used in Section 5 as a quantitative dimension.

3.5 Visual Displays

The characteristics of the visual scene, as determined by the indirect viewing displays, influence driving performance. In particular, the effects of the display compression on scene resolution and spatial distortion and the display dynamic resolution are of interest to this study.

3.5.1 Scene Resolution

The resolution of the scene is reduced by display compression since fewer pixels are used to draw the elements in the video return. In optical terms, the display modulation transfer function acts as a low pass spatial filter for the vision process as determined by the pixel resolution. Display compression of the scene shifts the spatial cut-off frequency of the filter to a lower value, thereby reducing the detail that can be seen. The far scene appears smoother, and terrain detail only becomes visible at closer distances. In particular, the decrease in scene resolution reduces the visibility of the terrain detail that generates the velocity flow field. The field is shortened since the flow appears to originate from a point in the scene that is closer to the front of the vehicle. The flow appears faster and to accelerate as the vehicle approaches the scene elements.

3.5.2 Scene Distortion

The display compression distorts the spatial geometry of the scene. At increased compression ratios, an object appears more distant than it actually is while the approach path bends outward and the apparent speed increases as the object approaches the vehicle. The object appears to move farther laterally and faster as it is approached. In a vehicle turn, the center of rotation that is to the side (with a turn radius determined by the steering wheel setting) is distorted forward so as

to be visible in the side displays for the wide and extended compressed scenes. Furthermore, the rate of turn that is apparent on the side displays is different from that experienced by the driver. For reference, these scene distortions are shown in Figures B-2 through B-4, which are distortion plots of the real-world map plane overlaid onto the display world plane as derived in Appendix B for the different compression ratios used in this study.

3.5.3 Display Dynamics

The LCD uses a block crystal realignment method to refresh the display. During sudden changes in direction such as in rapid turns and going over berms, bumps, and other steep rises in terrain, the display refresh cannot keep pace with the changing scene, which results in a loss of image quality. Because of the motion blurring of the video return, the display loses dynamic resolution. The result is a temporal blurring in the display modulation transfer function. The display appears to be out of focus without a definite image plane.

3.6 Driving Task

The driving task performed by the participants is described in terms of the control activity, the display stimuli, and the cognitive resources that are used by the driver in operating the vehicle. An allocation of the functions and tasks to the human resources and the driver's interface to the machine are described. Also described is a task analysis listing the subtask sequences and the information cues of the display, as well as the task environment.

3.6.1 Task Description

Considering a driving course designated by pairs of markers, the driver navigates the course from the locations of the marker pairs in the scene and by recalling his or her knowledge of the route from a mental map of the course. This is followed by a task-specific rule-based selection of the next marker pair and an approach path to the pair. Finally, the driver executes skill-based driving of the vehicle along the approach path and between the marker pair with speed control based on the velocity flow field of the scene before he or she repeats the process.

As with any driving task, vehicle control at the skill-based level may be thought of as a two-dimensional tracking task with lateral control to maintain lane position and longitudinal control for speed. The lateral control is a second order tracking task with prediction based on a preview of the course ahead and the heading of the vehicle. The longitudinal control is a first order tracking task with command input given by the internal goal of the driver and by the disposition of the road markers. The tracking display presents three channels of visual command information to be tracked along two axes. Lateral tracking is commanded by the course, while longitudinal tracking is commanded by a distributed set of input consisting of the flow of motion along the course and the distances to the markers. To drive proficiently, the driver needs to see the course

ahead within a primary visual attention lobe of forward vision, which extends from a few meters ahead of the vehicle to a few hundred meters directly in front (Wickens, Gordon, & Liu, 1998).

While this is a valid description of highway driving, the road course used in this study was a successive sequence of short lane segments separated by marker pairs. For this reason, soldiers navigating the course employed the cognitively demanding rule and knowledge-based levels to find the next set of markers and the following lane segment, as well as to prepare and monitor the skill-based looking and acting activities used for lane passage.

3.6.2 Task Allocation

Table 2 is a function and task allocation chart proposed for soldiers driving the course. The table allocates the tasks to the resources of the human operator, the operator interface, and the mental model of the process. The chart lists processors for the perceptive, cognitive, and motor activities of the human, which are exercised by performance of the tasks. The column of the chart for the operator interface lists the event in the driving scenario that elicits each task, the portion of the scene showing the display cue needed for the subsequent action, the cue feedback from the display, and the response by the driver. Finally, the portion of the mental model that is exercised with the task is listed as situational or task specific. The situational mental model refers to course localization and is based on a mental map of the course. Here, SA is the awareness of the location and orientation of the vehicle on the course and the location of the next marker pair. The task-specific mental model refers to the procedural knowledge used to operate the vehicle between marker pairs. Referring to Table 2, the function of operating the vehicle is separated into three tasks: navigating, approaching, and driving between the marker pair. Following marker passage, the driver navigates by finding the nearest pair on the course from the far scene on the display and the mental map of the course and then selecting an approach path. He or she then drives the vehicle along the approach path, using the velocity flow field on the front scene to judge speed until he or she nears the marker pair. The driver then steers by using the near scene to align on the pair and accelerates between them to drive through.

3.6.3 Task Analysis

Figure 8 is a task analysis flow diagram separating the driving task into a sequence of subtasks. Following training, the driver used a strategy of maximize the course speed while minimizing the marker strikes. In this strategy, he used braking, steering, and acceleration to approach a pair of markers "head on" and then accelerated between them. As has been noted before, the driver navigated the course by first finding the next marker pair from the mental map and the display scene and then selecting an approach path that supports the driving strategy. The driver manually adjusted course speed from the velocity flow field on the display scene. To do this, the driver must first find the velocity field on the

Table 2. Allocation of Functions and Tasks

		Human operator						Human operator interface				Mental model	
		Perceptual		Cognition			Motor					Maintenance	
Function	Task	visual	skill	rule	supervisory	ocular	manual	Eliciting event	Interface display	Feed-back	Ensuing action	task	situation
Operating vehicle													
	Navigation	x	x	x	x	x		through marker pair	far scene	nearest marker pair	select approach	x	x
	Approach control	x	x	x		x	x	path selected	front scene	velocity field	brake/steer upon approach	x	
	Drive through	x	x	x		x	x	near pair on path	near scene	alignment on pair	steer/ accelerate between pair	x	

display, evaluate the flow by comparing it to that learned in training, and then adjust speed and course by manually controlled actions. As he or she neared the marker pair, the driver checked orientation and manually steered to align the vehicle so that he or she could drive directly between the markers. This serial sequence of activities is reasonable, considering the time window available to the driver for approaching each marker pair.

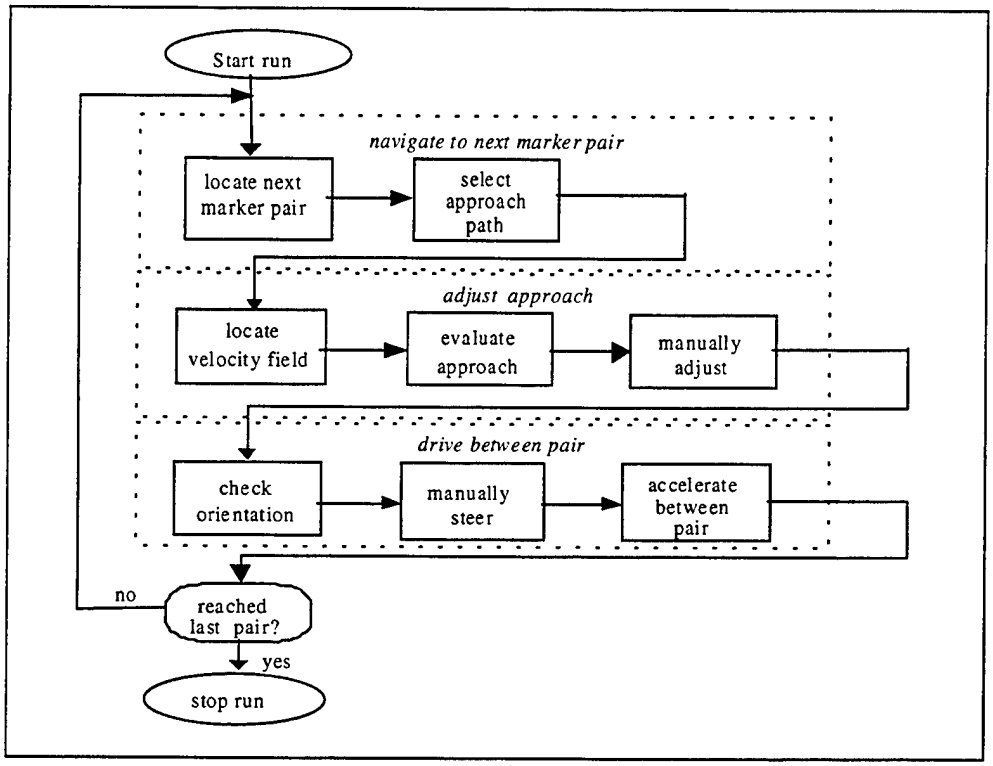

Figure 8. Task Analysis Flow Diagram for the Driving Task.

3.6.4 Display Information

Figure 9 is a sketch of a driving scene, showing the different visual display elements that the driver uses in decision making during task performance. Since the vehicle-mounted camera array looks downward on the roadway, the display shows the markers of the closest pair as farther apart, lower on the display, and larger than those farther away. A perspective of the route is outlined on the display by a succession of marker pairs with the markers of each successive pair appearing closer together, smaller, and higher in the scene.

Superimposed on the scene are encircled elements that correspond to the types of decisions made by the driver. For example, over-trained, automatic skill-based reasoning acquired from driving one's automobile is used to steer around roadway obstacles as they approach the vehicle in the vision field. Rule-based, schematic reasoning acquired in training is used to select the next marker pair, the approach path, and speed from the display. The velocity flow field of the

display, which shows the movement of the vehicle, originates from this region since it is here that terrain details become large enough to be visible and appear to flow past the vehicle. Finally, supervisory, knowledge-based reasoning associated with the far scene is used to monitor the rule-based schema, and as the course is traveled, to restructure it for changing driving conditions.

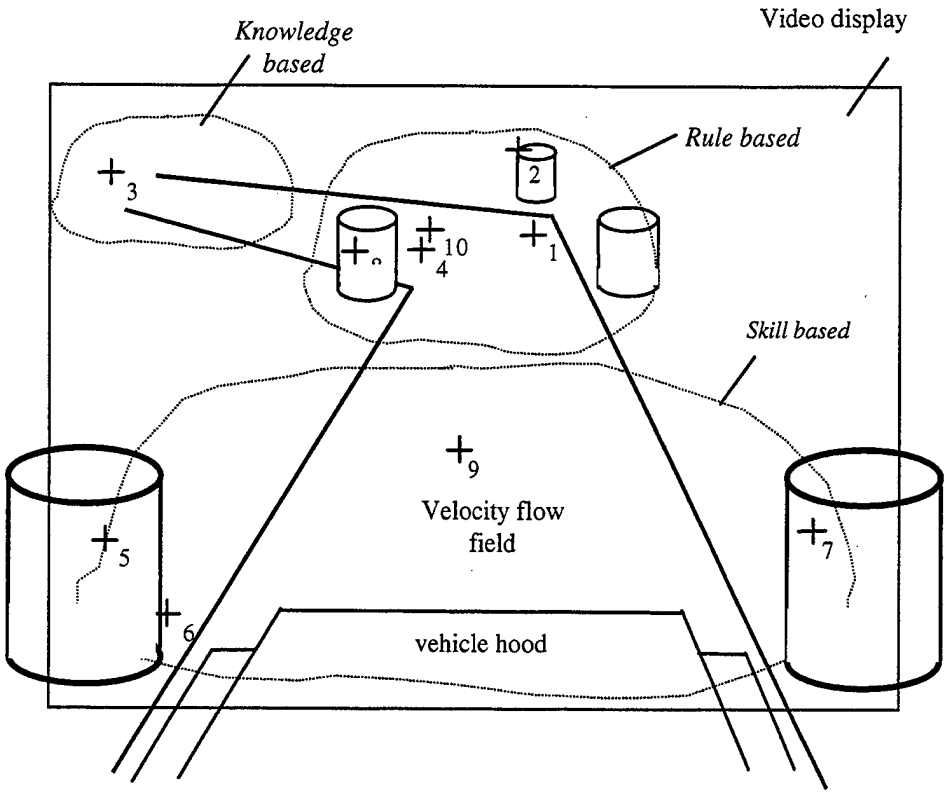

Figure 9. Cognitive Functional Areas of the Driving Scene.

"Tick" marks on the drawing indicate feasible eye fixation points that the driver may make during the performance of the task. Here, the driver (as indicated from his or her eye movements) is noticing the bend in the course (ticks 1, 4, and 10), the barrels marking the bend (ticks 2 and 8), the far bend (tick 3), obstacles (tick 6) to the vehicle's passage, the next barrel pair (ticks 5 and 7), and the velocity flow field (tick 9). Associated with these ocular fixation points is a stream of decisions that start with a supervisory evaluation of the road ahead and the impact on the driving schema. Included in this evaluation are the recall of the route from the mental map and the location of the next marker pair on the course. This is followed by a task-specific, rule-based selection of the next marker pair and the approach route and speed control based on the driving schema. Finally, the driver executes skill-based driving around the obstacle before repeating the process.

3.6.5 Task Environment

With the indirect vision system, the driver is physically isolated in the vehicle and experiences darkness, heat, noise, and vibrations. With the light shields in place, the only light seen is from the displays and the low-level ambient light reflected from the cab interior. The light shielding isolates the driver from the experimenter, and the only contact is through speech at the start and end of a trial run. Engine noise further isolates the driver from the environment. In addition to the sunlight on the cab roof, the LCDs generate heat during operation, a process that raises the internal cab temperature. An exhaust fan mounted behind the driver circulates air from outside through the cab. The vibrations seen by the driver on the display are slightly different in amplitude and frequency from those that he or she receives physically from the vehicle frame. This is true because the driver sits on the left side of the vehicle and the cameras are mounted in the center.

3.7 Road Course

The road course, located at Aberdeen Proving Ground (APG), Maryland, is a 0.36-mile (590-meter) stretch of S-curves, berms, and straight-aways marked by 48 pairs of barrels spaced along the course at roughly 12-meter intervals. The barrels of each pair are separated by 114 inches (1.33 times the vehicle width), with a striped barrel on the left and a plain one on the right when one is traveling the course in the counterclockwise direction.

There is a perimeter road surrounding the course, which was used for initial familiarization with the vision systems. A 140-meter training course of similar design is near the research course. The research and training courses and perimeter road are part of the ground vehicle experimental course, a 13-acre site developed for teleoperated and on-board ground vehicle experiments. For safety, concrete "Jersey" barriers surround the site. (See Figure 10 for a course schematic.)

3.8 Participants

Eight male military personnel from the Army, Air Force, and Marines at APG, who have good eyesight (acuity 20/20 to 20/30, normal or corrected by glasses or contacts) served as participants in this study. Table 3 lists the demographics and visual acuity of the participants, along with their education level and prior driving experience for reference.

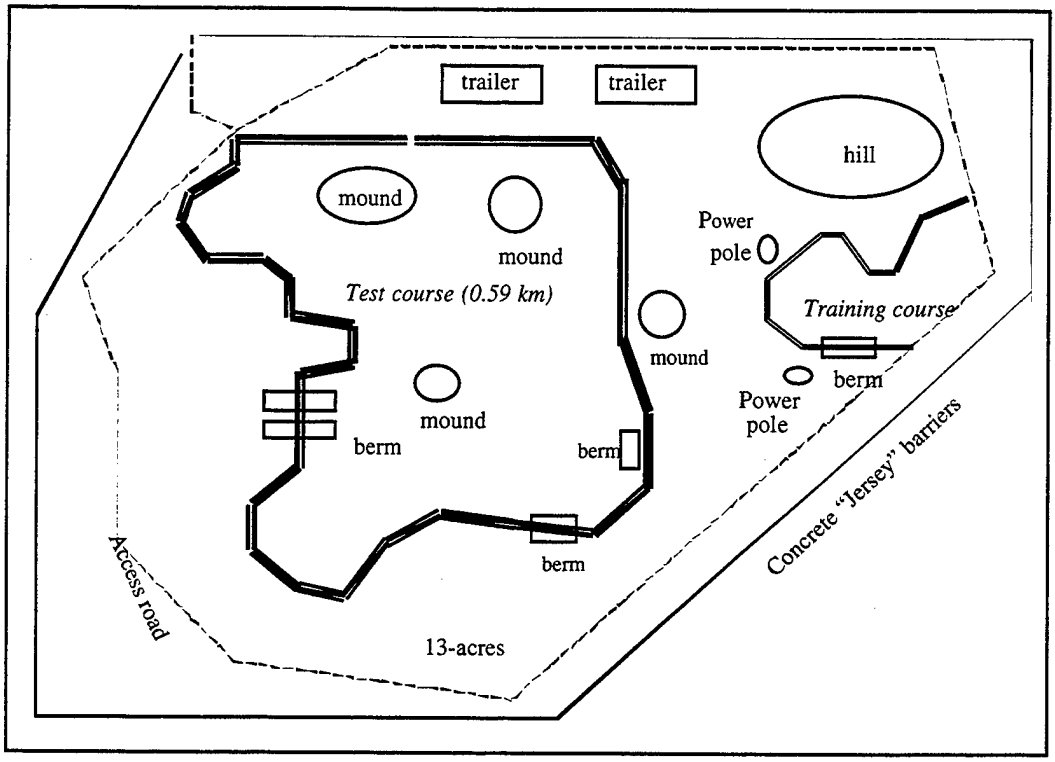

Figure 10. Ground Vehicle Experimental Driving Courses.

Table 3. Demographics and Visual Acuity of the Participants

Participant	Service	MOS[a]	Rank	Age	Education	Visual acuity	Driving experience
S1	AF	T2A751	E5	30	12	20/20	races car
S2	AF	T2A751	E4	24	15	20/20	POV[b]
S3	AF	2A771	E6	37	14	20/30	trucks
S4	AF	2A770	E6	36	14	20/25	trucks off road
S5	AF	25051	E4	25	13	20/20	POV
S6	AF	25051	E4	29	15	20/20	POV
S7	Marine	2161	E3	18	12	20/20	trucks, motorcycle
S8	Army	35E/51A	CPT	36	16	20/20	trucks off road

[a]MOS = military occupational specialty
[b]POV = privately owned vehicle

3.9 Experimental Design

The experimental design was a within-subject, single factor, fixed factorial experiment with repeated measures on the vision system and the participants as a random factor. The null hypothesis was that there is no difference in performance with vision system.

3.9.1 Independent Variables

Independent variables were the four levels of vision during driving (direct and indirect vision camera FOV of near unity, wide, and extended).

3.9.2 Dependent Variables

Dependent variables were the time to transverse the road course and the number of course barrels struck, the heart rate, and the root mean square (rms) head movement while the participants were on the course, and the ratings from a battery of questionnaires and examinations.

3.10 Questionnaires and Examinations

A battery of standardized questionnaires was administered to the participants to examine the differences in perceived effects on driving, which were induced by the vision systems. The battery of questionnaires consisted of four sets that measure the subjective workload, the affective state, and different levels of cognitive reasoning, including planning. The first set includes workload attention allocation, perceived workload, motion sickness, and SA. The second set is an affective battery of examinations, while the third set is a cognitive battery of examinations. Finally, a planning map examination is included as a fourth set.

3.10.1 Subjective Effects

The first battery set, which measures the subjective effects of the vision systems on different aspects of the task workload, consists of the following items.

3.10.1.1 Attention Allocation Loading

This is a questionnaire used for rating the allocation of attention to the visual, auditory, cognitive, and motor processing channels of the human operator according to loading factors (McCracken & Aldrich, 1984). These loading factors are used in task analysis workload simulations (Allender, Salvi, & Promisel, 1998). The questionnaire (see Appendix C) consists of a set of four 7-point, bipolar scales for rating the attention loading on each channel, with verbal anchors for corresponding activities overlaid on the scales.

3.10.1.2 National Aeronautics and Space Administration (NASA) Task Loading Index (TLX) Workload Questionnaire

The NASA TLX workload questionnaire (Hart & Staveland, 1988) is used for rating the perceived workload in terms of task demand and interaction. The NASA TLX is a multi-dimensional rating procedure for the subjective assessment of workload. Workload has been defined as a hypothetical construct that represents the cost incurred by the human operator to achieve a specific performance level. The construct is composed of behavioral, performance, physiological, and subjective components that result from the interaction

between a specific individual and the demands imposed by a particular task. The questionnaire (see Appendix C) consists of six scales that relate to the demands imposed on a subject and the interaction of the subject with the task. The Mental, Physical, and Temporal scales measure the demands, while the Effort, Frustration, and Performance scales relate to the interaction with the task.

3.10.1.3 Motion Sickness

A motion sickness questionnaire was used for the subjective estimation of motion sickness (Kennedy, Lilienthal, Berbaum, Baltzley, & McCauley, 1989). The questionnaire (see Appendix C) lists 4-point, bipolar rating scales consisting of verbal descriptors for the level of sickness of 16 symptoms such as general discomfort, eyestrain, dizziness, and nausea, among others. Based on data from a factor analysis of simulator sickness experiences, a procedure has been developed (Kennedy, Lane, Lilienthal, Berbaum, & Hettinger, 1992) for reducing the scores to subscales for the symptomatic components of oculomotor stress (eyestrain), nausea, and disorientation, and a measure of total severity.

3.10.1.4 Situational Awareness Rating Technique (SART) Questionnaire

The SART questionnaire (Selcon, Taylor & Koritsas, 1991), which was used for rating SA (Taylor, 1988, 1989; Taylor & Selcon, 1994), was designed to measure subjective ratings of non-attention factors such as domain knowledge or schemata and experience, the cognitive nature of the information received while a person is performing a task, and the workload needed to process the information. The questionnaire (see Appendix C) uses ten independent 7-point bipolar dimensions, which are then classified into three major domains of situation demand, supply, and understanding. The ten dimensions of the questionnaire are Instability, Variability, and Complexity of the situation for the demand domain; the Arousal, Spare Mental Capacity, Concentration, and Division of Attention for the supply domain; and the Quantity, Quality, and Familiarity of the information for the understanding domain. The questionnaire is the result of a study by Taylor (1988, 1989) that involved subjective ratings of bipolar awareness constructs elicited from aircrews about their experience and knowledge. Taylor reportedly found that ten independent bipolar constructs emerged from the 44 constructs provided by the aircrew, as determined by eliciting frequency, principal component loading, and inter-correlation clustering. These constructs were reduced by Taylor to the ten dimensions of the SART questionnaire.

3.10.2 Affective Effects

The second set consists of affective questionnaires that measure the perceived emotional state and components. These questionnaires are a part of ARL's Comprehensive Psychological Stress Assessment battery, which is used to provide a diagnosis of the various components of stress (Mullins & Fatkin, 1995;

Fatkin & Hudgens, 1994; Fatkin, King, & Hudgens, 1990; Glumm et al., 1997). The set consists of the two questionnaires described next.

3.10.2.1 The Subjective Stress Scale

The Stress scale (Kerle & Bialek, 1958) detects significant affective changes in one's emotional state. Participants select one word from a list of 15 adjectives that best describes how they feel either "right now" or during a specific time period or event. The scale is thought to be a measure of the overall "anxiety" or "worry" state attributable to stressful situations.

3.10.2.2 The Multiple Affect Adjective Checklist-Revised (MAACL-R) (Today form[4])

The MAACL-R (Zuckerman & Lubin, 1985) is used to measure changes in five primary affective aspect components of stress with changes in stressful situations. The participants check all words that describe their feelings from a one-page list of 132 adjectives. The primary affective components that are calculated from the selected adjectives are (a) anxiety, or uncertainty about a specific situation; (b) depression, or sense of failure about one's own performance; (c) hostility, or frustration regarding environmental circumstances or performance; and (d) positive effect, or sense of well-being. An overall distress score, dysphoria, or negative affect is calculated from the anxiety, depression, and hostility scores. The Today form has been found to be useful for research in which changes are expected in specific affects in response to stressful situations. Participants are instructed to answer according to how they either feel "right now" or how they felt during a specific time period or event. The form is easily administered, completed within 1 or 2 minutes, and provides critical information about the dynamics of the stress experienced by the respondents. Each subscale score indicates the level or intensity of the stress response, as well as the primary stress components contributing to the response.

3.10.3 Cognitive Effects

The third set consists of cognitive questionnaires that measure the effects of stress and endurance on verbal short-term memory, logical reasoning, mathematical calculations, and spatial rotation ability. These are part of the ARL-developed Cognitive Performance Assessment for Stress and Endurance battery of paper-and-pencil tests (Fatkin & Mullins, 1995). The assessment is administered as a booklet that contains four timed tests. Participants are provided with at least two practice sessions for familiarity with the test battery and to decrease learning effects (Baddeley, 1968). As used in this study, the assessments consist of the following timed tests.

[4]The questionnaire can be administered as a trait measure (the General form) or a stress perception measure (the Today form).

3.10.3.1 Verbal Memory Test

Short-term memory is evaluated with lists taken from word usage text (Thorndike & Lorge, 1944). Each list consists of 12 one- or two-syllable words with the most common usage rating (100 or more per million). The participant has 1 minute to study the list of 12 one- or two-syllable words and then another minute to recall the words on the list.

3.10.3.2 Logical Reasoning Test

This reasoning test evaluated the participants' understanding of grammatical transformations of sentences of various levels of syntactic complexity (Baddeley, 1968). Each item consists of a true or false statement about the order of letters in a letter pair. The test is balanced for the following conditions: positive versus negative, active versus passive, precedes versus follows, order of statement letter presentation, and order of letters in letter pairs (equivalent to balancing for true-false). Letter pairs are selected to minimize acoustic and verbal confusion. The participants have 1 minute to specify whether 32 statements about logical items consisting of letter pairs are true or false.

3.10.3.3 Addition Test

Used to test working memory, this task consists of 15 three-digit, two-number addition problems, with the numbers selected from a random number table (Williams & Lubin, 1967; Williams, Gieseking, & Lubin, 1966). The participants have 30 seconds to complete the test.

3.10.3.4 Spatial Rotation Test

Spatial skills are assessed with a mental rotation task adapted from Shepherd's work (1978). The test consists of spatial rotational problems. Each problem has a test pattern and three reference patterns, one of which is identical to the test pattern rotated. The patterns are in the form of a six-by-six grid enclosed within a hexagon measuring 2.8 cm with areas of the grid filled to create random patterns. To the right of each test pattern are three similar patterns. The task is to select the pattern that is identical to the test pattern when rotated. The problems are balanced for the number of grids filled (7, 9, or 11), pattern density (adjacent blocks filled versus one break between pattern blocks), and rotation of the correct answer (90, 180, or 270 degrees). The participants have 2 minutes to complete the 18 problems in the test.

3.10.4 Planning

The fourth set examines route planning in which the participant has 30 seconds to select the shortest path between two referenced buildings on a road map (see Appendix C). These exercises were derived from the literature (Bailenson, Shum, & Uttal, 1998; Tkacz, 1998) but otherwise have not been tested extensively for validity.

Finally, an exit questionnaire (see Appendix C) was used for the subjective evaluation of the vision systems by the perceived effects on image input, driver state, and control activities, and system performance.

3.11 Control of the Experiment-wise Type I Error

A problem in statistical analysis is the control of the experiment-wise Type I error. This is because the chance that a measure will erroneously prove to be significant increases statistically with the number of analyses performed. In all, a total of 61 measures was collected per vision system treatment for each participant. This includes the 47 measures collected in each trial: course time, number of barrel strikes, heart rate, average head movement, six workload questions, 10 SART questions, 16 motion sickness questions, one subjective stress state, five affective aspect components for the MAACL, and five scores for the cognitive processing problems. In addition, 14 ratings were collected for each treatment condition in the exit questionnaire. The strategy for controlling the Type I error is based on a judicious selection of the measures for analysis. Careful consideration is given to the statistics involved since inflated Type I error can result from an analysis without corrections for lack of sphericity and departures from normality in the within-subjects effects. The Holm simultaneous testing procedure (Neter, Kutner, Nachtsheim, & Wasserman, 1996) is used to partition the overall alpha level of 0.05 among the family of planned separate analyses. The Holm procedure is a more powerful form of the Bonferroni procedure, which is used to control family-wise Type I error. The approach is now described in greater detail.

Several techniques are used to reduce the data for analysis from the questionnaires. Different researchers have developed these questionnaires and we treat the results in separate analyses. First, factor analysis (Cooley & Lohnes, 1971) is used to reduce the measures to factorial components for statistical analysis. The number of factorial components used in the analysis equals the number of groupings that are recognized in the literature as being appropriate for the questionnaire. This is true, except for those cases when no such standard exists, and here, only two factorial components are used. A univariate statistical analysis is applied to each factorial component in turn, starting with the first factorial since this component contains the largest portion of the variance, until significance is attained, if at all. The components are analyzed by parametric methods unless the components are non-normal distributions, in which case, a non-parametric method of analysis is applied to the first component. In this way, only one (or two) analysis is applied to each factorial decomposition. Following significance of the factorial component, the data for the measures are analyzed according to standard practice for the questionnaire.

It is standard practice to reduce the data for the perceived performance questionnaires: workload, SA, and motion sickness, to single measures by a weighted summing of the component scales. For example, the NASA TLX

workload questionnaire (Hart & Staveland, 1988) consists of six bi-polar scales with semantic anchors, three scales for task demand and three for task interaction. A single grand measure of workload may be calculated by a weighted summing of the ratings of the component scales (Hendy, Hamilton & Landry, 1993). Also of interest are the sums for the task demands and interaction. In contrast, the SART questionnaire consists of ten bi-polar scales, three scales for situational demands, four for supply, and three for situational understanding. A single overall measure of SA is calculated from the sum of the ratings for the supply and understanding, minus the sum of the ratings for the demand scales (Selcon, Taylor, & Koritsas, 1991; Taylor, 1988, 1989). Of interest are the sums for the demand, supply, and understanding domains. Finally, the motion sickness questionnaire (Kennedy et al., 1992) consists of 16 multiple choices. In data reduction, these are mapped to numerical scales that are grouped into ratings for a nausea symptom, a disorientation symptom, and an oculomotor symptom. A single measure of total severity is calculated from the weighted sum of these ratings.

In some cases, we reduce the number of analyses performed by analyzing together multiple measures that are correlated by a multivariate analysis of variance (MANOVA) appropriate for repeated measures designs (Schutz & Gessaroli, 1987) to determine the overall significance. However, there are limitations in the application to this experiment because of the small sample size. Considering the subject sample size of eight, the multivariate analysis is limited to two dependent variables for valid matrix manipulation; a minimum number of subjects required per group is given by the total number of observations per subject (Schutz & Gessaroli, 1987). The statistical power of the test may be low since according to the literature for small sample sizes, the power of a MANOVA is suspected to be less than that of separate repeated measures univariate analyses of variances (RM ANOVA). This is reported for sample sizes of less than 20, plus the number of treatments ($n = k + 20$), although some authors (Vasey & Thayer, 1987) suggest that the sample limit is lower ($n = k + 6$). This is true even for correlated measures. Furthermore, the MANOVA is more sensitive to departures from parametric distributions at small sample sizes resulting in inflated Type I errors. The application of a parametric MANOVA requires multivariate normal distributions for the dependent measures within each subject group and equality of the variance-covariance matrices between groups (Pedhazur, 1982). However, the within-subjects effects do not need to satisfy sphericity. Furthermore, while the MANOVA does not require multivariate circularity (equal variances and covariances) of measures between groups, it should be satisfied to maintain statistical power (Schutz & Gessaroli, 1987). With equal sample sizes, the Pillai-Bartlett trace as a MANOVA test statistic is most robust in terms of Type I error to violations of the parametric requirements.

As an additional control of the Type I errors, adjustments are made in the univariate RM ANOVAs via the Greenhouse-Geisser correction of the degrees of

freedom for reduced sphericity in within-subjects effects. The MANOVA is an overall statistical test and does not indicate the separate contributions of the multiple dependent variables to the differences between the treatments. For this reason, separate tests are made of the dependent variables via RM ANOVA. In a parametric analysis, the distributions for the dependent measure must satisfy normality and homogeneity of variances without correlation of the variances with the means, as well as sphericity for the within-subjects effects (equal variances of the pairwise differences) since the number of treatments exceeds two. To maintain the error rate for all pairwise comparisons, the contrast of *post hoc* comparisons between treatment means are computed with the Tukey Honestly Significant Difference (HSD) Test from the mean differences and the ANOVA error residual (Keppel, 1982). In those cases when the distributions for the dependent measure are not normal, a nonparametric Friedman ANOVA by ranks is used for univariate analysis, followed by a Scheffé pairwise comparison test for the contrast of rank means.

Once the planned analyses are completed, the overall family-wise alpha level of 0.05 is partitioned among the statistical tests with the Holm simultaneous testing procedure (Neter et al., 1996) to control the Type I error. With this procedure, the alpha level is partitioned among the family of tests, according to the ranking of the (two-sided) probabilities of significance. With each acceptance of the alternate hypothesis, the family-wise alpha level is adjusted for the tests remaining. This process is continued until a test is reached for which the null hypothesis applies, at which time, the null hypothesis is accepted for this and all remaining tests.

3.12 Training and Research Procedures

At the start of the experiment, the participant was trained with the battery of test questionnaires, familiarized with driving the vehicle by direct vision, and introduced to the test course layout and the training and test procedures. To allow the participant time to assimilate the different tasks, this phase was separated into supportive stages of successive driving and questionnaire training as now described. As advised by the ARL Soldier Stress and Performance Research Team, the participants were trained twice with the questionnaires with sufficient time between for familiarization.

Following the signing of the volunteer affidavit (see Appendix C), the participant was given an orientation and safety briefing. The participant's demographics data and prior driving experience were recorded at this time. The participant was trained with a battery of the test questionnaires, an event that took 45 minutes to complete.

With the experimenter on board as safety officer, the participant drove the experimental vehicle with direct vision several times around the perimeter road to become familiar with the driving characteristics of the HMMWV.

Following another exercise with the battery of questionnaires, the participant then drove the vehicle with direct vision on the training course several times to become acquainted with the training procedure.

The experimenter then drove the participant over the research course at a slow speed, first in the clockwise direction and then in the counterclockwise direction, while the participant held a map of the course. This was done to familiarize the participant with the general layout of the driving course, thereby allowing him to build a mental map. The acquisition of a mental map of the course reduced the need for cognitive evaluation by the participant for route determination during driving.

The participant then completed another set of the questionnaires to establish a baseline. During this time, the vehicle was prepared for the first of the experimental trial sessions by the installation of the displays, camera lens, and light shields in the cab area as appropriate.

The participant then entered the experimental phase of the study. In this phase, the participant was trained and tested about the vehicle with the vision systems in a counter-balanced manner according to the Latin square scheme of Table 4. For each such set of trials, the participant first drove the vehicle with the experimenter on board several times around the perimeter road to become familiar with the driving characteristics of the HMMWV with the vision system. He then drove the vehicle on the training course while the experimenter timed him, recorded barrel strikes, and critiqued his performance. Again, the participant was instructed to drive as fast as he wanted to (but not to exceed a safe course speed for safety reasons) without intentionally striking barrels on the course. The participant repeated this process at least five or more times with stops between runs to allow struck lane markers to be erected, until his speed and strikes performance reached asymptotic levels. After each run, the experimenter discussed consistent guidance in driving strategies with the participant for increasing his speed while reducing barrel strikes.

Table 4. Participants' Schedule

Participant	Cameras' FOV			
	direct	near unity	wide	extended
S1	1	3	2	4
S2	4	2	3	1
S3	3	1	4	2
S4	2	4	1	3
S5	1	3	2	4
S6	4	2	3	1
S7	3	1	4	2
S8	2	4	1	3

During an experimental trial, the participant first drove the vehicle over the research course in the clockwise direction from start to finish and then after stopping for struck barrels to be replaced, drove in the counterclockwise direction. The second run was made to counterbalance any bias in the data from the participant having to turn consistently in one direction on the research course. Furthermore, the second run reduced the chance that the participant would eventually learn a procedural pattern for driving the course, while reinforcing his mental map of the course layout that had been learned in training. The course times and errors as measured by barrel strikes were recorded during the trial runs. During the test run, the participant's heart rate was recorded with the wrist recorder and his head movements were recorded on the on-board PC via the head tracker.

Following the experimental trial, the participant was allowed 45 minutes to complete a set of the battery of questionnaires. The participants reported that this was enough time for them to recover from the physical demands of driving the vehicle. During the rest break, the need to answer the questionnaires prevented them from mentally reviewing the driving task and thereby interfered with their learning the course at the level of skilled automatic responses. During this period, the vehicle was outfitted for the next vision system by the installation of the displays, camera lens, and light shields in the cab area as appropriate.

At the end of the experiment, the participant answered an exit questionnaire and was debriefed before being released by the experimenter.

The experimentation site was closed to other vehicular and foot traffic during the study. In all exercises with the participant driving, the experimenter served as safety officer while occupying the passenger's seat on the vehicle and was able to see the external front from that position. The experimental vehicle had been modified so that the safety officer could activate the braking system from the passenger's seat in case the video system stopped working—an incidence that happened only once because of a loose connector during a training run. The participant and safety officer were required to wear safety belts at all times while in the vehicle.

4. Statistical Results

Reported here are the results of the statistical analyses of the task performance, physical workload (as measured by the heart rate and head movements), attention allocation, perceived performance (workload, SA, and motion sickness), subjective stress state and affective aspect components, cognitive processing, and the exit evaluation.

4.1 Participants

In all, ten persons participated in the study, of which, the last two were dropped from the analysis. While the driving performance of the ninth participant matched that of the others, he exhibited no concern for his own safety and lost control of the vehicle several times during the experiment. The tenth participant decided to stop because of nausea followed by vomiting that occurred in the second trial run with the indirect vision system. One participant among the eight in the analysis exhibited motion sickness during his last two scheduled trials, which was severe enough for him to stop before completing the first run of the next-to-the-last trial and to abort the last trial after training. His performance in the next-to-the-last trial was extrapolated from that in his incomplete run and performance of the last trial from his training data. A study of the data showed a high correlation between training and research performance for the other participants completing the experiment for the times (two-tailed test $p < .001$, Pearson Correlation $R^2 = 0.904$, N = 28) and the errors (two-tailed test $p < .001$, Pearson Correlation $R^2 = 0.714$, N = 28) across treatments.

4.2 Task Performance

The task performance is determined by the course times and number of barrel strikes averaged across the clockwise and counterclockwise course runs. The correlation of the averaged course times and the barrel strikes is significant at the $p < .004$ level (two-tailed test) with a Pearson Correlation coefficient of 0.607 for the 32 samples. For this reason, the time and strike measures are analyzed with a MANOVA. The dependent measures in this analysis are the natural logarithmic transformation of the course times and the arcsine transformation of the strike counts. The time data for the indirect vision treatments are skewed toward the low values, and the transformation normalizes the distribution. Similarly, while the distributions for count data are commonly not normal, the arcsine transformation of number counts is close to normal in distribution. Here, the transformation is defined (Dixon & Massey, 1969) as the arcsine of the square root of the number of incidents divided by the total number possible (N = 96). The MANOVA is an overall statistical test and the measures are analyzed by separate univariate RM ANOVAs with an accompanying *post hoc* contrast of comparisons between treatment means.

4.2.1 Overall Performance

The task performance as measured by course times and barrel strikes is significantly different for the viewing treatments. The multivariate omnibus MANOVA test of within-subjects effects is significant ($p < .002$, Pillai's trace = .75, F = 4.199, df = 6, error df = 42).

4.2.2 Course Times

The course times are significantly different for the viewing treatments and for the most part, the treatment means are significantly different from each other. The

univariate RM ANOVA test of within-subjects effects is significant ($p < .001$, F = 15.031, df = 2.697, error df = 18.878), following the Greenhouse-Geisser correction (GGI $\varepsilon = 0.899$) of the degrees of freedom for reduced sphericity. A Tukey HSD multiple pairwise comparison test of the treatment means shows direct viewing to be significantly faster than the indirect viewing treatments. On the average, the direct view driving is 1.21 times faster than that for the near-unity FOV ($p < .006$), 1.26 times faster than the wide FOV ($p < .003$), and 1.34 times faster than the extended FOV ($p < .001$). Furthermore, the near-unity FOV is 1.11 times significantly faster than the extended FOV ($p < .047$); however, the wide FOV is not significantly different from the near-unity or extended FOVs. Figure 11 is an exploratory data analysis (EDA) "box-and-whisker" plot (Velleman & Payne, 1992) of the course times for the viewing treatments. The box plot figure shows the median, the "hinges" (first and third quartiles), and the maximum and minimum values that are not outliers for the distribution of each viewing treatment. Although not on this diagram, values more than 1.5 times the box lengths (inter-quartile range) from the quartiles are designated as outliers, and values more than three box lengths as extremes. The box plots for the course times show a monotonic increase in median times with increase in camera FOV.

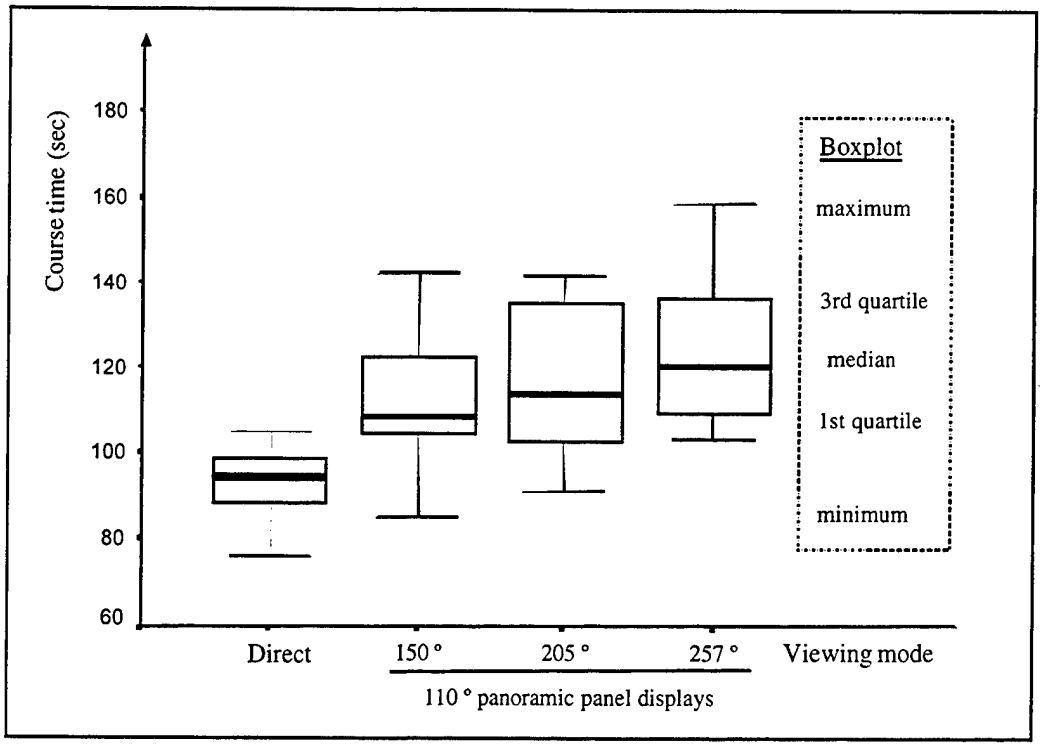

Figure 11. Course Time Box Plots for Viewing Treatments.

4.2.3 Lane Marker Strikes

The barrel strikes are significantly different for the viewing treatments. The univariate RM ANOVA test of within-subjects effects shows significant differences ($p < .035$, F = 4.414, df = 1.923, error df = 13.464), following the

Greenhouse-Geisser correction (GGI = 0.641) of the degrees of freedom for reduced sphericity. However, a Tukey HSD multiple pairwise comparison test of the treatment means shows no significant difference between direct viewing and the indirect viewing treatments, and the cameras' FOVs are not significantly different from each other. Figure 12 is an EDA box plot of the barrel strikes for the viewing treatments. The box plots show a monotonic increase in barrel strikes with increase in camera FOV; however, the distribution variances for the indirect vision are wide spreads.

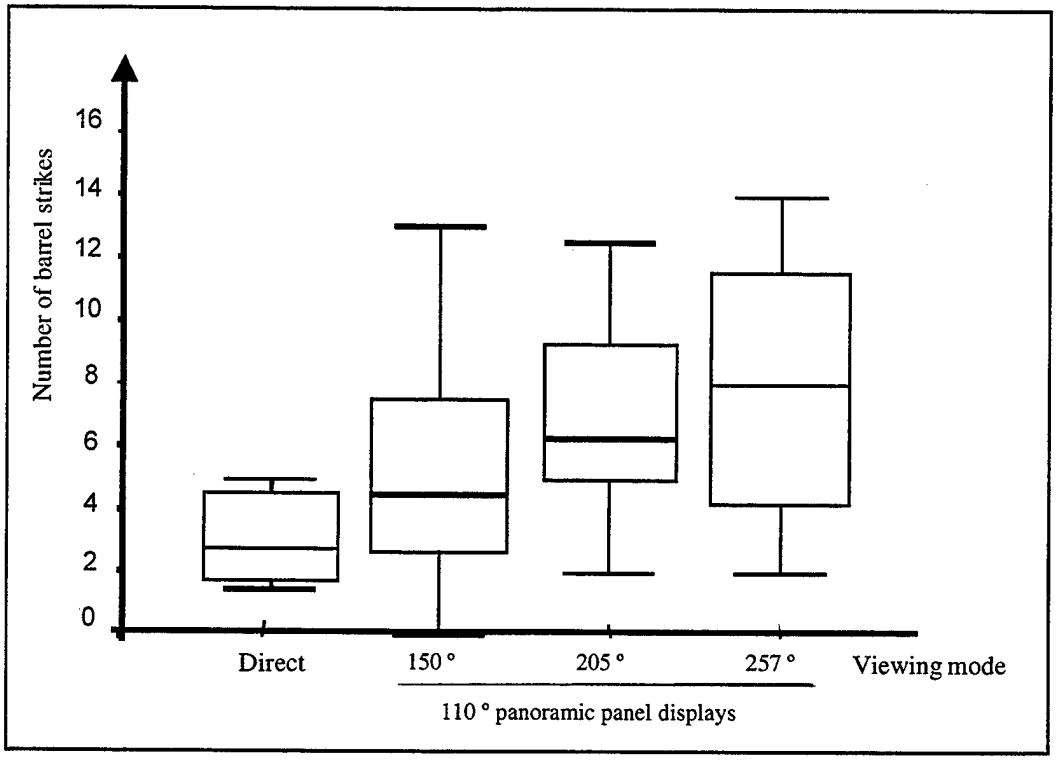

Figure 12. Marker Strike Box Plots.

4.3 Physical Workload

The heart rate and head movements during driving are measures of the physical workload. For both measures, equipment malfunction resulted in missing data from the factorial design. For the heart rate monitor, conditions for a good sensor-to-skin contact are a tight chest band and the participant is sweating. These conditions were not obtained in a few runs, which resulted in missing data (three data points for the fourth participant and two for the eighth participant, for a total of five missing data points from 32). One way of analyzing such data with an RM ANOVA is by estimating the missing data from the data of adjacent cells (Keppel, 1982); however, this is an ineffective process at small sample sizes. Instead, the approach used in this study was to apply a multiple linear regression analysis to the heart rate data as a function of the course time and barrel strikes, following a correlation analysis for significance, since these are all

dependent measures of the same treatments. Another problem is that in some runs, the recordings were momentarily interrupted by breaks in skin conductivity that resulted from vibrations in the chest band while the participant drove over the rough terrain. A study of the heart rate data shows that the maximum heart rate is representative of the sample over a trial. For this reason, both the maximum and average heart rates over the trial runs are analyzed; however, there is little difference in the analyses, and the results for the maximum heart rate are reported.

Similar comments apply to the head-tracking data when the power to the on-board computer was occasionally interrupted by physical vibrations over the rough terrain of the course. In this case, data were collected for only six of the eight participants, and 8 cells are missing from the total 24 available. Here, the effect of learning is not counterbalanced across trials. For example, the data for the near-unity FOV are drawn from the first two test trials, while those for the wide FOV are from the last two trials. Again, the data are often incomplete for a trial run, and the average across a run is used. The head tracking is computed as the rms sum of the location (inches) and angular displacement (degrees) about a bore-sighting point established at the start of each run. As before, the head-tracking data collected are analyzed with a multiple linear regression as a function of the course time and barrel strikes.

4.3.1 Heart Rate

The maximum heart rate shows significant correlation with the logarithm of the course times (two-tailed test $p < .001$, Pearson Correlation $R^2 = -.733$, N = 27) and the arcsine of the barrel strikes (two-tailed test $p < .006$, Pearson Correlation $R^2 = -.512$, N = 27). The times and strikes are significantly correlated (two-tailed test $p < .004$, Pearson Correlation $R^2 = .536$, N=27) because of collinearity between the predictor variables. A multiple linear regression analysis with the stepwise method (enter criteria, $p \leq .05$; remove criteria, $p \geq 0.10$) shows a significant linear decrease in maximum heart rate with course time ($p < .001$, F = 29.01, df = 1, error df = 25) but not barrel strikes, which are excluded. Figure 13 is a regression line and scatter plot for the maximum heart rate (beats per minute) as function of the natural logarithm of the course time (in seconds).

4.3.2 Head Movements

The rms head movement shows minimal correlation with the arcsine of barrel strikes (two-tailed test $p < .059$, Pearson Correlation $R^2 = 0.432$, N = 16) and no correlation with the logarithm of course times. A multiple linear regression analysis shows no significant linear change of the head tracking with the arcsine of the barrel strikes ($p < .059$, F = 4.233, df = 1, error df = 14).

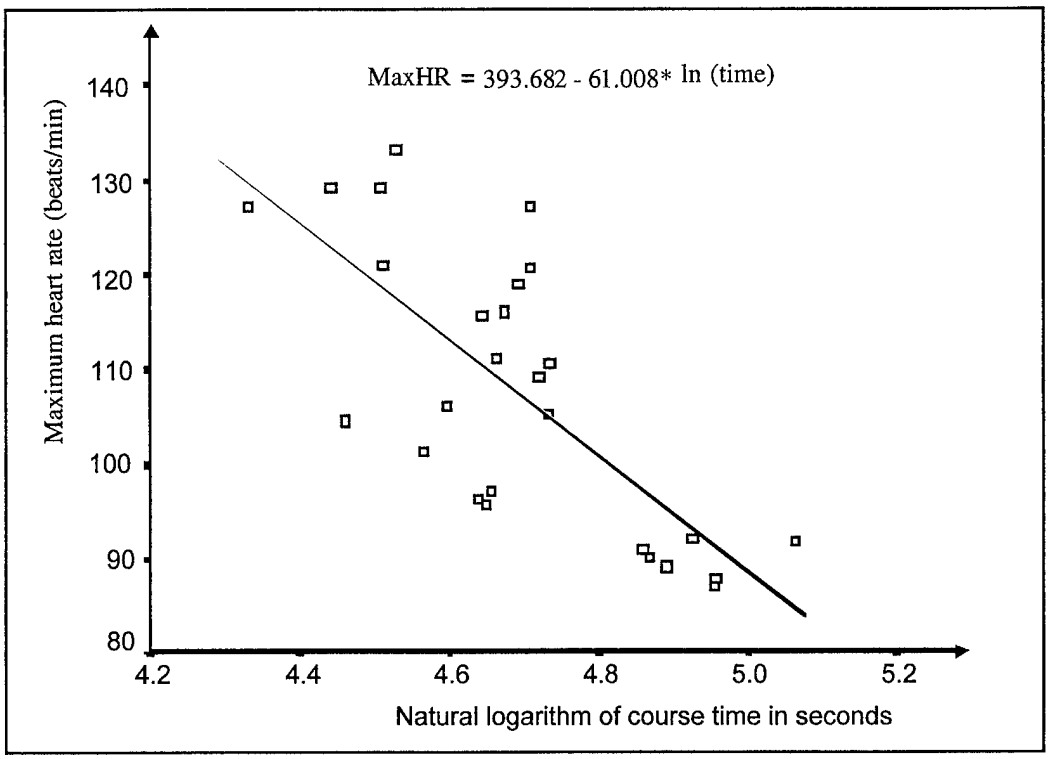

Figure 13. Maximum Heart Rate as a Function of Course Time.

4.4 Attention Allocation Loading Factors

The allocations of the participant's attention resources to the human auditory, visual, cognitive, and psychomotor processing channels are not significantly different for the viewing treatments as estimated by the attention allocation loading factors (McCracken & Aldrich, 1984). Figure 14 shows a factorial component loading diagram for the allocations to the four channels, following reduction to two components with a factor analysis that uses principal component analysis as the extraction method (82.034% total variance explained), and Vaximax rotation with Kaiser normalization. A study of the rotated component weight matrix shows that the cognitive channel (0.929, 0.140) dominates one component, the auditory channel (0.177, 0.921) dominates the other component, and vision (0.785, 0.536) and psychomotor (0.537, 0.573) are divided between both components.

Application of an RM ANOVA shows that neither factorial component varies significantly with treatments. Figure 15 shows an EDA box plot of the first component for the viewing treatments. Along with the box plots, the figure shows the outlier values marked by an open circle (o) and the extremes marked by an asterisk (*). As a confirmation of these results, the separate applications of a univariate RM ANOVA test of within-subjects effects show no statistically significant differences among the viewing treatments for each of the four channels. The box plots of Figures D-1 through D-4 in Appendix D for the visual,

cognitive, auditory, and psychomotor channel allocation scores show that this is partly attributable to the large variances in the distributions. For reference, the figures show the verbal anchors for the equivalent behavioral functions that correspond to the loading factors (see Appendix C).

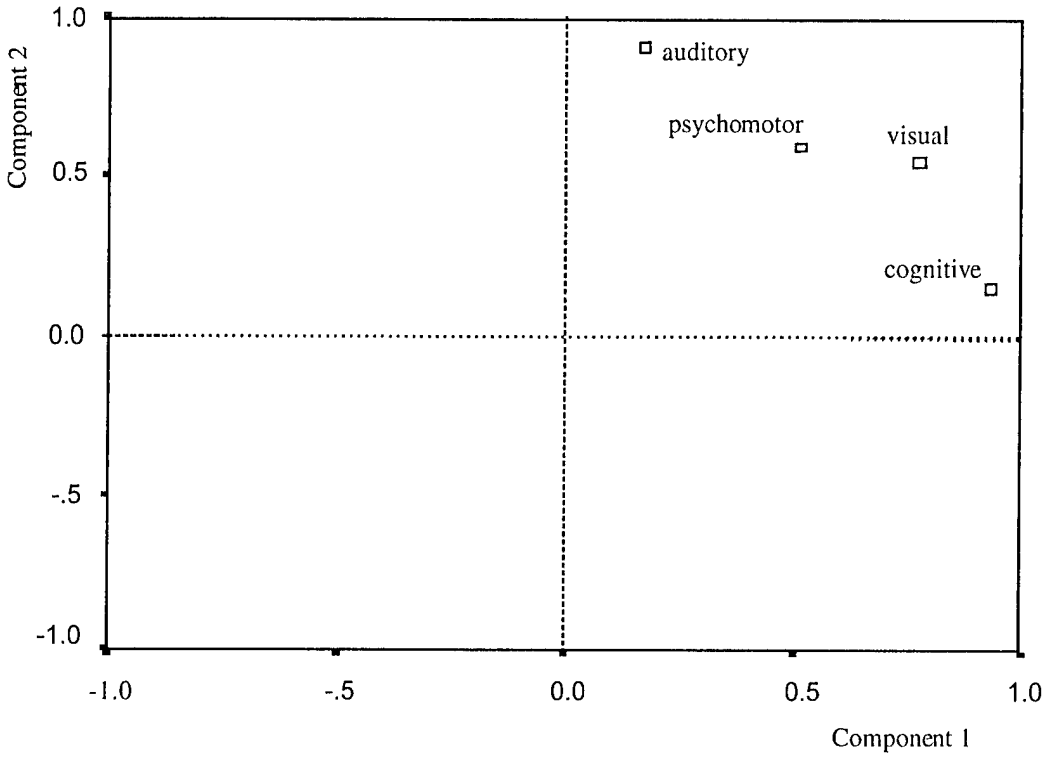

Figure 14. Attention Allocation Factorial Component Plot in Rotated Space.

4.5 Perceived Performance

The perceived performance is measured by the ratings from the questionnaires for the NASA TLX workload, SART, and motion sickness.

4.5.1 NASA TLX Workload Battery

The perceived workload is significantly different for the viewing treatments as determined by an analysis of the first factorial component. Figure 16 shows a factorial component loading diagram for the six TLX scales, following reduction to two components with a factor analysis that uses principal component analysis as the extraction method (80.845% total variance explained), and Vaximax rotation with Kaiser normalization. As noted in the key on the figure, the TLX scales are shape coded by their status as task demand or interaction. A study of the rotated component weight matrix shows that the demand components of perceived workload are aligned with the first factorial component: mental (0.912, 0.2090), physical (0.911, -.001), and temporal (0.875, 0.251). While the effort component (0.039, 0.927) of task interaction is aligned with the second factorial

component, the performance (0.882, 0.291) is aligned more with the first factorial, and the frustration (0.484, 0.599) is distributed between both components.

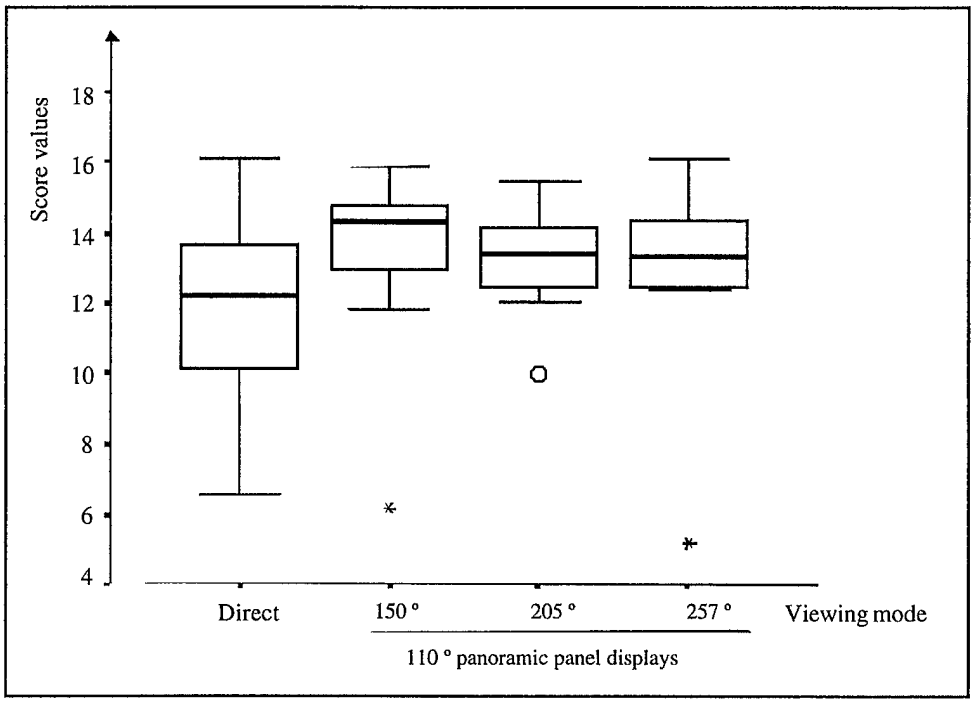

Figure 15. Attention Allocation First Factorial Component Box Plots.

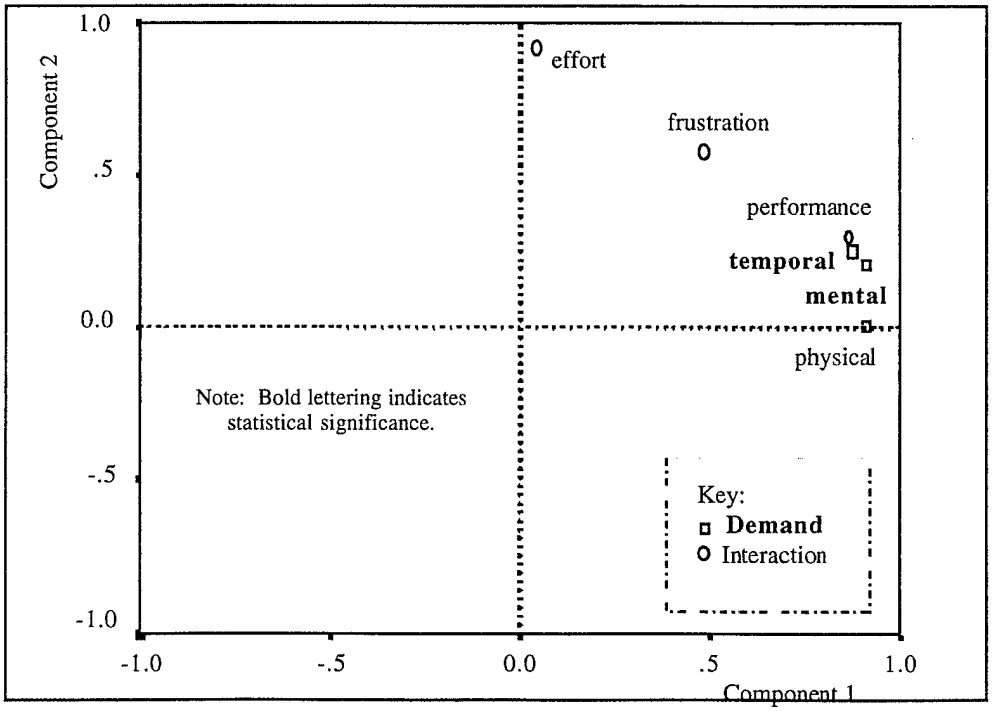

Figure 16. TLX Factorial Component Plot in Rotated Space.

Figure 17 shows an EDA box plot of the first factorial component for the viewing treatments. A univariate RM ANOVA test of within-subjects effects is significant by viewing treatments ($p < .001$, F = 11.704, df = 2.203, error df = 15.422, GGI = 0.734) for the first component but not the second. For the first component, a Tukey's HSD test was applied to the treatment means for multiple pairwise comparisons. The test shows direct viewing to be significantly different from the camera FOVs for indirect viewing (near unity: $p < .006$, wide: $p < .005$, extended: $p < .003$). However, the indirect viewing FOVs are not significantly different from each other.

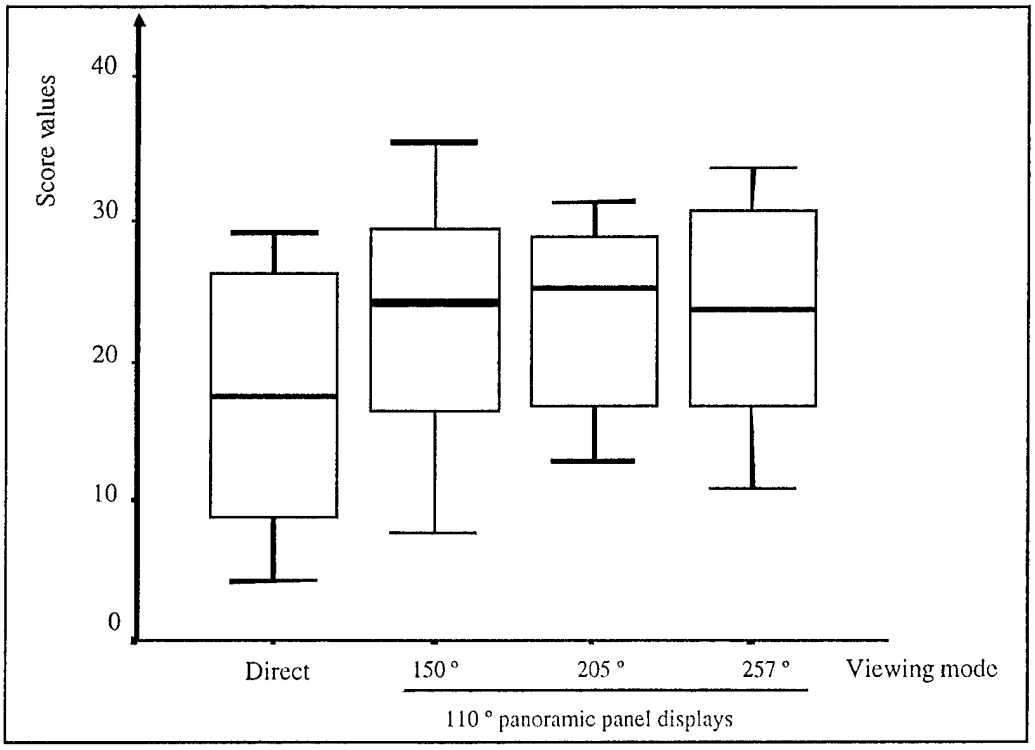

Figure 17. TLX First Factorial Component Box Plots.

The grand sum of the workload is significantly less for direct viewing than for indirect viewing. Figure 18 shows EDA box plots of the sum for the viewing treatments. The univariate RM ANOVA test of within-subjects effects is significant ($p < .004$, F = 7.251, df = 2.454, error df = 17.176), following the Greenhouse-Geisser correction (GGI = 0.818) of the degrees of freedom for reduced sphericity. A Tukey HSD multiple pairwise comparison test among treatment means shows direct viewing to be significantly different from the camera FOVs for indirect viewing (near unity: $p < .022$, wide: $p < .006$, extended: $p < .001$). However, the indirect viewing FOVs are not significantly different from each other.

A bivariate correlation shows that the sums of the task demand and interaction scores are significantly correlated with each other (two-tailed test $p < .001$,

Pearson Correlation = .710, N = 32). Application of a MANOVA shows that the demand and task interaction sums vary significantly with treatments ($p < .002$, Pillai's trace = .772, F = 4.01, df = 6, error df = 42).

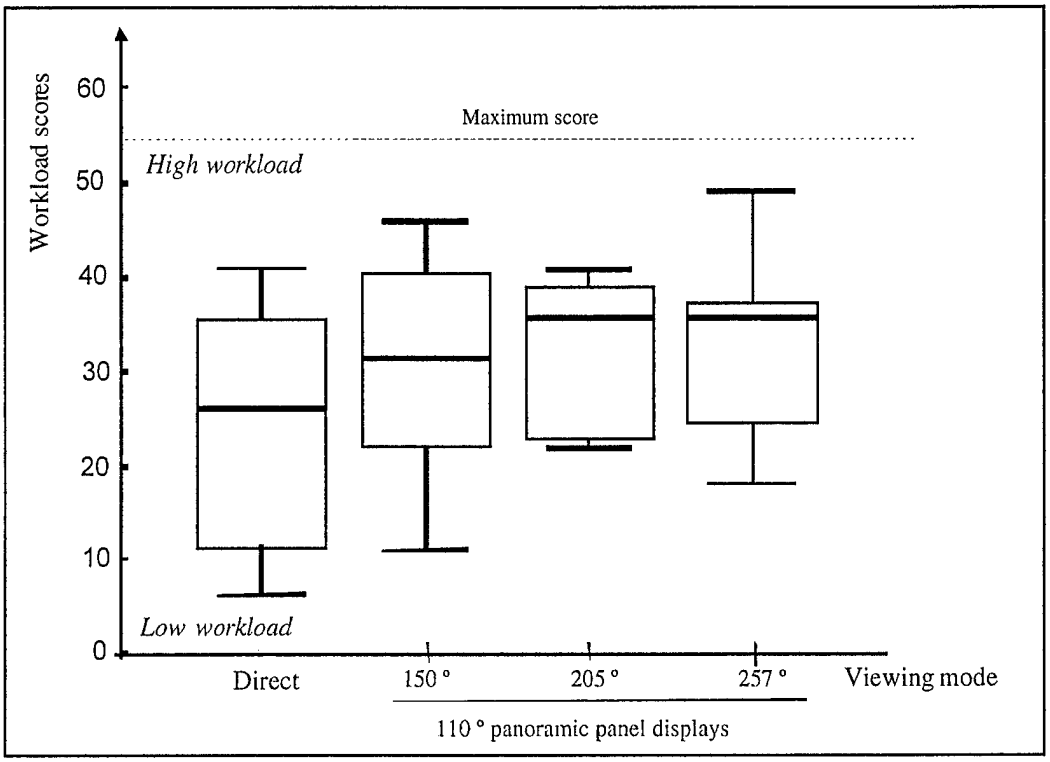

Figure 18. TLX Grand Sum Box Plots.

Considering the task demand, an RM ANOVA univariate test of within-subjects effects is significant for the sum of the demand components ($p < .001$, F = 14.701, df = 2.469, error df = 17.285), following the Greenhouse-Geisser correction (GGI = 0.823) of the degrees of freedom for reduced sphericity. Figure 19 shows EDA box plots of the demand sum for the viewing treatments. A Tukey HSD multiple pairwise comparison test among treatment means shows direct viewing to be significantly different from the camera FOVs for indirect viewing (near unity: $p < .002$, wide: $p < .006$, extended: $p < .002$). However, the indirect viewing FOVs are not significantly different from each other.

Considering the ratings for the demand components, the univariate RM ANOVA tests of within-subjects effects are significant for the temporal demand ($p < .004$, F = 9.925, df = 1.759, error df = 12.312, GGI = 0.586). This is also true for the mental demand ($p < .010$, F = 8.807, df = 1.380, error df = 9.662, GGI = 0.460) but not at all for the physical demand ($p < .156$, F = 2.060, df = 2.295, error df = 16.063, GGI = 0.765). A Tukey HSD multiple pairwise comparison test among treatment means for the temporal demand shows direct viewing to be significantly different from the camera FOVs for indirect viewing (near unity:

$p < .010$, wide: $p < .008$, extended: $p < .011$). However, the indirect viewing FOVs are not significantly different from each other. Similar comments apply to a Tukey HSD multiple pairwise comparison test among treatment means for the mental demand. The test shows direct viewing to be significantly different from the camera FOVs for indirect viewing (near unity: $p < .011$, wide: $p < .024$, extended: $p < .009$), but the indirect viewing FOVs are not significantly different from each other. For reference, Figures E-1, E-2, and E-3 in Appendix E show EDA box plots of the demand components for the viewing treatments.

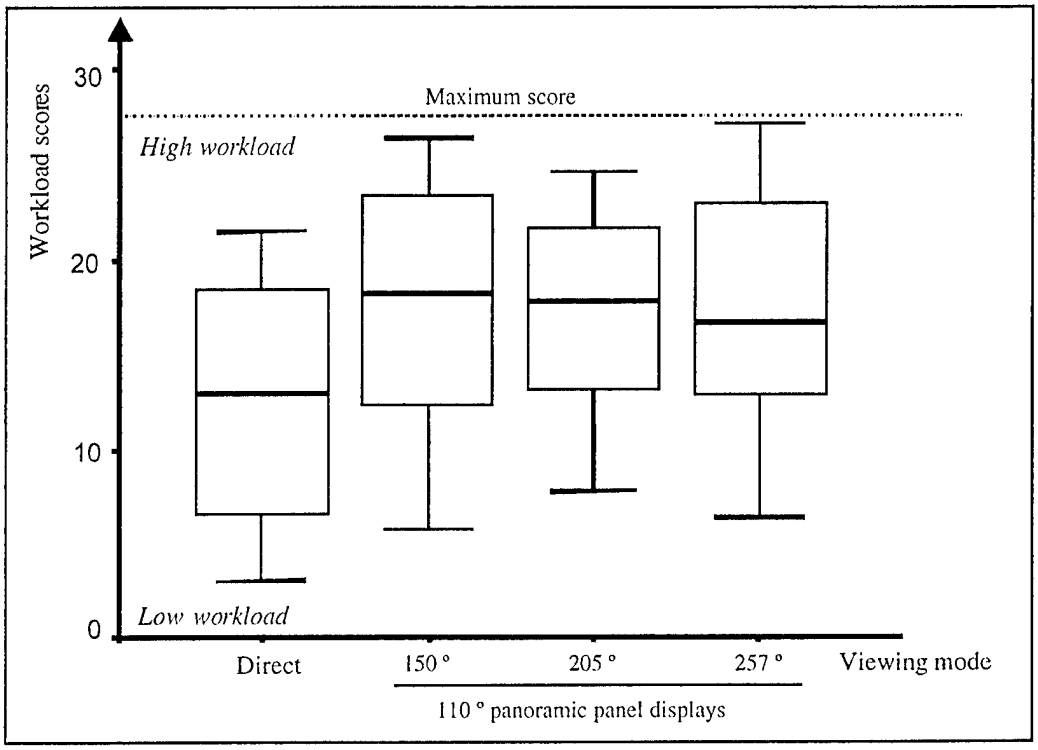

Figure 19. TLX Demand Sum Box Plots.

In contrast, the sums of the interaction components are not significant different by viewing treatments ($p < .159$, F = 2.076, df = 2.076, error df = 14.866, GGI = 0.708). For reference, Figure 20 shows EDA box plots of the interaction sum for the viewing treatments, and Figures E-4, E-5, and E-6 show the same for the interactive effort, performance, and frustration scores, respectively.

4.5.2 Situational Awareness Rating Technique (SART)

The SART scores for SA are significantly different for the viewing treatments as determined by an analysis of the first factorial component. Figure 21 shows a factorial component loading diagram for the ten scales following reduction to three components with a factor analysis that uses principal component analysis as the extraction method (75.875% total variance explained), and Vaximax rotation with Kaiser normalization. As noted in the key on the figure, the scales

are shape coded by their status as SA demand, supply, or understanding. A study of the rotated component matrix shows that the demand ratings are aligned with the first factorial component: instability (0.933, 0.056, -.234), variability (0.901, -.022, -.227), and complexity (0.943, 0.089, -.007). Similarly, the understanding ratings are aligned with the second factorial component: information quantity (0.310, 0.802, -.012), information quality (-.087, 0.944, 0.084), and familiarity (-.115, 0.870, -.057). However, the supply ratings are largely distributed among the three factorial components: arousal (0.354, 0.425, -.227), mental capacity (-.288, -.057, 0.711), concentration (0.191, 0.509, 0.692), and attention (-.230, -.160, 0.822).

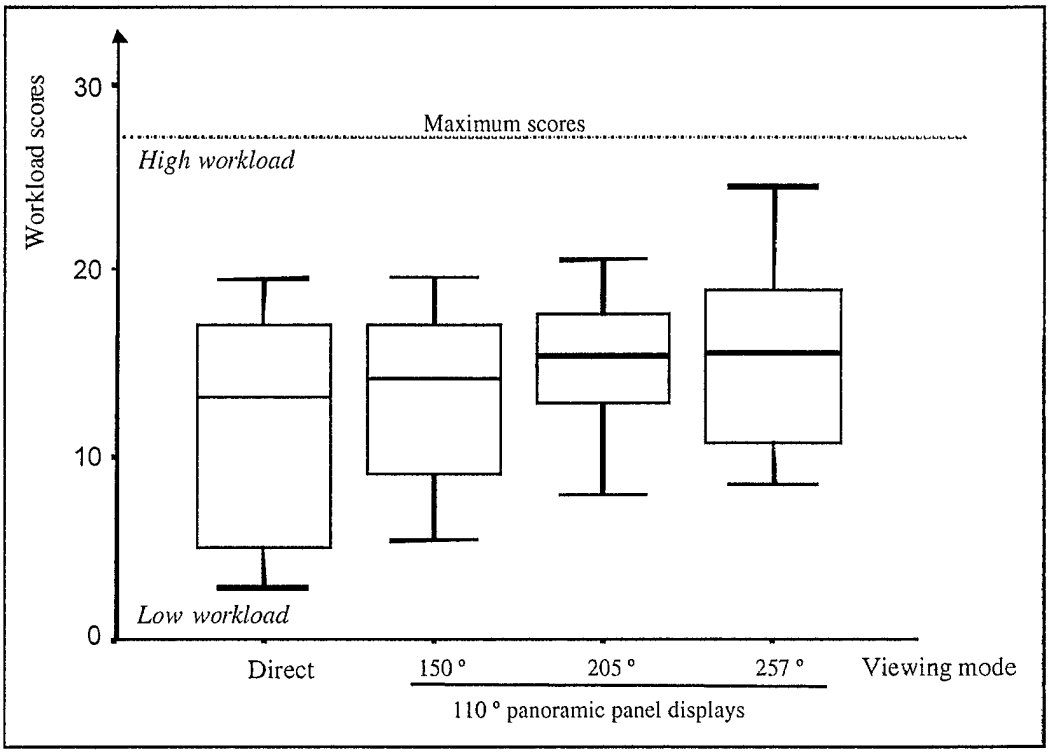

Figure 20. TLX Interaction Sum Box Plots.

Figure 22 shows EDA box plots of the first factorial component for the viewing treatments. The plots show the distributions of the first component to be heavily skewed for direct viewing. A nonparametric (NP) RM Friedman ANOVA test by ranks is significant ($p < .008$, chi-square = 11.886, df = 3, N =8) for the first component. Applications of RM ANOVA univariate tests are not significant for the second and third factorial components.

The overall rating of SA for the direct viewing is not significantly different from that for the indirect viewing FOVs. The overall SA rating is the difference between the sum of the components for the supply and the demand added to those for the understanding. Figure 23 shows EDA box plots of the SA ratings for

the viewing treatments. An RM ANOVA univariate test of within-subjects effects is not significant ($p < .062$, F = 3.33, df = 2.106, error df = 14.739, GGI = 0.702).

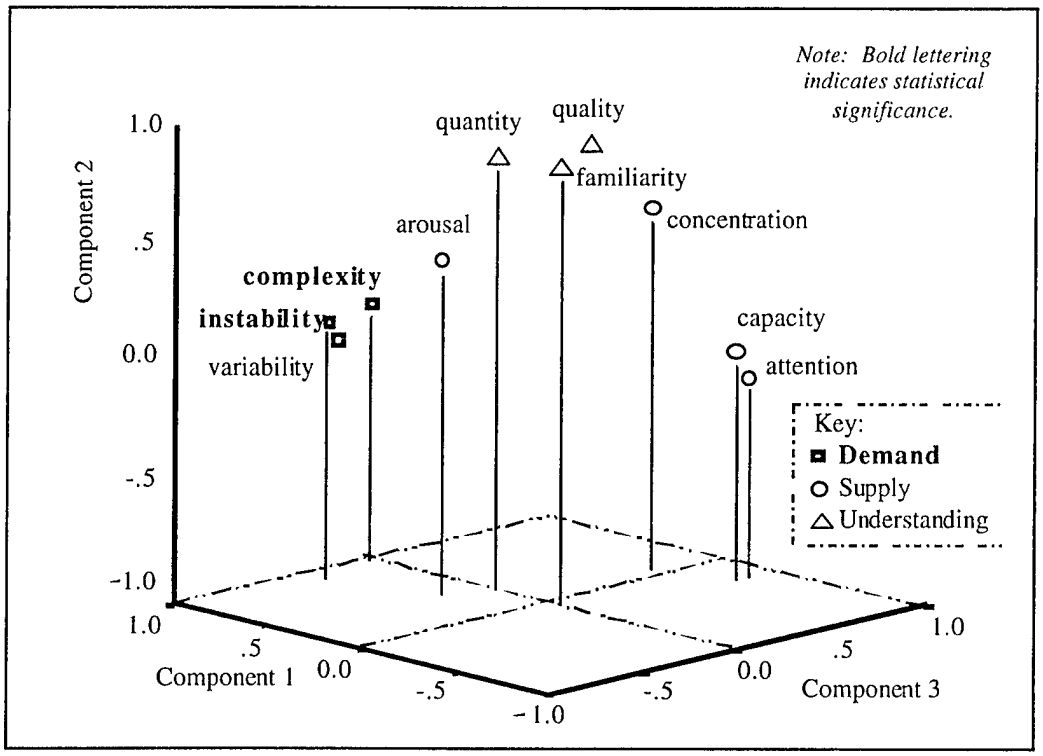

Figure 21. SART Factorial Component Plot in Rotated Space.

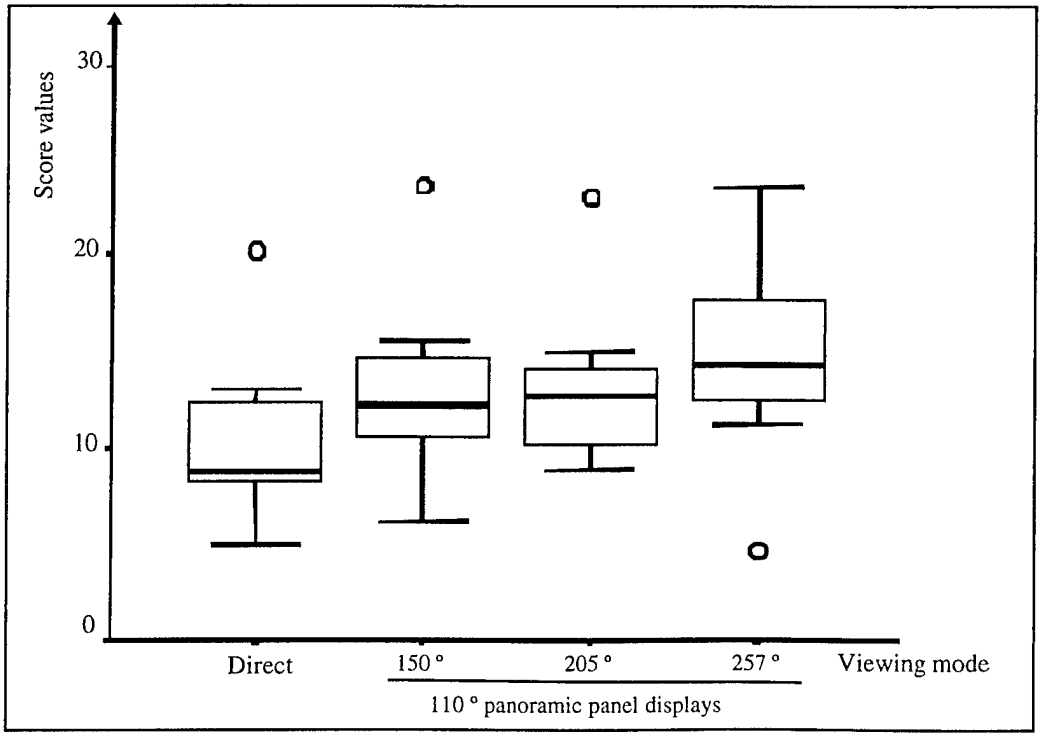

Figure 22. SART First Factorial Component Box Plots.

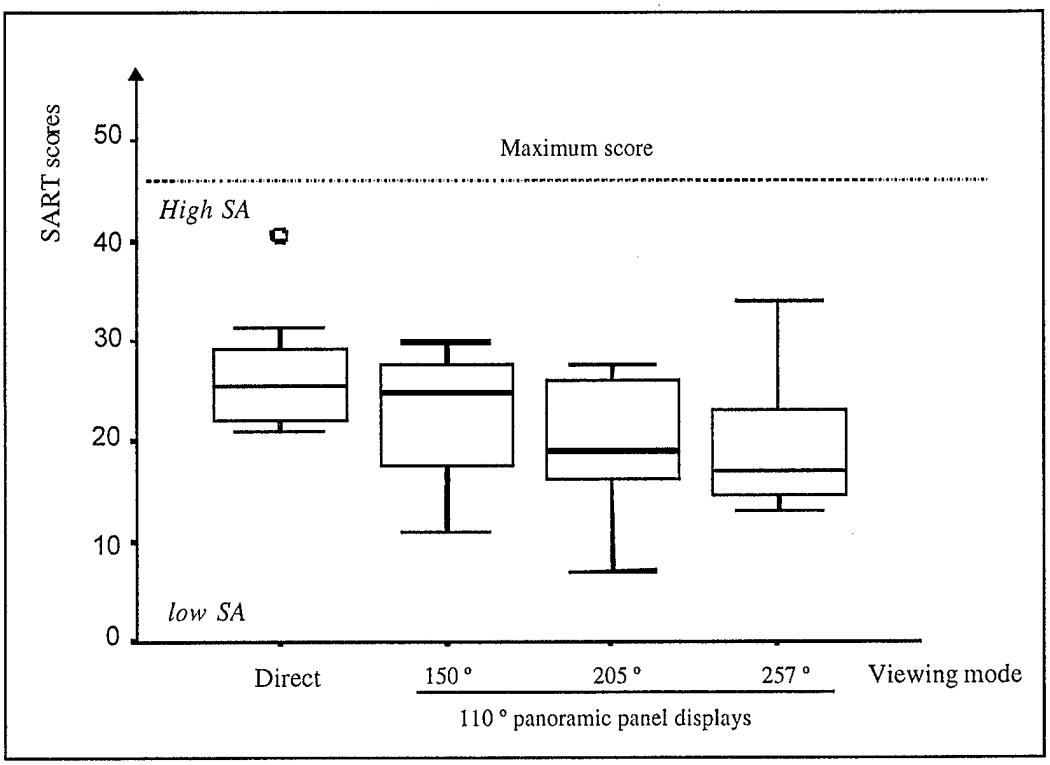

Figure 23. SART Grand Total SA Box Plots.

A bivariate correlation analysis shows no significant correlation among the sums of the scores for the SART demand, supply, and understanding. Considering the SART demand sum, a NP Friedman RM ANOVA test by ranks is significant ($p < .012$, chi-square = 10.917, df = 3, N = 8). Figure 24 shows EDA box plots of the demand sum for the viewing treatments; the plot shows the distributions to be skewed with outliers. Considering the ratings for the SART demand components, an NP Friedman test is significant for the instability demand ($p < .013$, chi-square = 10.765, df = 3, N = 8) and the complexity demand ($p < .013$, chi-square = 10.857, df = 3, N = 8) and not at all for the variability demand ($p < .190$, chi-square = 4.765, df = 3, N = 8). For reference, Figures F-1, F-2, and F-3 in Appendix F show EDA box plots of the components for the viewing treatments; the plots show the distributions to be skewed with outliers.

An NP Friedman RM ANOVA test by ranks shows that the SART supply and understanding sums differences are not significant by viewing treatments. For reference, Figure 25 shows the supply sum box plots, and Figures F-4, F-5, F-6, and F-7 show the box plots for the arousal, spare mental capacity, concentration, and division of attention supply, respectively. Similarly, Figure 26 shows the understanding sum box plots, and Figures F-8, F-9, and F-10 show box plots for the information quality, quantity, and familiarity, respectively.

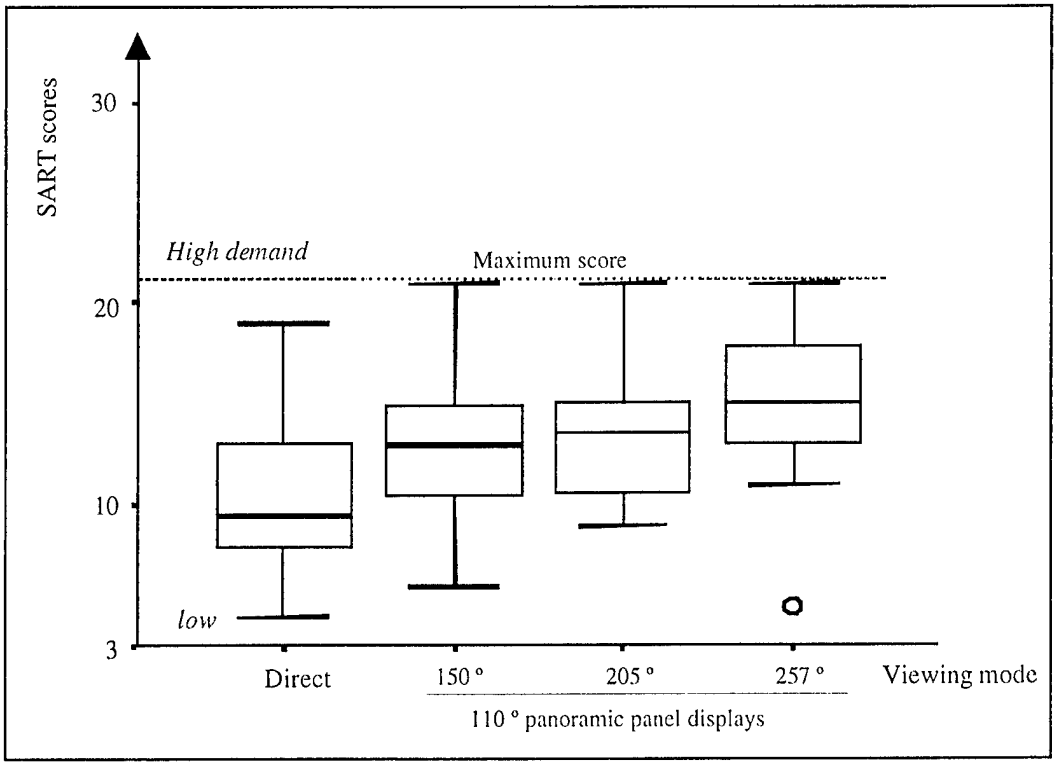

Figure 24. SART Demand Sum Box Plots.

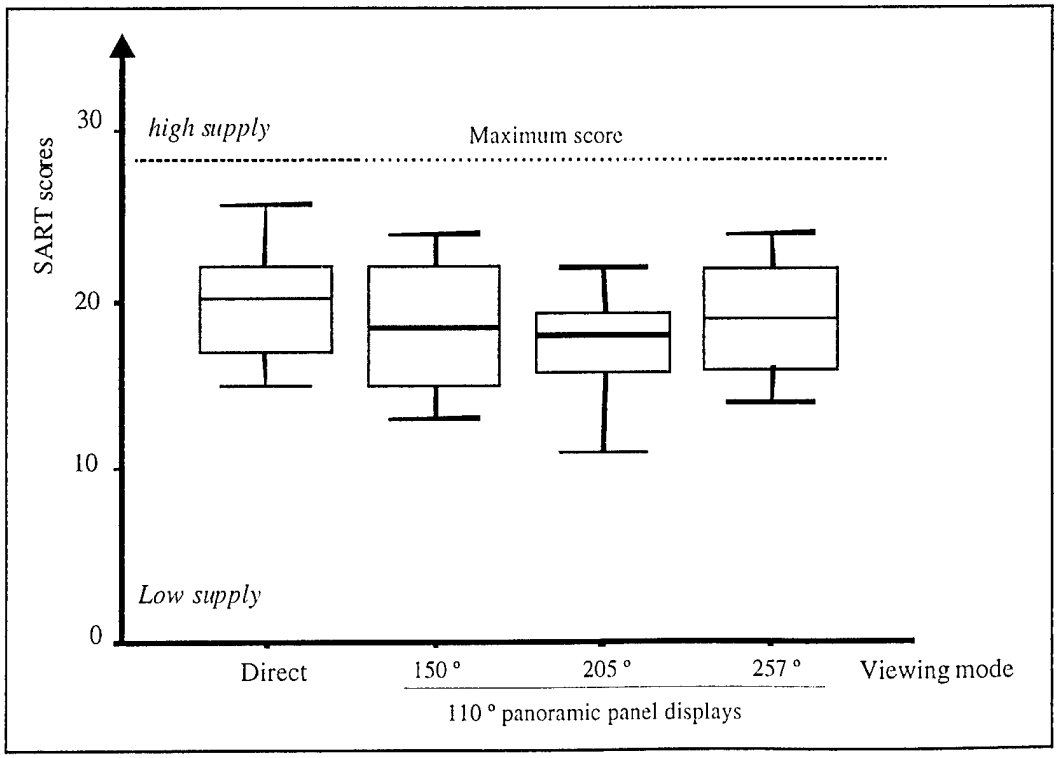

Figure 25. SART Supply Sum Box Plots.

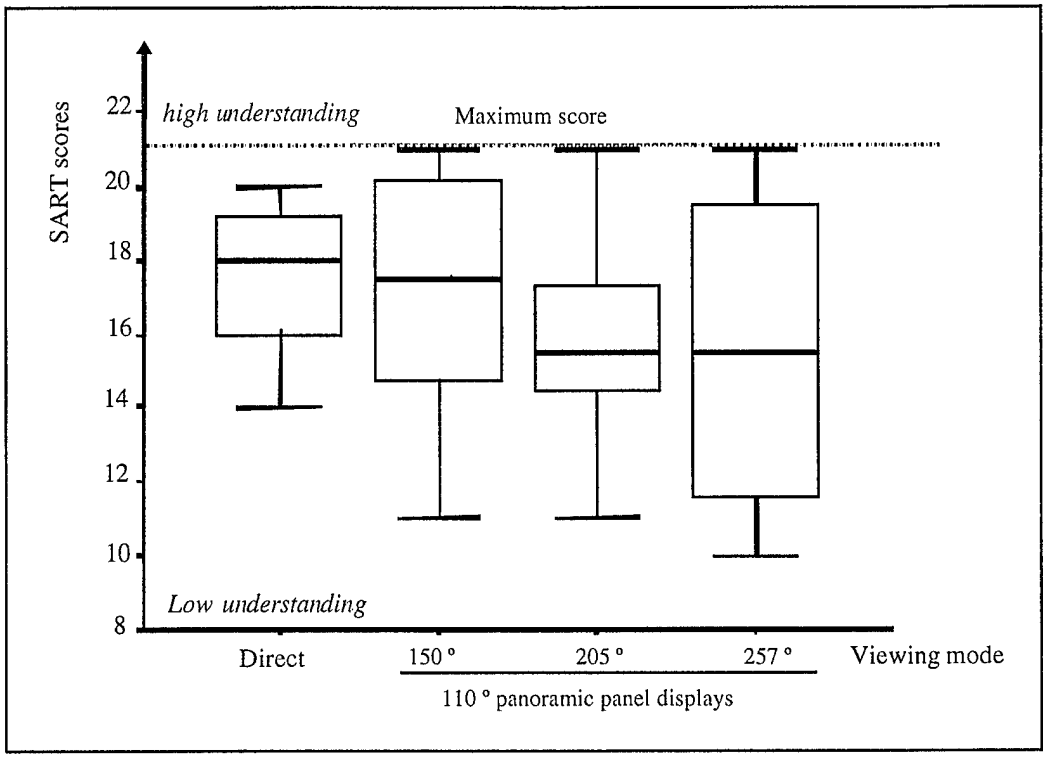

Figure 26. SART Understanding Sum Box Plots.

4.5.3 Subjective Estimation of Motion Sickness

The motion sickness scales for the direct viewing are significantly less than those for the indirect viewing FOVs as determined by an analysis of the first factorial component. Figure 27 shows a factorial component loading diagram for the 16 motion sickness scales, following reduction to three components with a factor analysis that uses principal component analysis as the extraction method (83.259% total variance explained) and Vaximax rotation with Kaiser normalization. As noted in the key on the figure, the scales are shape coded by their status as nausea, oculomotor, or disorientation symptoms (Kennedy et al., 1992); those scales used in multiple symptoms are only coded for one symptom.

Considering the distribution of the ratings on the factorial plot of Figure 27, the first factorial component reflects dizziness and loss of orientation; the second component reflects cognitive impediment because of oculomotor difficulty; the third component reflects physical impediment and increased salivation because of nausea. While not an exact mapping to the nausea, disorientation, and oculomotor symptoms determined by Kennedy et al. (1992), the interpretations are similar.

Figure 28 shows EDA box plots of the first component for the viewing treatments. The plots show the distributions to be heavily skewed with outliers.

A nonparametric RM Friedman test by ranks is significant for the component ($p < .004$, chi-square = 13.105, df = 3, N = 8).

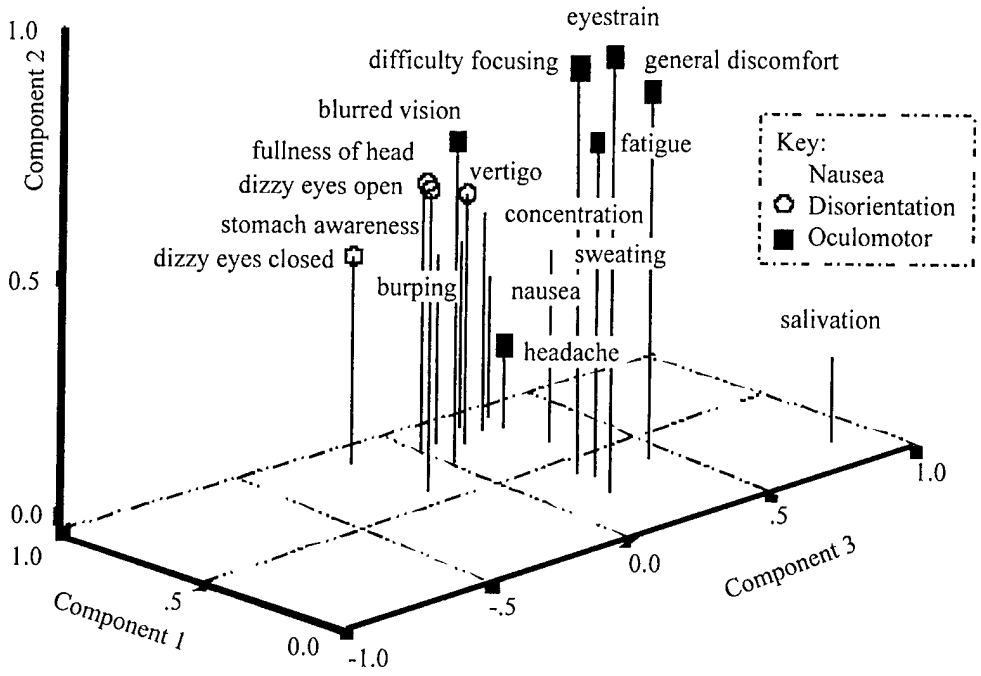

Figure 27. Motion Sickness Factorial Component Plot in Rotated Space.

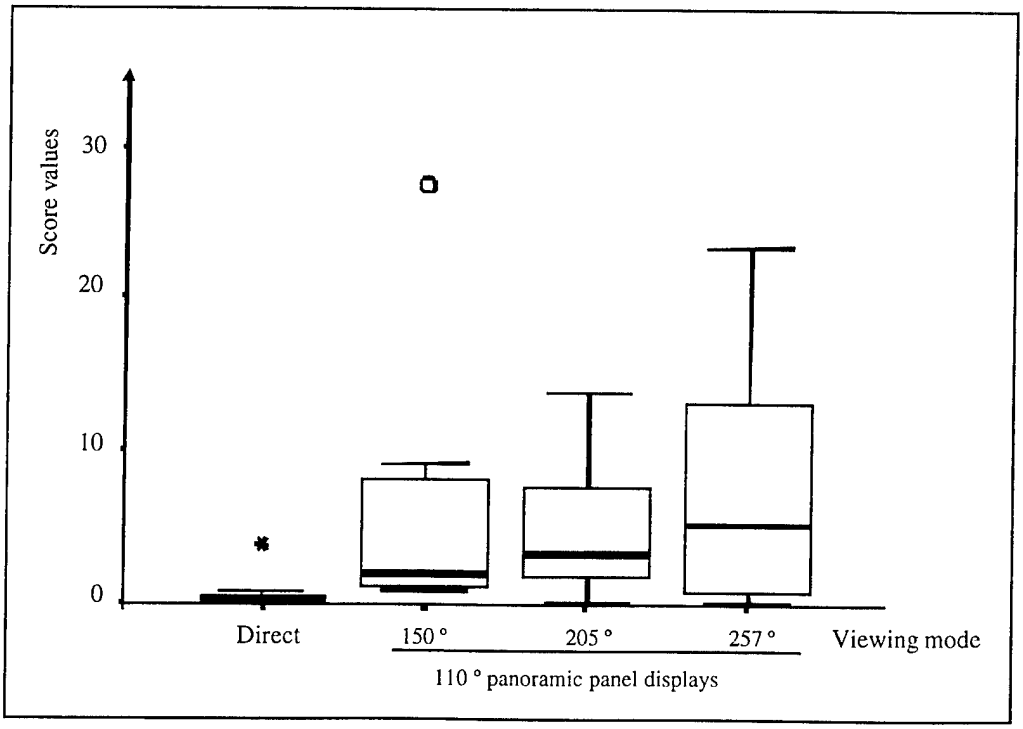

Figure 28. Motion Sickness First Factorial Component Box Plots.

The total severity motion sickness scores for the direct viewing are significantly less than those for the indirect viewing FOVs. Figure 29 shows EDA box plots of the total severity as a function of the viewing mode. The distribution for the direct viewing is largely skewed toward low values. A nonparametric Friedman ANOVA test by ranks applied to the motion sickness scores shows significant differences across treatments ($p < .005$, chi-square = 12.789, df = 3, N = 8).

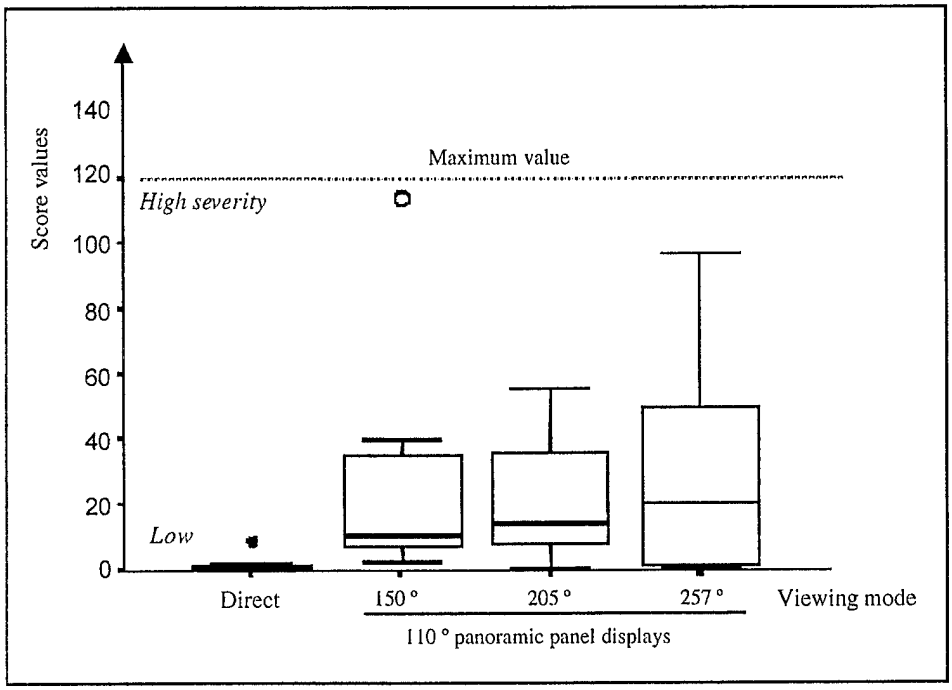

Figure 29. Motion Sickness Total Severity Box Plots.

Similar comments apply to the nausea, oculomotor, and disorientation symptoms for which box plots are plotted in Figures 30, 31, and 32. Again, the distributions for the direct viewing are largely skewed toward low values. Friedman tests show significant differences among treatments for the nausea symptoms ($p < .008$, chi-square = 12.762, df = 3, N = 8), oculomotor symptoms ($p < .015$, chi-square = 10.414, df = 3, N = 8), and the disorientation symptoms ($p < .017$, chi-square = 10.183, df = 3, N = 8).

A review of the 16 motion sickness ratings shows that the distributions are largely skewed toward the lower ratings with high value outliers; this is especially true for the direct viewing but also in many cases for the narrower FOVs. The implication is that most participants experienced slight motion sickness which increased with FOV. A nonparametric RM Friedman test by ranks applied to each of the scales in turn shows that eyestrain ($p < .011$), difficulty in focusing ($p < .013$), and sweating ($p < .012$) are major sources of significance. General discomfort ($p < .021$), difficulty in concentrating ($p < .025$), vertigo ($p < .023$), and burping ($p < .021$) contribute as well. Finally, stomach awareness ($p < .049$) and fullness of head ($p < .049$) are significant sources of motion

sickness. For reference, box plots for the ratings are shown in Appendix G in Figures G-1 through G-16.

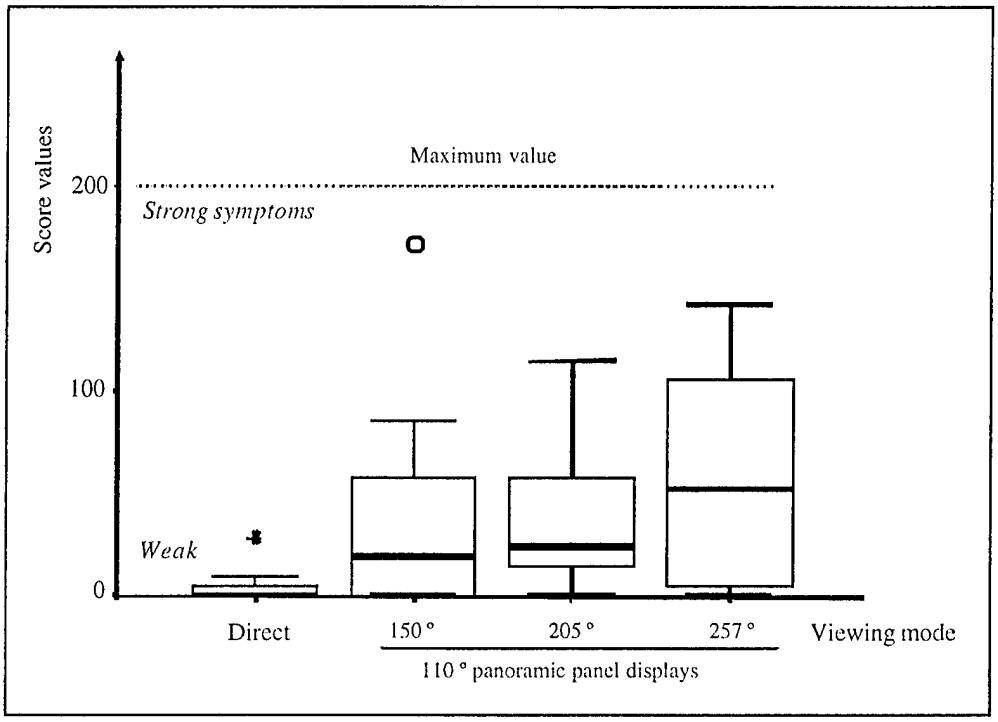

Figure 30. Motion Sickness Nausea Symptoms Box Plots.

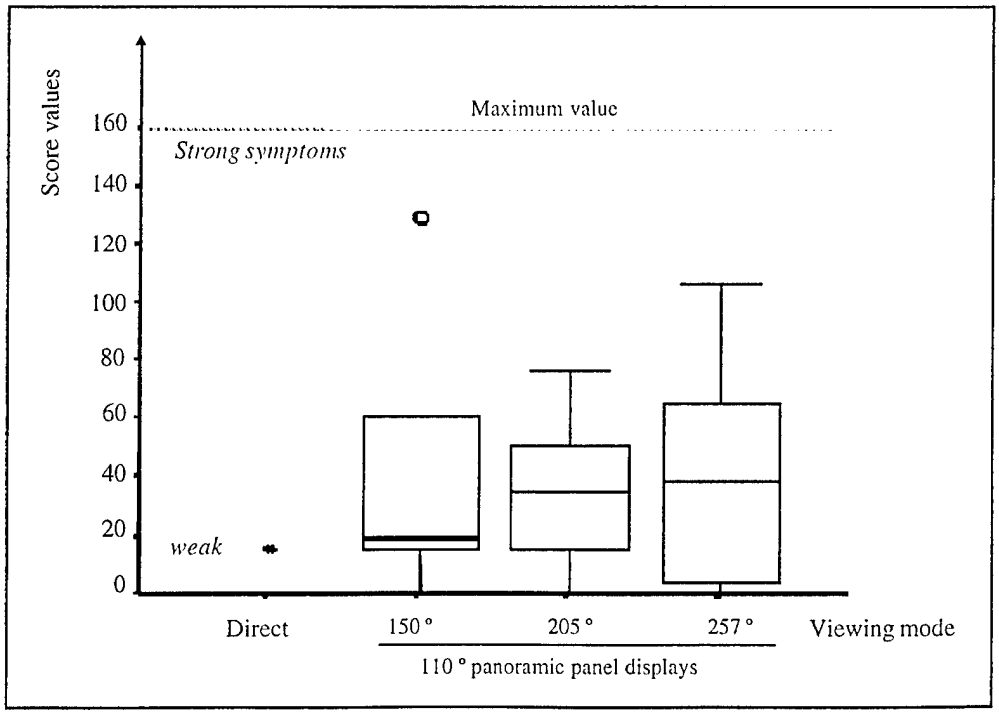

Figure 31. Motion Sickness Oculomotor Symptoms Box Plots.

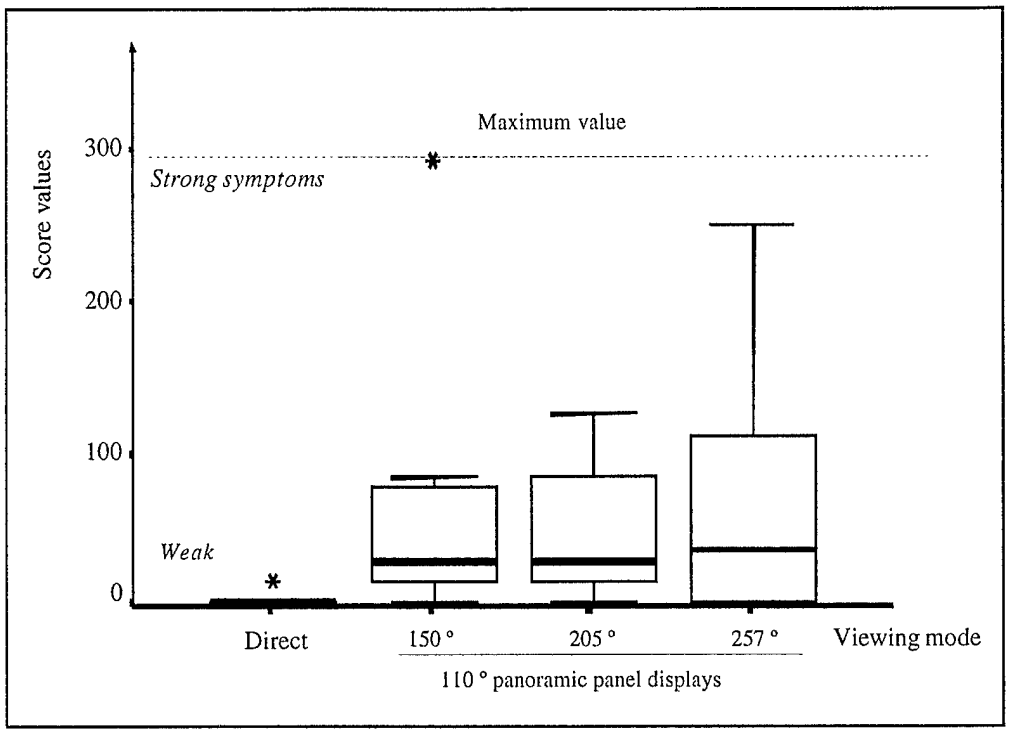

Figure 32. Motion Sickness Disorientation Symptoms Box Plots.

4.6 Subjective Stress State and Affective Aspect Components

A mistake in the preparation of questionnaire packages resulted in the omission of checklists for the subjective stress state and affective aspect components from the fourth run packages for the Participants 2 through 5. Essentially, this resulted in four missing data values for each measure. One way of analyzing these data is with a repeated measures ANOVA with adjustments for missing data (Keppel, 1982) from adjacent cells; however, the statistical power is low for small sample sizes. Instead, the approach used in this study, following a correlation analysis for significance, was to apply a multiple linear regression analysis to the affective data as a function of the course time and barrel strikes since they are dependent measures of the same treatments. A bivariate correlation analysis shows that the stress state is only slightly correlated with the anxiety ($p < .055$), depression ($p < .046$) and negative ($p < .032$) aspects and not at all with hostile ($p < .623$) and positive ($p < .448$) aspects of the affective components. For these reasons, the stress state and aspect components are studied in separate regression analyses. The data from the five aspect components were reduced to two factorial components with a factor analysis, and these components were then studied in separate regressions as a function of the course times and barrel strikes.

4.6.1 Subjective Stress Scale

The subjective stress state increases with course trial time. A bivariate correlation shows a significant correlation of the subjective stress state with the course times (two-tailed test $p < .001$, Pearson Correlation = .618, N = 28) but not the barrel

strikes. A multiple linear regression analysis via the stepwise method (enter criteria, $p \leq .05$; remove criteria, $p \geq 0.10$) shows a significant linear increase in subjective stress state with course time ($p < .001$, F = 16.031, df = 1, error df = 26) but not barrel strikes, which are excluded. Figure 33 shows a regression line and scatter plot for the subjective stress state as a function of course time.

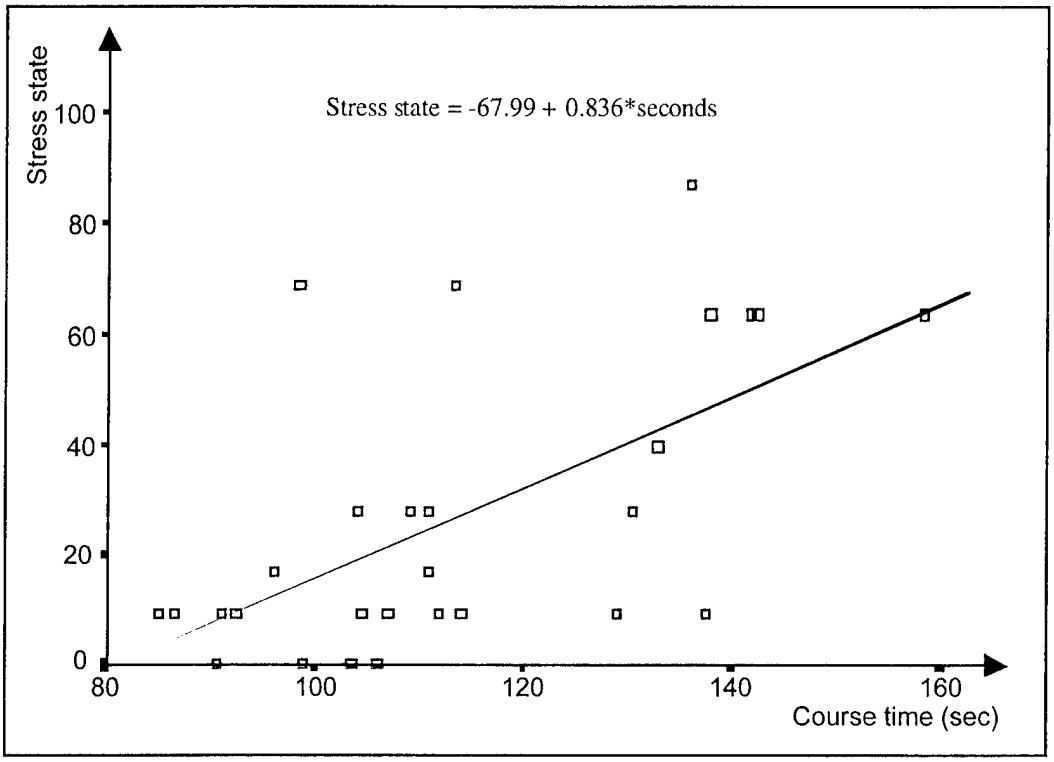

Figure 33. Subjective Stress State as a Function of Course Time.

4.6.2 Affective Aspect Components

The affective aspects have no significant relations to the course times and barrel strikes. The data from the five aspect components were reduced to two components with a factor analysis that used principal component analysis as the extraction method (74.846% total variance explained) and Vaximax rotation with Kaiser normalization. Figure 34 shows a factorial component loading diagram. A correlation analysis shows no significant relation between the factorial components, and separate regression analyses show no significant relations of the components to the course times and barrel strikes.

A study of the rotated component weight matrix shows that the positive aspect (0.135, -.825) dominates one component; anxiety (0.928, -.058) and the negative aspect (0.946, 0.320) are the major contributors to the other component; and depression (0.374, 0.683) and hostility (0.496, 0.574) are divided between both components. A bivariate correlation analysis shows that the positive aspect is not correlated with any of the other aspects, while anxiety ($p < .001$), depression

($p < .002$), and hostility ($p < .001$) are highly correlated with the negative aspect but not with each other. Furthermore, hostility and depression are correlated ($p < .025$). Considering the distribution of the aspects on the factorial plot, the first factorial component reflects uncertainty about the task, while the second component reflects confidence in one's abilities. In separate regression analyses, neither aspect component was significantly related to the course times and barrel strikes.

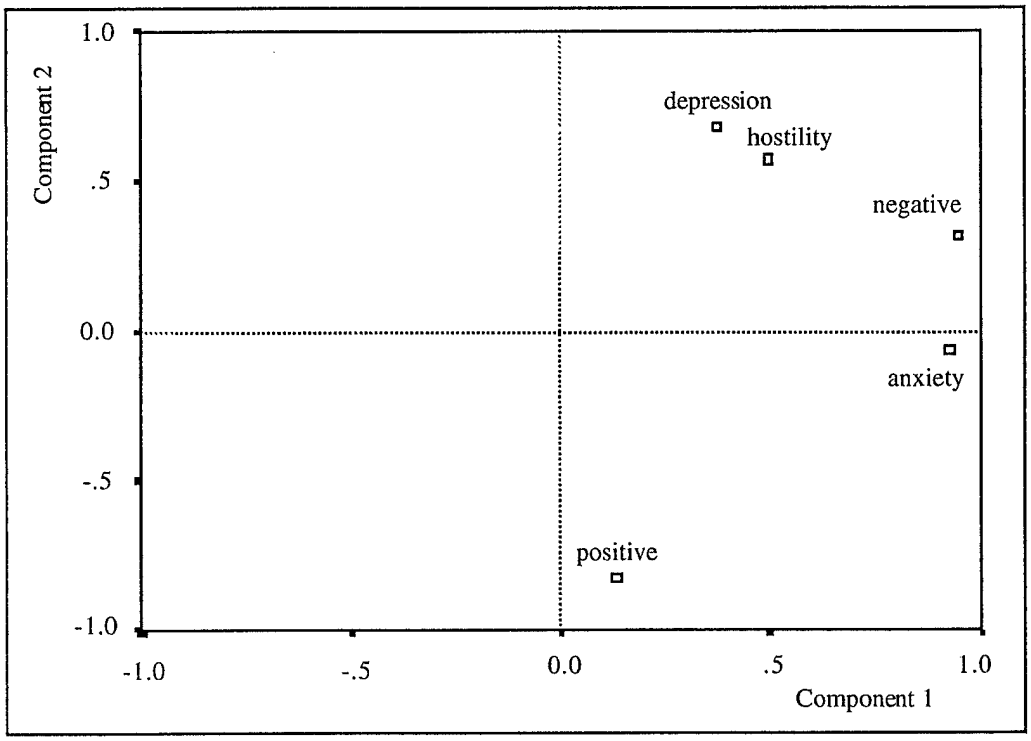

Figure 34. Affective Aspects Factorial Component Plot in Rotated Space.

4.7 Cognitive Performance Battery

The data from the five cognitive performance tests were reduced to two components with a factor analysis that used principal component analysis as the extraction method (58.426% total variance explained) and Vaximax rotation with Kaiser normalization. Figure 35 shows a factorial component loading diagram. Application of an RM ANOVA to each component shows no significant difference by treatments. See Figure 36 for a box plot of the first factorial component.

A study of the rotated component weight matrix shows that logical reasoning (0.776, 0.022) and spatial rotation (0.866, 0.014) are the major contributors to the first component. Map route selection (-0.303, 0.803) dominates the other component, while addition (0.528, 0.558) and word recall (0.130, 0.431) are divided between both components. A bivariate correlation analysis shows that

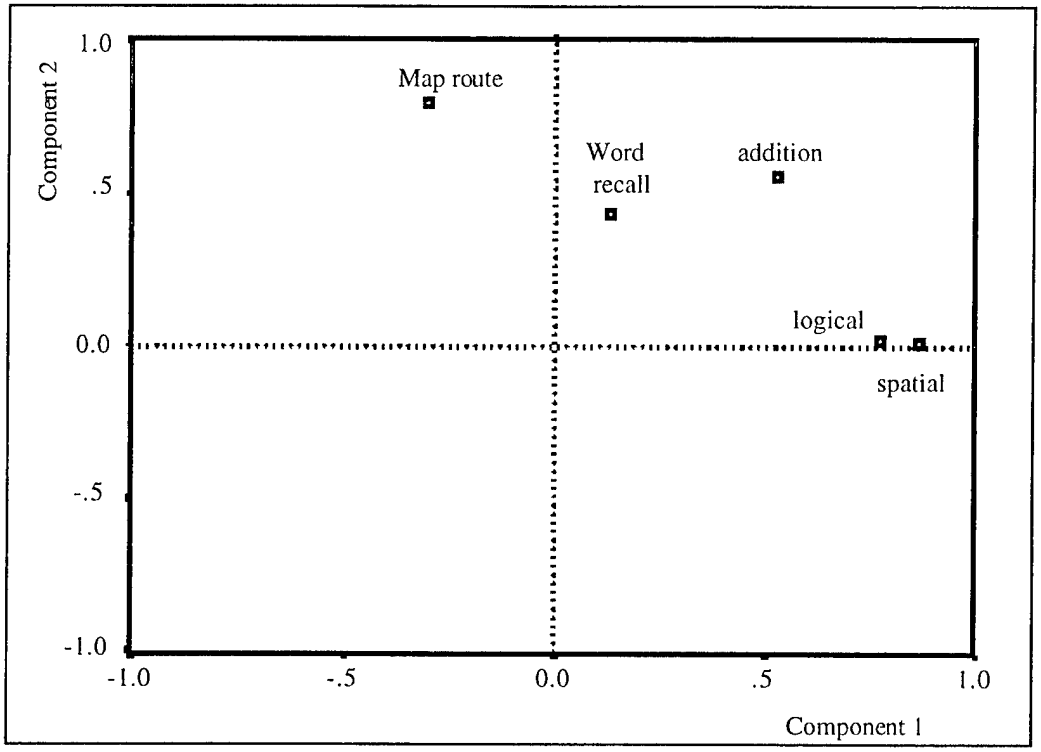

Figure 35. Cognitive Factorial Component Plot in Rotated Space.

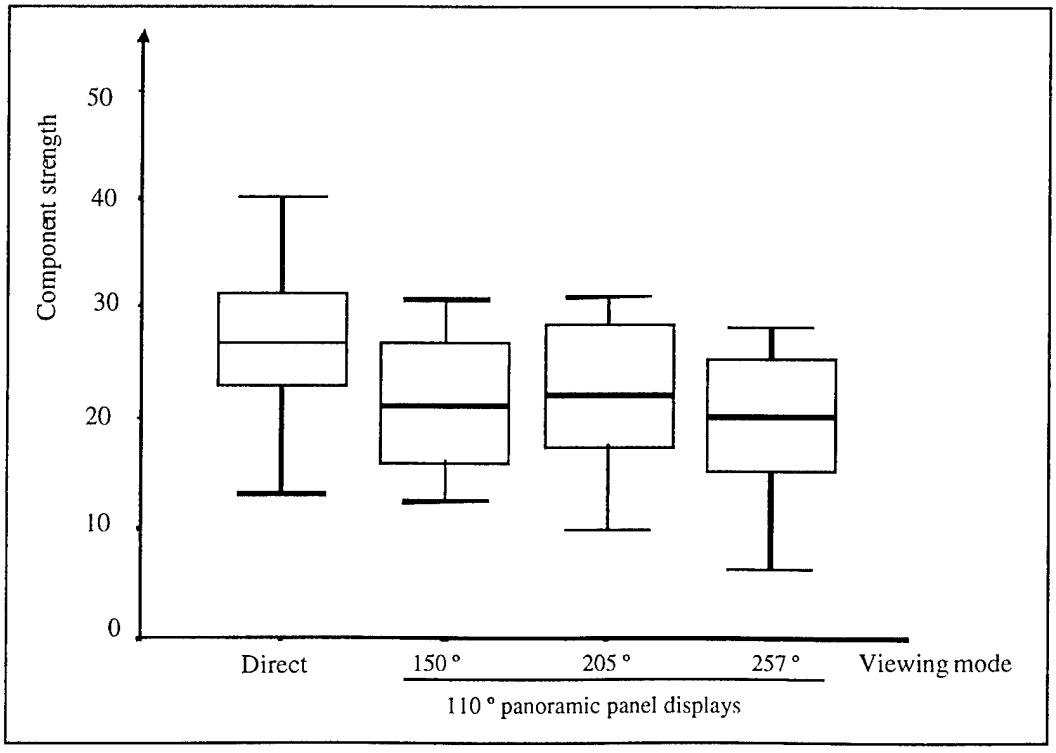

Figure 36. Cognitive First Factorial Component Box Plots.

the spatial rotation is significantly correlated with the logical reasoning ($p < .003$) and only slightly with addition ($p < .023$). Considering the distribution of the tests on the factorial plot, the first factorial component reflects intuitive reasoning, while the second component reflects deductive, serial reasoning. The box plots of Figures H-1 through H-5 in Appendix H show the distributions for the tests to be highly skewed with outliers. Separate RM Friedman tests show that all the tests (logical reasoning, arithmetic [addition] test, spatial rotation, word recall, and map route selection) are non-significant.

4.8 Exit Evaluation

The results of the exit evaluation are significantly different for the viewing treatments as determined by analysis of the first factorial component. In the exit evaluation (see Appendix C), the participants were asked to rate the viewing systems on 14 bi-polar (7-point) scales with semantic anchors, for the input from the displays, their driving task activities and cognitive loading, and their output as measured by the performance of the vehicle. The display ratings were the perceived image quality, FOV, refresh rate, and time delay; the driving activity were the eyes, head, feet, and steering movements; the cognitive ratings were the workload, motion sickness, and stress; and the performance ratings of the vehicle were the course speed, accuracy, and overall rating. The evaluation was completed by seven of the eight participants; counterbalancing is not a statistical concern since they completed the evaluations after the study.

The data from the 14 scales were reduced to two components with a factor analysis that used principal component analysis as the extraction method (51.964% total variance explained) and Vaximax rotation with Kaiser normalization. Figure 37 shows a factorial component loading diagram. As noted in the key on the figure, the scales are shape coded by their status as display input, driver activity, cognitive loading, or vehicle output. Figure 38 shows EDA box plots of the first factorial component as a function of the viewing mode. The distributions appear to be close to normal with comparable variances. Applications of an RM ANOVA show significant differences among treatments for the first component ($p < .009$, F = 5.841, df = 2.601, error df = 15.608, GGI = 0.867) but not for the second component ($p < .070$, F = 3.124, df = 2.333, error df = 13.9968, GGI = 0.778). A Tukey HSD multiple pairwise comparison test of treatment means for the first component shows significant differences between the direct and indirect viewing (unity: $p < .019$, wide: $p < .026$, extended: $p < .011$) but no differences among the indirect systems.

A study of the rotated component weight matrix shows interesting clusters of the rating scales. The display and vehicle performance ratings dominate the first component, and the operator activities and workload dominate the other component, except for steering activities, stress, and motion sickness, which are divided between both components. Considering the distribution of the ratings on the factorial plot, the first factorial component reflects the vehicle system by the

status of the display input and performance output, while the second component reflects the driver's controller activity and cognitive loading.

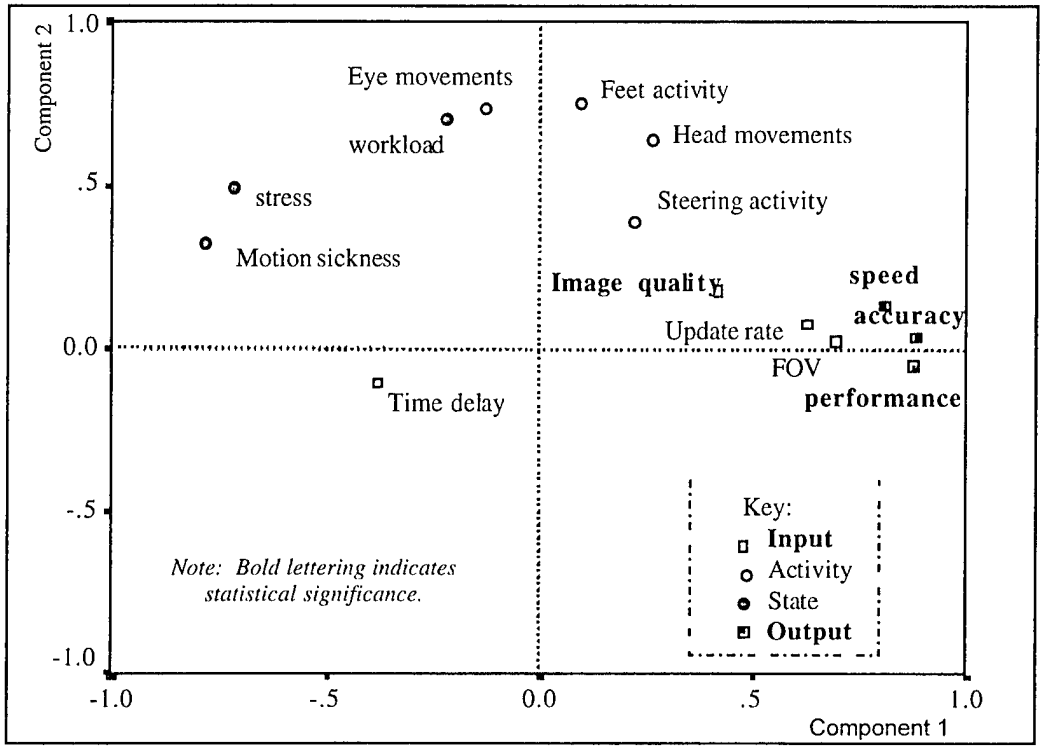

Figure 37. Evaluation Factorial Component Plot in Rotated Space.

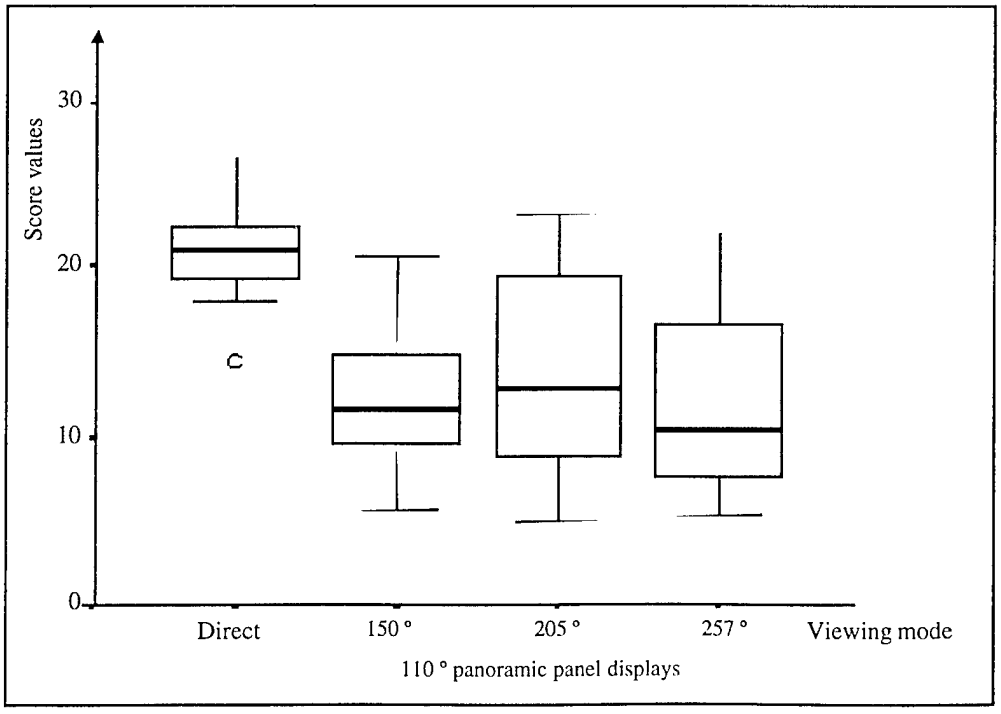

Figure 38. Evaluation First Factorial Component Box Plots.

Furthermore, the positive values of the system performance component appear to be clustered with the controller activities of the driver's state, while the information processing activities and the stress and motion sickness states are associated with the negative system values. This is particularly true for motion sickness which can be caused by increasing display time delay.

We consider statistics for rating components formed from the evaluation scores for the display input, vehicle output, driver activity, and cognitive loading. An NP RM ANOVA shows significant differences among treatments for the display input component ($p < .007$, chi-square = 12.047, df = 3, N = 7). The display input component is defined as the sum of the image quality, refresh rate, and FOV, minus the time delay. The box plots of Figure 38 show the distributions for the component to be highly skewed with outliers. Similarly, application of an RM ANOVA shows significant differences among treatments for the output ($p < .027$, F = 4.350, df = 2.472, error df = 14.835, GGI = 0.824) and the activity ($p < .052$, F = 4.91, df = 1.762, error df = 10.575, GGI = 0.587) but not the cognitive state ($p < .151$, F = 2.191, df = 2.100, error df = 12.599, GGI = 0.700). As shown by the box plots in Figures 39 through 42, the distributions for these components are more closely parametric with comparable variances. The activity component is the sum of the eye, head, steering, and motor movements. The cognitive loading component is the sum of the workload, stress, and motion sickness. The performance output component is the sum of the vehicle speed, accuracy, and overall ratings.

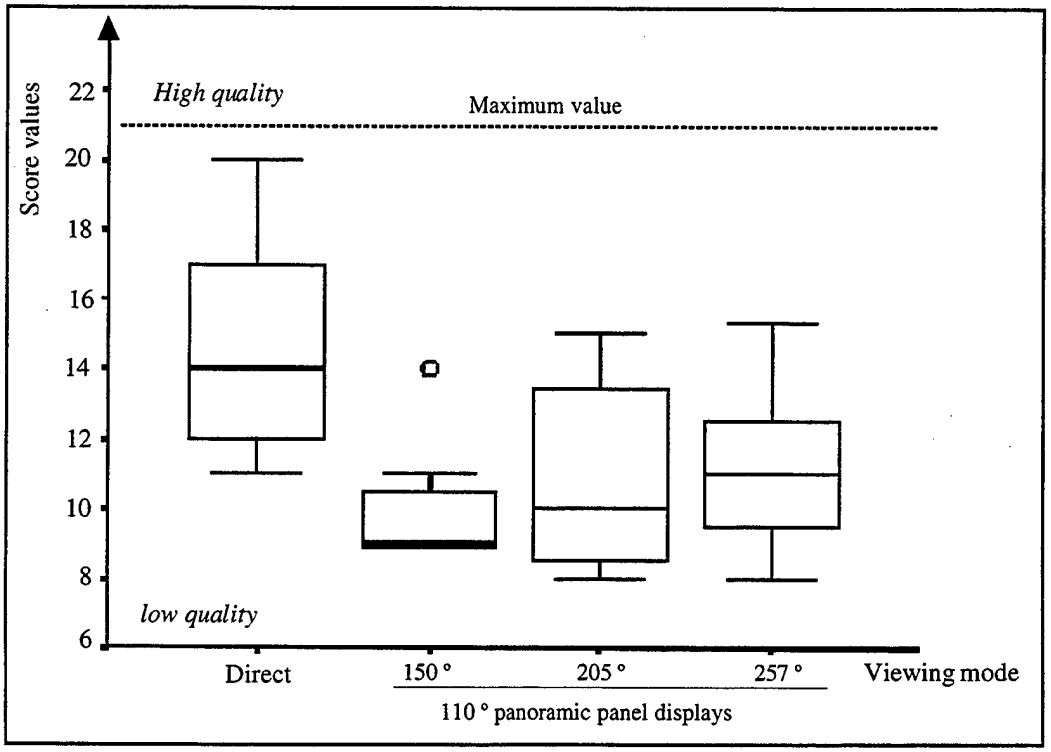

Figure 39. Display Input Rating Box Plots.

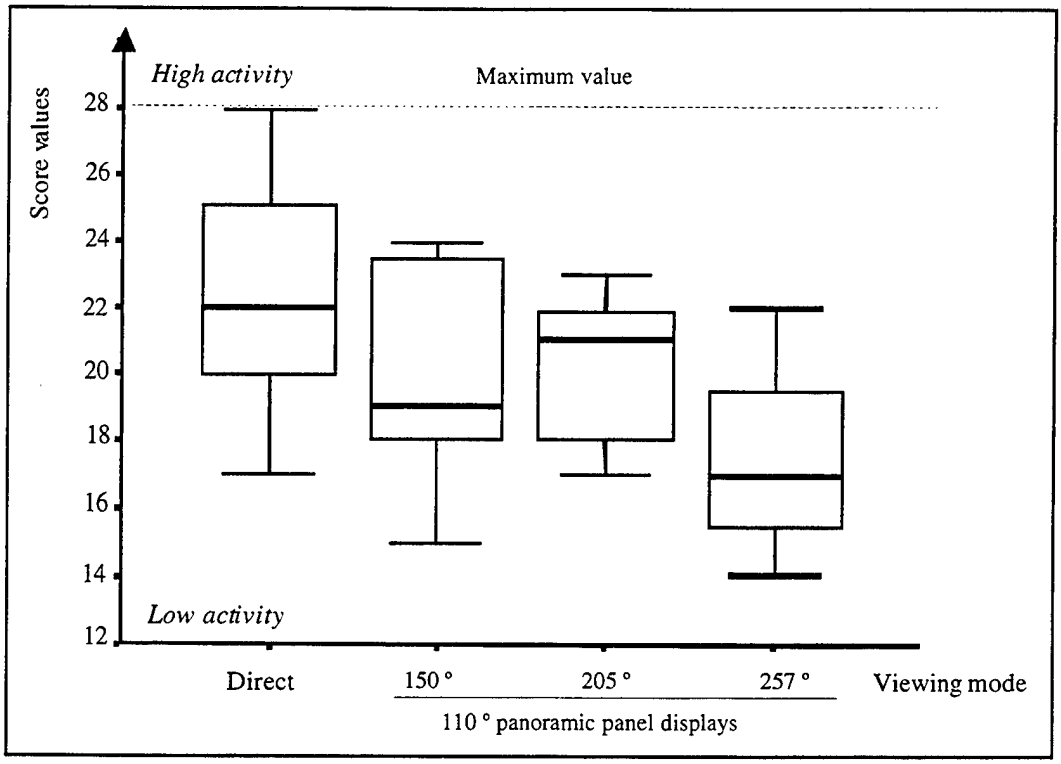

Figure 40. Control Activity Box Plots.

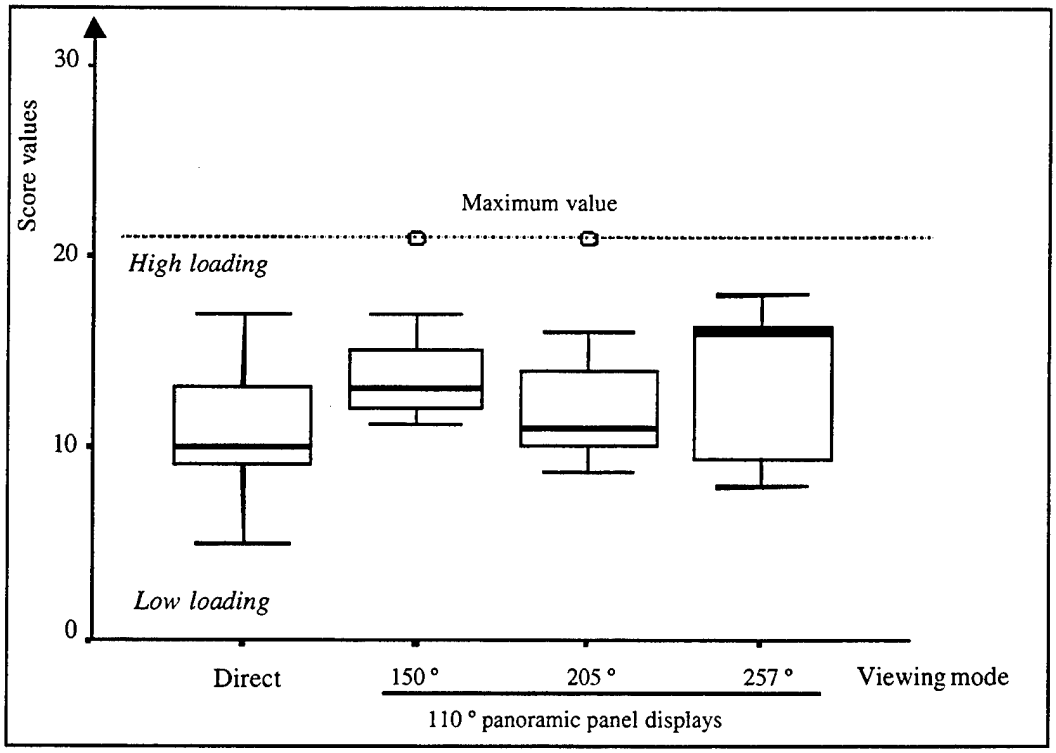

Figure 41. Cognitive Load Box Plots.

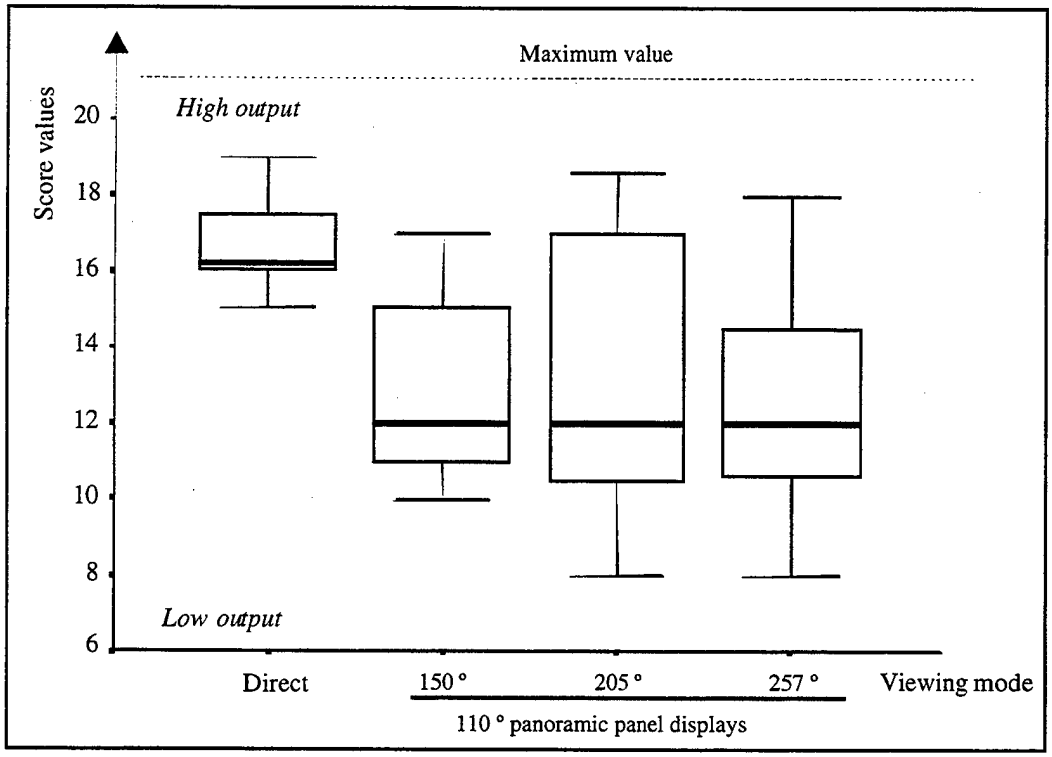

Figure 42. Performance Output Box Plots.

Considering the individual ratings, the significant correlations are listed in Table 5, along with the corresponding probability. The bivariate correlation analysis shows that the ratings for the display image quality are significantly correlated with those for the refresh rate but not those for the time delay or FOV. The eye movement ratings are correlated with those for the head movements. The workload ratings are correlated with those for the pedal activity and the stress. The steering activity ratings are not correlated with any of the other scores. The stress ratings are correlated with those for the display refresh rate and FOV, the motion sickness, and the vehicle speed, course accuracy, and overall performance. The motion sickness scores are correlated with the stress ratings and the ratings for the refresh rate, FOV, speed, accuracy, and overall performance. The vehicle speed ratings are correlated with those for the display refresh rate and the course accuracy. The course accuracy ratings are correlated with those for the display FOV. Finally, the overall performance ratings are correlated with those for the display FOV, vehicle speed, and course accuracy.

The box plots of Figures H-1 through H-14 in Appendix H show many of the distributions for the individual ratings to be highly skewed with outliers. Separate NP Friedman RM ANOVA tests by ranks applied to the input ratings show that the scores with significant differences among treatments are the image quality ($p < .008$, chi-square = 11.760, df = 3, N = 7) and the refresh rate ($p < .029$, chi-square = 9.058, df = 3, N = 7). Similarly, as part of the activity rating, head

Table 5. Pearson Correlation Matrix for Significant Evaluation Ratings (N = 28)

Note: Probability of significance (two-tailed test) in Italics.

		Display Input				*Control activity*				*Operator state*			*Vehicle output*		
		Image quality	Update rate	Time delay	Field-of-view	Eye movements	Head movements	Steering activity	Pedal activity	Workload	Stress	Motion sickness	Vehicle speed	Accuracy	Performance
Display input	Image quality		0.375* *0.049*												
	Update rate										-.472* *0.011*	-.490 ** *0.008*	0.547 ** *0.003*		
	Time delay														
	Field-of-view										-.434* *0.021*	-.399* *0.036*		0.548 ** *0.003*	0.736 ** *0.000*
Control activity	Eye movements						0.704 ** *0.000*								
	Head movements														
	Steering activity														
	Pedal activity									0.504 ** *0.006*					
Operator state	Workload										0.579 ** *0.001*				
	Stress											0.791 ** *0.000*	-.466 ** *0.012*	-. 591 ** *0.001*	-.555 ** *0.002*
	Motion sickness												-.598 ** *0.001*	-.597 ** *0.001*	-.601 ** *0.001*
Vehicle output	Vehicle speed													0.723 ** *0.000*	0.627 ** *0.000*
	Accuracy														0.889 ** *0.000*
	Performance														

Correlation significance (two-tailed): * at the 0.05 level, ** at the 0.01` level

movement is significant ($p < .004$, chi-square = 11.145, df = 3, N = 7). For the cognitive state, workload ($p < .046$, chi-square = 8.023, df = 3, N = 7) and motion sickness ($p < .038$, chi-square = 8.423, df = 3, N = 7) are significant, as is the course speed ($p < .011$, chi-square = 11.071, df = 3, N = 7).

4.9 Family-wise Significance

The statistically significant analyses are ranked ordered by the (two-sided) probabilities of significance in Table 6 along with the corresponding overall alpha level computed by the Holm procedure. The table shows that family-wise significant differences result among the treatments for the analyses of the overall performance, heart rate, TLX workload, SART SA, motion sickness, stress state, and the exit evaluation. The analyses for the head movements, attention allocations, affective aspects, and cognitive processing are not significant at the 0.05 family-wise level.

Table 6. Statistically Significant Rankings of the Family of Statistical Tests

Rank	Measure	Test	Probability	Holm alpha-level
1.0	Heart rate	Regression analysis	.001	.0045
2.0	Affective stress state	Regression analysis	.001	.0050
3.0	Overall performance	MANOVA	.002	.0056
4.0	TLX workload factorial components	MANOVA	.005	.0062
5.0	Motion sickness factorial component	NP RM ANOVA	.005	.0071
6.0	SART SA factorial component	NP RM ANOVA	.008	.0083
7.0	Exit Evaluation factorial component	RM ANOVA	.009	.0100

For each of the significant multivariate analyses, we can further consider a separate analysis of the component measures using the Holm procedure to control the (sub) family-wise 0.05 alpha level. For the overall performance, the analyses for the course times and barrel strikes are family-wise significant. For the TLX workload, the analyses of the grand sum and the demand sum are significant but not the analysis for the interactive sum. Furthermore, the analyses of the temporal and mental demands are significant but not the analysis of the physical demand. Similarly, for the SART SA, while the analysis for the SA demand is significant, analyses for the SA measure, SA supply, and SA understanding are not. Continuing, the instability and complexity ratings of SA Demand are significant, while the variability is not. While the total severity and nausea, oculomotor, and disorientation components of the motion sickness are family-wise significant, the ratings for each of the components are not. Finally,

the display input of the exit evaluation is significant because of the image quality, but the remaining components are not.

The mean treatment measures for the direct viewing are significantly different from those for the each of the indirect viewing treatments as determined by the application of a *post hoc* pair-wise comparison test. This is true for the course time and the first factorial component of the TLX workload, motion sickness, SART SA, and the exit evaluation. Furthermore, while the mean direct viewing course time is significantly different from the course times for the different indirect treatments, the mean time for the indirect near-unity treatment is different from that for the extended viewing treatment. Finally, the regression coefficient of the course time is significantly different from zero for the heart rate and affective stress state analyses.

4.10 Usability Evaluation

In exit interviews, all participants rated the near-unity camera's lens as more useful for steering; however, the cameras with the wider FOVs were rated as more useful for navigation since they allow the driver to see farther for path selection.

---

5. Discussion

Discussed are the driving task load as determined by the driving performance, the physical and metabolic exertion used to perform the task, the cognitive state of the driver, and the resultant mental workload. A predictive model is described for the course speed as a function of the display compression ratio. The results from an earlier driving study with an HMD are used to check the validity of the model. Heart rate is derived as a function of the compression ratio from the relation to the course speed, and the metabolic workload is predicted from the heart rate and course times. The changes in cognitive state and mental workload with vision system are discussed.

5.1 Driving Performance and Task Load

Course speed and error rate are discussed, and predictive models are developed for these variables as a function of the display compression ratio. The perceived speed of travel is discussed. The performance ratings from the exit evaluation are summarized.

5.1.1 Performance Ratings

Driving performance was rated higher for the direct vision than with the indirect vision systems. Compared to the ratings for the direct vision, the exit evaluation

shows a trend of reduced performance ratings for the indirect vision. This is true for the course speed, lane-following accuracy, and overall performance. These trends can be seen in Figures H-12 through H-14.

5.1.2 Course Speed

Average driving speed is greatest for the direct viewing and decreases with increasing camera FOV. This follows since the eight participants drove the 590-meter course with direct viewing at an average speed of 14.19 miles per hour (22.84 km/hr). In contrast, they drove with indirect viewing at 11.76 mph (18.92 km/hr) for the near-unity camera FOV, 11.28 mph (18.15 km/hr) for the wide FOV, and 10.13 mph (17.08 km/hr) for the extended FOV. That is, the near-unity FOV average speed was 82.84% of that for the direct viewing, the wide FOV speed was 79.49%, and the extended FOV speed was 74.77%.

Considering the driving task as self paced, with the driver adjusting his speed to acquire the scene-related information needed for control decisions, an equation has been derived (Smyth, 2000) relating vehicle speed to the display compression ratio (DCR). The equation is in the form of the product of the course speed times the compression ratio raised to a 1/3 power, with the product equal to a constant. Since the course times show statistically significant differences among treatments, the parameters of the equation are computed from these data with a regression analysis (adjusted R square = 0.328, $p < .0004$, F = 16.136, df = 1, error df = 30), resulting in

$$\text{speed (km/hr)} = 22.31 * \text{DCR}^{-0.332}.$$

The equation predicts that the average driving speed is greater for the direct vision and decreases with increasing camera FOV.

See Figure 43 for a plot of the speed as a function of the display compression ratio. The figure shows a scatter plot for the experimental data, the mean data values, and the estimated speed regression line with 90% confidence intervals (CI) for the sample means. The point labeled "HMD study" was not part of the analysis and refers to a separate experiment discussed next. The figure also shows the perceived speed that is predicted for the driver.

Considering the simplicity of the analysis, the close match between the predicted and average values is appealing; the mean data values are within the 90% CI for all treatments except the near-unity FOV. The predicted speed of 22.31 km/hr for direct vision is within 2.32% of the mean value. For the indirect vision, the predicted 18.16 km/hr is within 0.06% of that for the wide FOV, and 17.11 km/hr is within 0.18% of that for the extended FOV. While the predicted value of 20.13 km/hr for the near-unity FOV is within 6.39% of the mean value, the mean value is just outside the 90% CI. However, while the driver could see the vehicle hood with the other treatments, this was not true with the near-unity FOV since

the hood was just below the camera's narrower view. Without the hood as a guide, the drivers presumably had to be more careful in their control of the vehicle's approach to the markers, and this may account for the slower than predicted speed.

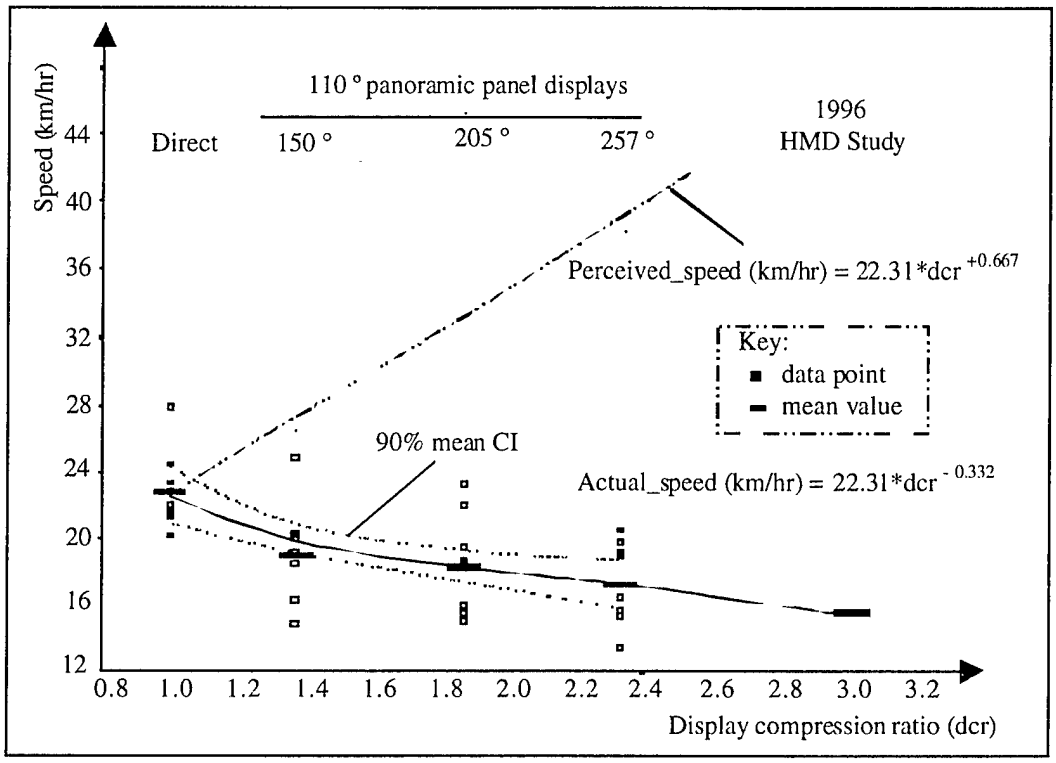

Figure 43. Course Speed as a Function of Display Compression Ratio.

5.1.3 Perceived Speed

For the indirect vision, the speed of travel is perceived to be greater than that for direct viewing and increases with compression ratio because of scene elongation. See Smyth (2000) for a derivation of the perceived speed as a function of the compression ratio. This effect is shown in Figure 43, in which although the predicted speed for indirect view driving is less than that for direct viewing and decreases with display compression ratio, the perceived speed is predicted to increase. Thus, although the drivers with indirect vision travel at a slower speed to maintain control with increased display compression, they perceive themselves to be traveling at a faster speed in direct proportion to the compression ratio. For this reason, they believe themselves to be traveling faster than they are and may decelerate, possibly resulting in a decrement in tactical performance.

5.1.4 Marker Strike Errors

On the average, fewer marker strikes were made with direct vision than with the indirect vision systems. However, the differences are slight, which suggests that the participants maintained a consistent driving strategy across viewing treatments. For example, the participants struck an average 3.19% of the markers with the direct vision driving. In contrast, they struck 5.534% with the near-unity FOV, 7.226% with the wide FOV, and 8.268% with the extended FOV of the indirect vision system. That is, the near-unity FOV error rate is 1.73 times that of the direct viewing, the wide FOV rate is 2.26 times, and the extended FOV rate is 2.59 times.

While, as reported in the statistical section, the marker strikes are significantly different by treatments, the treatment means are not significantly different among themselves. However, the strike error rates are significantly related to the display compression ratio according to a linear regression analysis (adjusted R-squared = 0.205, $p < .005$, F = 8.981, df = 1, error df = 30). The resulting linear predictor for the error rate as a function of the compression ratio is

$$\text{error rate}(\%) = -.068 + 3.728*\text{DCR}.$$

See Figure 44 for a plot of the error rate as a function of the display compression ratio. The figure shows a scatter plot for the error rate data, the mean error rate values, and the linear regression line for the estimated error rate with 90% confidence intervals for the mean error rate values. Again, the point labeled "HMD study" was not part of the analysis and refers to a separate experiment discussed next.

The figure shows that the mean data values are within the 90% CI for all treatments. While the actual rate is 14.70% less than the predicted rate of 3.81% for the direct vision, the predicted rates for the indirect vision are reasonably close to the actual values. For example, the predicted rate of 4.97% for the near-unity FOV is within 8.94% of the actual value, the predicted 6.59% rate for the wide FOV is within 4.47%, and the predicted 8.10% rate for the extended FOV is within 4.23% of the actual value. However, the differences in error are practically insignificant, and the implication is that the participants exercised a driving strategy that operationally performed at the same level of accuracy with both the direct and indirect vision systems.

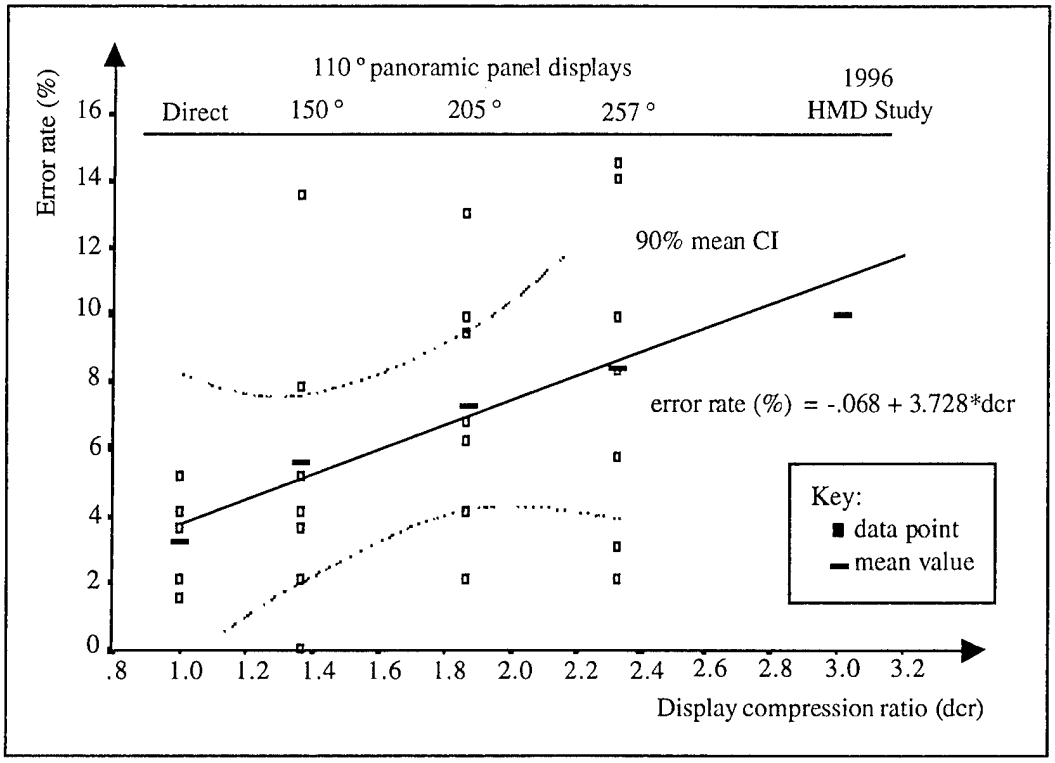

Figure 44. Marker Strike Error as a Function of Display Compression Ratio.

5.1.5 Comparison to an HMD Driving Study

The course speeds and error rates closely agree with those for an earlier study in which participants drove a course with indirect vision using an HMD with head-slaved camera video returns (Smyth & Whitaker, 1998). In that study, which was conducted on the same site but with a different model HMMWV, training regimen, and course layout, the participants drove at an average speed of 14.26 mph (22.95 km/hr) with direct viewing and 9.58 mph (15.41 km/hr) with the HMD. To reduce the need for head movement with the HMD, the participants were taught a similar driving strategy of first aligning the vehicle with a barrel pair during the approach and then accelerating through. With the narrow FOV of the HMD, the participant could just see both sides of the front hood at the same time by looking directly forward but could not see both barrels of a marker pair as he passed them. A participant turning his head to navigate around a barrel as he entered a turn would tend to lose track of the other one in the pair of markers.

At a 30-degree FOV, the HMD compresses the 56-degree FOV of the vehicle-mounted cameras used in the earlier study by a factor of 1.866; furthermore, the HMD with 180,000 rasters has 58.59% of the video resolution of the fixed panel displays (640 x 480 rasters) used in this study. For these reasons, the HMD has a 3.184 effective display compression ratio, which converts to a predicted course speed of 9.428 mph (15.17 km/hr) with the course speed equation (see

Section 5.1.2). As shown in Figure 43, this predicted value is within 1.56% of that measured in the HMD study. Furthermore, the direct vision average speeds are practically identical for the two studies (within 0.46%).

Similar comments apply to the error rates for the two experiments. While the direct vision error rate of 6.818% for the HMD study is 2.137 times that for the flat panel study (because of an HMD outlier value), the indirect vision rate of 10.511% is about the same as the 11.80% value (within 12.27%) predicted for the HMD (see Figure 44). This prediction is based on the regression equation for the flat panel indirect vision error rate (see Section 5.1.4) and the effective display compression ratio of 3.184 for the HMD. The implication is that participants will tend to drive with the same speed and error rate, using either an HMD or flat panel displays of the same video quality. Furthermore, the display compression ratio adjusted for video resolution may be a useful predictor of average driving performance, at least for the driving experimental paradigm used in these studies.

5.2 Operator's Machine Interface Loading

The driving performance model derived previously for the vision systems via the concepts of self-paced behavior by the driver and scene compression, is limited to short-term driving on the order of several minutes. However, the effects of machine interface loading on the driving performance must be considered. This is important because over time, excessive physical and mental loading can lead to driver fatigue, lower speed, and increased errors. Interface loading means the perceived loading for the displays and controls and the metabolic loading incurred while the vehicle is being operated. As an introduction to this topic, the quality ratings of the visual displays are first discussed.

5.2.1 Visual Display Quality Ratings

The visual display ratings from the exit evaluation show a trend of higher quality for driving with direct vision and reduced quality for the indirect vision. This is true for the display image quality, refresh rate, and FOV (see Figures H-1 through H-3). As shown in Figure H-4, no differences are noted for any apparent time delay.

5.2.2 Control Activity Loading

The control activity is composed of eye and head movements for acquiring information and feet and hand manual actions for controlling the vehicle. The control activity is discussed, along with these component measures as determined from the ratings from the exit evaluation. The heart rate is discussed and the metabolic workload is estimated from the heart rate.

5.2.2.1 Control Activity Ratings

The total control rating, determined by the summation of the evaluation ratings for the component measures, shows a trend of increased activity for driving with direct vision and the indirect wide FOV cameras and reduced activity with the near-unity and extended FOV cameras (see Figure 40).

5.2.2.2 Eye Movements

As with the control ratings, the eye movement ratings from the exit evaluation show a trend of increased activity for driving with direct vision and the indirect wide FOV cameras and reduced activity with the near-unity and extended FOV cameras (see Figure H-5).

5.2.2.3 Head Movements

While the measured head movements are not significantly different, the head movement ratings from the exit evaluation show a marked trend with far more movements with direct vision than with the indirect systems that have the same ratings. This is reasonable since the natural vision is of an open scene without restricted FOV, while the indirect viewing is restricted to the panel displays (see Figure H-6).

5.2.2.4 Hand and Feet Steering Activities

The hand steering and feet activity ratings from the exit evaluation are the same for all treatments. This is reasonable since the same course was driven in all cases (see Figures H-7 and H-8).

5.2.3 Metabolic Loading

Metabolic workload is estimated from heart rate, which is a function of the equivalent compression ratio through the course speed.

5.2.3.1 Heart Rate

Heart rate increased significantly with course speed because of the increased manual effort needed for driving. At the higher speeds, the driving task requires intense concentration to coordinate forceful arm and feet movements that are needed to rotate the steering wheel and move the accelerator and brake pedals for driving. As noted before in the statistical result section, heart rate is significantly related to course speed. The equation for the relation between speed and compression ratio (DCR) may be inverted to produce an equivalent DCR database for analysis (see Section 5.1.2). A linear regression analysis shows that the maximum heart rate is significantly related to the equivalent DCR (adjusted R-squared = 0.521, $p < .001$, F = 28.222, df = 1, error df = 29), following refinement of the analysis with the removal of one extreme outlier from the data. The result is a predictor for the maximum heart rate as a function of the compression ratio:

max HR (beats/min) = 129.627 - 13.353*DCR.

The relation predicts that the maximum heart rate is highest for the direct viewing and decreases with increased camera FOV for the indirect viewing.

Table 7 lists the predicted heart rate for the viewing treatments. In metabolic processes, heart rate may be used to predict oxygen consumption for dynamic tasks, and the corresponding average energy expenditure rate (in kilojoules per minute) is listed in the table (Kroemer, Kroemer, & Kroemer-Elbert, 1997). The relation of heart rate to expenditure rate is closely linear over the range listed. Listed also is the 1960 Borg subjective scale (modified 1985) rating of perceived exertion (RPE) predicted from the heart rate and the associated verbal anchors for the ratings (Kroemer et al., 1997). The implication is that the amount of physical exertion devoted to driving is "somewhat hard" for direct vision and for the indirect viewing decreases with camera FOV from "light" for the near-unity FOV to "very light" for the wide and extended FOV.

Table 7. Predicted Heart Rate, Subjective Assessment of Exertion, and Energy Expenditure

Viewing condition	DCR	Heart rate (beats/min)	Exertion Borg scale RPE	anchor	Energy expenditure rate (kJ/min)	total (kJ)
Direct	1.00	116.27	12	"somewhat hard"	28.135	140.48
150° FOV	1.36	111.47	11	"light"	25.735	146.74
205° FOV	1.86	104.79	10	"very light"	22.395	155.20
257° FOV	2.33	98.51	10	"very light"	19.255	162.99

5.2.3.2 Metabolic Workload

While physical exertion decreases slightly with compression ratio, the amount of work used to drive the course increases because of the much longer times. The predicted total energy expended (in kilo-joules) in driving the fixed course is listed in Table 7 for each treatment. As computed from the energy expenditure rate and the course time, the total energy expended is significantly related to the equivalent DCR (adjusted R-squared = 0.733, $p < .001$, F = 72.258, df = 1, error df = 25) through the course speed by regression analysis. The linear relation predicts that the total energy expended is least for the direct viewing and increases with increased camera FOV for the indirect viewing. The driving course was the same for each treatment and for this reason required the same physical work to maneuver the vehicle. The increase in energy expended may include a cognitive stress component as well as a physical one. The increase in control response sensitivity with display compression requires finer control

adjustments and increases the time and attention needed to physically maneuver the vehicle.

5.3 Operator's State and Mental Workload

The effects of cognitive loading on the driving performance must be considered. This is important because over time, excessive cognitive loading can lead to driver fatigue, lower speed, and increased errors. Furthermore, increased cognitive workload can result in a loss of SA for other problems, which can impact future decision making. Discussed are the operator state as determined by the attention allocation, the perceived task workload, SA, motion sickness, emotional stress, and cognitive abilities. The cognitive load ratings from the exit evaluation are summarized.

5.3.1 Cognitive Load Ratings

The cognitive load ratings from the exit evaluation show a trend of decreased ratings for driving with direct vision and the indirect wide FOV cameras and increased ratings with the near-unity and extended FOV cameras. This is true for stress and motion sickness, which are less for the direct and wide camera FOV (see Figures 41, H-10, and H-11).

5.3.2 Attention Allocation

The allocation of attention to the visual, auditory, cognitive, and psychomotor processing channels statistically remains the same across the viewing treatments. Table 8 lists the mean allocation loadings for the channels and the corresponding activities according to the McCracken and Aldrich's descriptors. The loadings are reasonable for the driving task since the participants tracked the barrel markers to follow the course and maintained the orientation of the vehicle relative to the barrel pairs for rapid passage. Thus, the attention loading on the visual channel is needed for tracking the barrels, following the approach path, and orienting the vehicle for passage. While driving, the participant needs to recall the mental model of the course for localizing during navigation. Thus, cognitive loading is needed for the participant to recall the mental map, encode the map for the scene, and then revise the map by encoding the location. The manual motor manipulation of the steering and driving controls is executed between consecutive stages of discrete adjustments made in response to the locations of the barrel markers. Finally, auditory loading occurs since the on-board experimenter verbally instructs the participant when to start driving the course and confirms when the end has been reached. Thus, auditory loading is needed for the participant to interpret semantic content of speech.

While the statistical consistency of the loadings implies that the nature of the driving task remains the same across treatments, there are trends of interest. As shown by the box plots of Figures D-1 through D-4 for the visual, cognitive, auditory, and psychomotor channels, these trends suggest that slightly more

intense attention was needed on all processing channels with the indirect vision systems than with the direct vision. For example, while the mean visual loading of attention for the direct vision driving is between those for "locating" and "tracking," the mean loading for the indirect vision systems is between those for "tracking" and "reading"—a more demanding task. Similarly, the mean cognitive loading for direct vision is between attention for "recall" and "judgment," while that for the indirect vision is between those for "recall" and "evaluation". Furthermore, the psychomotor loading for direct vision attention is for "manipulation," while that for indirect vision is for "discrete adjustments".

Table 8. Attention Allocation Loadings

Channel	Loading value	Corresponding activity
Visual	5.372	track, follow, maintain orientation
Auditory	4.812	interpret semantic content of speech
Cognitive	5.453	recall, encode, decode
Psychomotor	5.212	manipulation, discrete adjustment

5.3.3 Perceived Workload

Perceived workload for the driving task as measured by the NASA TLX scores is increased by indirect viewing because of a significant increase in task demand, particularly in the temporal and mental components. While indirect viewing significantly increases the workload, there are no significant differences among the indirect systems.

5.3.3.1 Quantitative Results

The total workload increases 31.89% from a mean score of 24.22 for direct vision to a grand mean of 31.95 (maximum possible 54) for the indirect vision systems combined. The demand sum increases 38.06% from a mean of 12.61 for direct vision to a grand mean of 17.41 (maximum possible 27) for the indirect vision systems combined. Similarly, the mental demand increases 48.41% from 4.34 to a grand mean of 6.44 (maximum possible 9) for the indirect systems, while the temporal demand increases 53.19% from 3.46 to 5.30.

While there are no significant differences in workload among the indirect systems, the box plots for the total workload (see Figure 18) show a definite monotonic increasing trend approaching an asymptote with display compression ratio. In contrast, while the box plots for the demand sum (see Figure 19) and the mental (see Figure E-1) and temporal (see Figure E-3) components show clear differences between direct and indirect viewing, the plots show no trends with display compression ratio for the indirect systems. The total workload is the

mathematical sum of the components, and a study of the box plots suggests that the trend is attributable to the nonsignificant increase in the interaction sum through the frustration component.

5.3.3.2 Sources of Workload

Workload refers to the application of procedural knowledge used to operate the vehicle between barrel pairs. Workload was increased with indirect viewing by the reduced viewing conditions that resulted from the relocation of the viewpoint with the cameras, restricted display FOV, and the lack of depth perception. Also, the reduced resolution and scene distortions that were produced by the scene compression increased workload by shortening the velocity flow field and decreasing the control sensitivity. These changes forced participants to suppress the overly learned responses acquired in direct view driving with conscious attention to the temporal and mental demands of the task. These topics are described further in the following paragraphs.

a. Change in viewpoint - Workload was increased with indirect viewing by the change in viewpoint with the cameras from the left side to the center. The cameras were mounted over the lateral center of the vehicle, and the participants had to drive with the road image in the center of the scene on the central display to remain on the road. In this process, they had to suppress their overly trained response learned with direct viewing, namely, keeping the road centered to the right while driving from the left side of the vehicle. This was a conscious activity that demanded attention and increased their cognitive workload.

b. Limited FOV - Workload was also increased with indirect vision by the limited view of the road from the central display. With the extended FOV, the central camera is just wide enough to see the full hood but not both barrels of a marker pair at the same time as they are passed. With the wide FOV, the central camera shows the central portion of the hood as far as the running light mounts. As he entered a turn, the driver, in turning his head to see the side display to navigate around a barrel, tended to lose track of the other barrel of the pair, possibly striking it. For this reason, participants learned a driving strategy of aligning the vehicle with the barrel pair to approach directly and then driving straight forward between the barrels. In this process, participants had to suppress their overly trained response learned with direct viewing, namely, steering around the barrels. Again, this was a conscious activity that demanded attention and increased their cognitive workload.

c. Lack of depth perception - Another reason for the increased workload is the lack of depth perception with indirect vision, which is attributable to the monocular cameras. The lack of depth perception forced the driver to estimate the positions of the barrels from their change in apparent size and movement. The difficulty of this process was increased by the scene distortion. As can be seen from the distortion plots in Figures C-2 through C-4 (see Section 3.5.2), an

object being approached by the vehicle would appear on the display to accelerate and move laterally. This effect is quickened and moved closer to the front hood with increased scene compression. As a result, the driver had to closely track the barrels as they were approached. This is in contrast to natural vision when the markers move in a predictable path toward the vehicle.

d. Scene compression - Other reasons for the increased workload with indirect vision are the apparent increase in course speed and the increase in control-to-display-response ratio with scene compression. As noted for the indirect vision (see Section 3.5.1), the velocity flow field is shortened and accelerated with scene compression. The decrease in scene resolution reduces the visibility of the terrain detail that provides the velocity flow field. The field is shortened since the flow appears to originate from a point in the scene that is closer to the front of the vehicle. Because of the increased lateral movements, the velocity field appears faster and to accelerate as the vehicle approaches the scene elements. The velocity field has a quickening effect as it is moved toward the hood of the vehicle. The strategy of reducing course speed to accommodate driving response times for a relatively consistent error rate retains an element of increasing temporal task demand with an accompanying mental load.

e. Decreased control sensitivity - The decrease in scene resolution with display compression increases the control-to-display-response ratio (Sanders & McCormich, 1993) and thereby decreases the control sensitivity. The driver made finer adjustments in control with feedback of the compressed visual image to obtain the same control as with the direct viewing system. The drivers reduce their driving speed to accommodate the rate of changes in course variations and maintain a consistent error rate during the conditions of reduced control sensitivity.

5.3.3.3 Analytical Validity

The factorial analysis reported in the Results section for the TLX scores appears to have face validity. Figure 16 shows that the two components of the factor analysis for this study agree in principle with the questionnaire construction (Hart & Staveland, 1988). The first factorial component corresponds to the task demand and the second component corresponds to task interaction. Here, the temporal, mental, and physical demands are aligned with the demand component. However, in this study, while the effort rating is aligned with the interaction component, the performance and frustration ratings have both demand and interaction components.

In the Results section, the NASA TLX workload battery was analyzed in terms of the overall sum and the components. The weighted sum of the ratings for the components is commonly used as an overall workload rating. In general, the summing weights are task specific, derived by pair-wise comparisons among the six factors by the participants for the particular task (Hart & Staveland, 1988).

However, it has been argued that the non-weighted sum of the component ratings is an equally effective measure of the overall workload (Hendy et al., 1993), and this approach was used in this study.

5.3.4 Situational Awareness

While there is no significant change in overall SA with viewing system, the demand on SA is increased by indirect viewing because of a significant increase in instability and complexity. The statistical constancy in overall SA is attributable to the large variation in data. Logically, this must be true since the supply and understanding components show no significant changes and the overall SA is the mathematical sum of the supply and understanding minus the demand.

5.3.4.1 Quantitative Results

SA demand increases 30.30% from a mean of 10.56 for direct vision to a grand mean of 13.76 (maximum possible 21) for the indirect vision systems combined. Similarly, instability demand increases 40.98% from 3.05 to a grand mean of 4.30 (maximum possible 7) for the indirect systems, while complexity demand increases 38.33% from 3.60 to 4.98. While the changes among the indirect vision systems are not statistically significant, the box plots for the demand sum (see Figure 24) and instability (see Figure F-1) show monotonic increasing trends with increasing display compression ratios. No such trend exists for the complexity box plots (see Figure F-3).

5.3.4.2 Sources of SA Demand

The increase in cognitive demand on SA with indirect vision is caused by the perceived increase in instability and complexity of the display scene. In the driving task, SA is the knowledge of the vehicle's location and position on the course and the location of the next barrel pair. The driver maintains an awareness of where the vehicle is and extrapolates the location of the next barrel pair from his mental map of the course. This knowledge is essential for coordinating the task-specific behavior with the barrel pairs.

The demand on SA was increased by the reduced viewing conditions that resulted from the relocation of the viewpoint with the cameras, restricted display FOV, and the lack of depth perception. These changes made it more difficult to extrapolate the mental map to the scene. Furthermore, the scene is distorted by the display compression (see Section 3.5.2), and the distortions increase the demand on awareness needed for course localization. At increased compression ratios, an object appears more distant than it actually is, while the approach path bends outward and the apparent speed increases as the object approaches the vehicle. The scene distortion tends to make course locating difficult since objects appear to accelerate and move laterally as they are approached. Possibly, the driver needs to momentarily evaluate his location on the course, and the

resolution of this confusion between what is perceived and the mental model of the natural world would increase the cognitive loading.

5.3.4.3 Analytical Validity

The factorial analysis reported in the Results section for the SART scores (see Section 4.5.2) appears to have face validity. Figure 21 shows that the three factorial components for the factor analysis agree with the questionnaire construction (Selcon, Taylor, & Koritsas, 1991). As noted in the Results, the 10 dimensions of the questionnaire are plotted in the figure for the factorial component space. The figure shows that the 10 dimensions tend to cluster according to the corresponding domains. The first factorial component matches with the demand domain, and the second component matches the understanding domain. While the third component generally matches the supply domain, the arousal and concentration ratings of this domain are distributed among the other components as well.

5.3.4.4 Relation of Workload to SA

A question remaining is the relationship between the perceived workload and SA for this study as exhibited by the TLX and SART ratings, since only the demand components for both workload and SA vary with the viewing systems. The decreased resolution and increased scene distortion resulting from display compression increase the cognitive demands on both the procedural driving task and the locating task associated with SA.

According to the literature, the demand and supply domains of the SART are reported to be measures of workload as well as SA. This view is supported by experimental studies of task difficulty and differences in experience in simulator flying (Selcon, Taylor, & Koritsas, 1991). These studies have reportedly shown that the SART and TLX ratings overlap in sensitivity to task difficulty. In these studies, canonical correlation between the TLX scores and the 10-dimensional scores of the SART shows a strong relationship between the Effort and Mental Demand on the TLX, and the Variability, Spare Mental Capacity, and the Complexity on the SART. Similarly, a strong correlation was reportedly found between Mental Demand on the TLX and the Demand on Attentional Resources on the SART. These relationships appear to reflect the variation in task difficulty.

However, while the overall TLX scores as well as the six scales are reported to be sensitive to task difficulty, they are not sensitive to differences in experience (Selcon, Taylor, & Koritsas, 1991). For the SART, six dimensions (instability, complexity, variability, spare mental capacity, information quantity, and information quality) as well as all the SART domain dimensions and the overall measurement are reported to be sensitive to task difficulty. The SART dimension of familiarity was only sensitive to experience, and the concentration and spare

mental capacity dimensions were sensitive to the Task Difficulty x Experience interaction.

Furthermore, Endsley (1993) reportedly would expect SART ratings to be significantly related to TLX scores, since demands on and supply of attention resources are indicators of workload, while understanding of the situation is an awareness component. Endsley has stated that SA is a precursor to performance in that a loss in awareness incurs a risk of performance error since decision making may be impacted. Further, workload is generated from the effort taken to achieve and maintain awareness as well as the decision making and actions that follow. However, the ability of the human to process information is limited, and an excessive flow of information and tasks may result in a loss of awareness. This is because the human can attend to only a subset of the required information because of attention narrowing and the resulting disruption of scan patterns.

5.3.5 Motion Sickness

The reports of motion sickness and motion after-effects were minimal for direct vision but significantly increased for the indirect vision system with increases in eyestrain, difficulty in focusing, and sweating. Also reported were incidences of general discomfort, stomach awareness, and vertigo, among others. Several participants reported motion after-effects following experimental runs. As mentioned before (see Section 4.1), one participant exhibited motion sickness during the last two experimental runs with the indirect vision, which was severe enough for him to stop before completing the first run and to abort the second run after training. Another participant not included in the analysis chose to stop the experiment because of nausea followed by vomiting which occurred in the second trial run with the indirect vision system.

5.3.5.1 Quantitative Results

The sums for the total severity and the nausea, oculomotor, and disorientation symptoms are significantly greater for indirect viewing, but there are no significant differences across the indirect systems. The total severity increases from a mean of 1.22 for direct vision to a grand mean of 26.00 (21.67% of the maximum possible 120) for the indirect vision systems combined. Similarly, the nausea symptom increases from 4.77 to a grand mean of 45.71 (22.85% of maximum possible 200) for the indirect systems; the oculomotor symptom increases from 1.90 to 37.90 (23.83% of maximum possible 159); and the disorientation symptom increases from 1.74 to 60.32 (20.66% of maximum possible 292). Although the box plots for the severity (see Figure 29) and symptoms (see Figures 30 through 32) show increasing trends with display compression, the data means for the near-unity and wide FOV cameras fall outside the 90% confidence intervals for quadratic regressive estimates to the data. Therefore, a reasonable estimate is minimal motion sickness with direct viewing and a significant increase with indirect viewing equally for all camera FOVs.

5.3.5.2 Time-wise Behavior

The motion sickness scores show no consistent time-wise pattern across participants with course runs. For example, although five participants started with moderate total motion sickness scores in the first run with the indirect system, they learned to adapt to the conditions and reported lower scores in the later runs. However, two participants could not adapt, and their motion sickness scores continued to increase with course runs. Finally, one participant continued to report moderate motion sickness across all indirect vision runs. While in this study, the participants drove for only several minutes at a time, whereas drivers of combat vehicles may be driving for several hours. It is important to note that the literature about flight simulator sickness (Baltzley, Kennedy, Berbaum, Lilienthal, & Gower, 1992) reports that symptoms may last as long as 1 hour after a flight session and for some pilots, more than 6 hours, with many of these being disorientation symptoms.

5.3.5.3 Sources of Motion Sickness

The prevalent theory about the cause of motion sickness is sensory conflict, in which the visual system, the vestibular system, and the proprioceptors conflict with each other or with expectations based on previous experience. There are two main categories of sensory conflict: either the information from the visual system and that from the vestibular system are incompatible with each other, or the information from the canals and otoliths within the vestibular system provides conflicting signals (Pausch, Crea, & Conway, 1992). The particular mechanics of indirect vision driving that induce motion sickness are now described in greater detail.

a. Conflict in viewpoint - The change in camera viewpoint with the indirect viewing may induce motion sickness. Motion sickness is provoked by sensory conflict between the visual field and sensorimotor activities that involve the vestibular system through body and head movements (Yardley, 1992). Since the driver sat on the left side of the vehicle and the cameras were mounted in the center, the vibrations seen on the display were slightly different in amplitude and frequency from those that were received physically from the seat through the vehicle frame. The slight inconsistency between the visual and physical vibrations may not be disconcerting to all drivers. However, the one participant who was an experienced vehicle driver was so disturbed by the indirect vision driving that he tried to drive while sitting in the center of vehicle. This occurred just before he aborted the study because of extreme motion sickness (not included in the analysis). That a more experienced driver would have an increased chance of acquiring motion sickness is because he or she will have a clearer expectation of performance and therefore sense a greater discrepancy (Pausch, Crea, & Conway, 1992).

b. Display characteristics - The wide 110-degree FOV for the displays may induce motion sickness because of motion in the peripheral vision. An

analogous experience, simulator sickness, generally occurs more frequently and intensely with a wider FOV display since it provides more ocular stimulation (Kennedy, Fowlkes, & Hettinger, 1989; Scribner & Gombash, 1998). Another source of motion sickness may have been the lack of natural binocular stereovision and the accompanying depth perception, which causes a discrepancy between the scene and that expected from direct viewing (Pausch, Crea, & Conway, 1992). However, binocular stereovision that is artificially induced by binocular rivalry between offset images presented to both eyes has been reported to increase simulator sickness in teleoperations (Scribner & Gombash, 1998). Presumably, this is because the stereo-optics are "slaved" to the vehicle and not to movements of the driver's head as in natural vision.

c. Scene distortions - The sensorimotor conflicts may have been further aggravated by the distortions in the display scene, especially during vehicle turns. See Appendix B for a derivation of scene distortions as a function of display compression. With the wide FOV, the far corners on the side displays appear to rotate rather than slide in turns. With the extended FOV, the side display scene visually appears to rotate at a faster rate than the vestibular system senses that the vehicle is turning. Furthermore, because of the reduced resolution for terrain detail, the bottom portion of the display does not appear to refresh as fast as the vehicle is moving. Even in forward motion, objects in the central display appear to accelerate laterally as they are approached. The results may be an increase in disorientation and nausea symptoms caused by the distorted visuals (Pausch, Crea, & Conway, 1992).

d. Image motion blurring - Many participants in this study reported incidences of motion sickness during a rapid course turn or when they went over the berms. This may be attributable to the block crystal realignment method of image refresh that is employed in LCDs. As noted before, the display refresh could not keep pace with the changing scene during a rapid turn and while the vehicle went over the berms on the course. This resulted in the display appearing out of focus because of the temporary motion blurring of the video return with the accompanying loss of dynamic resolution. In some participants, this may have induced a lack of convergence accommodation that resulted in blur-driven asthenopia symptoms. As reported in the literature, motion sickness, especially asthenopia symptoms (Ebenholtz, 1992), can be produced by insufficiencies in visual stimulation. These symptoms can arise from lack of binocular convergence, inappropriate accommodative responses to blurred images, unequal image sizes in the two eyes, unequal focusing capability in each eye, and from inadequate fixation or pursuit responses. Furthermore, visual after-effects, consisting of illusory and unstable perception after exposure, have been reported to follow asthenopia symptoms (Ebenholtz, 1992).

e. Task environment - The task environment as reported previously for the indirect vision tends to increase sensitivity to motion sickness because of

sensory isolation while soldiers ride in the enclosed compartment. While the direct vision driving was performed with unrestricted, natural vision from an open cab, the indirect vision driving was from an enclosed cab. As noted before, the driver experienced physical isolation, darkness, heat, and noise during the test run with the indirect vision systems, which differed from conditions for direct vision driving. The imposition of these conditions upon the participant may have been interpreted as a loss of control, a condition that increases susceptibility to motion sickness (Pausch, Crea, & Conway, 1992).

5.3.6 Subjective Stress State

The subjective stress state is significantly related to the equivalent DCR (adjusted R-squared = 0.368, $p < .001$, F = 16.738, df = 1, error df = 26) through the course speed by a regression analysis. The result is a predictor for the stress state as a function of the compression ratio (DCR),

$$\text{stress state} = -4.161 + 16.856*\text{DCR}.$$

The relation predicts that the stress state is lowest for direct viewing and increases with increased camera FOV for indirect viewing. The predicted affective state ratings are listed in Table 9, along with the corresponding verbal anchors (Kerle & Bialek, 1958). The ratings increase from 12.70 ("fine") for direct viewing to 18.60 ("comfortable") for the near-unity FOV, 27.19 ("steady") for the wide FOV, and 35.11 ("not bothered") for the extended FOV. However, considering the insignificant variation of the other mental measures with camera FOV, an averaged stress rating of 27.19 ("steady") is probably the best estimate for the indirect vision.

Table 9. Predicted Affective Stress State for Viewing Treatments

Viewing condition	DCR	Affective stress rating	anchor
Direct	1.00	12.70	"fine"
150° FOV	1.36	18.60	"comfortable"
205° FOV	1.86	27.19	"steady"
257° FOV	2.33	35.11	"not bothered"

5.3.7 Affective Aspects

The affective aspect components of stress were not significantly influenced by the course speed, at least as measured by the components of the factor analysis. The distribution of the affective aspects in the factorial component plot of Figure 34 shows that the first factorial component is aligned with the negative

aspect of emotion and may be interpreted as reflecting uncertainty about the task. The second component is aligned with the positive aspect and reflects confidence in one's ability. The implication is that while the stress state changes with viewing treatments, the confidence of the participants in their abilities and knowledge of the task remains the same.

5.3.8 Cognitive Functions

The performance of the cognitive functions was not significantly influenced by the viewing treatments; however, the box plots show a trend for reduced performance following the indirect viewing. This is true for the logical reasoning (see Figure H-1), addition (see Figure H-2), and word recall (see Figure H-4) tests. In contrast, the box plots for spatial rotation (see Figure H-3) and map planning (see Figure H-5) show a trend of increased performance for driving with direct vision and the indirect wide FOV cameras and decreased performance with the near-unity and extended FOV cameras. The distribution of the cognitive tests on the factorial component plot of Figure 35 suggests a dichotomy of functions. Here, the first factorial component may be interpreted as corresponding to intuitive, holistic reasoning, while the second component corresponds to deductive, serial reasoning. Note that both the spatial rotation and map planning tests involve geometrical patterns; however, while both involve intuitive reasoning, map planning involves serial reasoning as well.

5.3.9 Spatial Priming

A trend in the data suggests that the wide FOV has a priming effect on spatial cognitive functioning on the same order as direct viewing. This is reasonable since the wide FOV was intentionally selected by the researchers to provide a balance between scene resolution and route perspective much as occurs with natural vision. As noted in the discussion, this trend is not only apparent in the data for spatial rotation and map planning but exists in the data for other measures as well. For example, the eye movements (see Figure I-5 in Appendix I) reported by the participants in the system evaluation show an increased activity at the same level for both the direct and the wide FOV viewing. The source of this priming may be in the eye movements used for task-specific steering and situational course selection during driving. The wide FOV may better support the consecutive processing of both problem stages and the spatial conversion involved in the translation between them from a global perspective to an egocentric perspective needed for driving. The advantages of this priming effect are supported by trends in the data of the system evaluation for the reported workload (see Figure I-9), stress (see Figure I-10), and motion sickness (see Figure I-11), which are decreased to the same levels for both the direct and wide FOV viewing.

5.4 Summary of Driving Results

The average values for the statistically significant task performance and mental workload results are summarized in Table 10 for direct and indirect driving. The mental workload measures include the total severity rating of motion sickness, the NASA TLX perceived workload, the SART SA demand, and the estimated subjective stress. While the data for the task performance (i.e., driving speed and lane accuracy) vary significantly with camera FOV for the indirect driving, data for the mental workload measures are averaged across the three camera treatments. The values for the motion sickness, perceived workload, and SA demand are reported as the percentage of the total score possible on the corresponding questionnaire (see discussion sections), averaged across the eight participants. In addition, listed for motion sickness are the number of participants of the total participants in the experiment who aborted at least one trial. In addition to the results for the flat panel displays, the average results for task performance and the number of participants aborting because of motion sickness are listed for the 1996 driving study with the HMD.

Table 10. Summary of Driving Results

Configuration	Driving speed (km/hr)	Accuracy percent strikes	Metabolic workload	Motion sickness	TLX workload (percent)	SART SA-D[a] (percent)	Subject stress
Direct driving	22.84	3.19	1.00	1.02% *0/10*	44.85	50.28	12.70
Flat panel display Near unity FOV-150°	18.92	5.53	1.04	21.67% *2/10*	59.17	65.52	27.19
Flat panel display Wide FOV-205°	18.15	7.23	1.10	21.67% *2/10*	59.17	65.52	27.19
Flat panel display Extended FOV-257°	17.08	8.27	1.16	21.67% *2/10*	59.17	65.52	27.19
Helmet-Mounted Display	15.41	10.51	-	- *1/8*	-	-	-

Note 1. For motion sickness, TLX, SART demand on SA ([a]SA-D), and subjective stress, statistical significant differences occur between direct and indirect treatments. For MS, TLX, and SART, the values are expressed as a percentage of total score on the questionnaire.
Note 2. Motion sickness expressed as percent of total severity across eight subjects from questionnaire, and number of subjects who aborted test of total tested.
Note 3. Metabolic workload expressed as ratio of indirect vision treatment workload to direct treatment workload.

5.5 Participants' Comments

Comments by the participants provide some insight into the mental workload that is incurred while soldiers drive with the indirect vision system. Some of these comments are now summarized by topic.

5.5.1 Camera FOV

One participant reported that the near-unity FOV was more comfortable and easier to use to navigate than the wide or extended FOV because of the more realistic image. He liked the wide FOV but had difficulty seeing what he was approaching. He felt encapsulated and uncomfortable with the extended FOV since the display images were too close together, and he had trouble concentrating and felt disoriented.

In contrast, another participant reported that he preferred the wide and extended FOV since he could see the hood and more of the course ahead. With the wide FOV, the side cameras helped since they were closer together and let him navigate. Although the objects were smaller, the relative size was the same and he was still able to drive. With the extended FOV, he saw more of the scene on the central display; however, the side cameras were not as helpful. Still another participant felt that all displays made him queasy. The screen image with the near-unity FOV seemed a true image but he could not keep it in focus. With the wide FOV, he became dizzy and disoriented after going over the middle berms since when the cameras moved up and down, he easily got lost; however, straight driving was possible. The cameras for the extended FOV made him dizzy; the display objects appeared to be passing faster than they should have been, and the horizon on the side displays appeared inconsistent with the ground objects.

5.5.2 Vehicle Hood Reference

A participant reported that seeing the hood of the vehicle was comforting as a frame of reference since it was easier to track, but it did not necessarily improve performance. The runs with the near-unity FOV seemed more natural and comfortable since without the hood in view, the participant was able to concentrate on the trend of the vehicle's movement from the flow pattern instead of the nearest set of barrels.

5.5.3 Side Displays

One participant reported that the side displays were helpful in turns since sharp turns, slow or fast, were probably the most disorienting tasks. As he turned toward an object such as a barrel, he was able to consistently track it as a driver normally would in direct viewing. This was most apparent as the barrels or other objects move from a side panel to the front panel. His initial impression was that the side panels were of use only when he was deliberately looking for something such as a turn from a road or when he was checking for traffic. When the right

side panel stopped working during a training run, he thought that he could continue with only minor difficulty. The next right turn he encountered proved that he was using the side panels more than he had realized.

5.5.4 Display Visual Dead Space

A participant reported losing track of barrels in the visual dead space when the markers passed from the side display to the front in a turn with the near-unity FOV. He could not predict the track fast enough from the flow pattern for steering and he had to shift his visual attention between screens. However, he could see as far as the next barrel pair and by properly aligning the vehicle, could navigate between them.

5.5.5 Depth Perception

One participant reported that the shift in visual focus when he looked from the far scene to the near scene was uncomfortable because of the lack of depth perception on the displays. When driving, he tended to shift his attention from a point of view ahead of the vehicle to right in front as he approached a set of barrels, and he then tried to fit the hood between the barrels. This was a bit uncomfortable because there was no accompanying shift of visual accommodation as he looked from the far to the near.

Depth perception problems were reported to be most apparent when drivers performed tasks peripheral to the actual experiment and when they made turns. For example, turning around to reverse direction on the practice course and trying to judge the clearance between the vehicle and the course retaining wall was a bit unnerving. Another example is turning onto the test course and trying to judge the clearance between the vehicle and the stop sign. Tight turns on the actual course were also difficult but less bothersome because the participant did not worry about hitting a barrel. Judging distance with a direct approach was much easier.

5.5.6 Scene Distortions

One participant reported a rotation effect with the wide FOV on the far corners of the side displays. With the extended FOV, the turn rate in the scene on the side displays was different from that felt in the vehicle. The bottom half of the displays did not refresh as fast as the vehicle was moving. The participant reported feeling that he was sliding in a turn, with accompanying motion sickness, headache, and stomach nausea.

Another participant reported that with the wide FOV, objects appeared to move faster on the displays than they actually were and appeared slightly blurred when the vehicle bounced while going over rough ground. With the extended FOV, since objects appeared so much smaller, they seemed farther away than they actually were, and he misjudged distances.

5.5.7 Object Discrimination

One temporally disorienting feature of the panel displays was how much a dark shadow looked like a solid object. The early morning shadows from the trailers across the course perimeter road looked like a solid black block object sitting in the road.

6. Conclusion

Increasing the camera's FOV for indirect vision driving with a fixed display size decreases the speed of travel because of scene compression. While the vehicle is traveling slowly, the perceived speed is faster, possibly resulting in a decrement in tactical performance. Because the physical exertion is less at the decreased speed of travel for indirect vision, the estimated heart rate decreases with indirect vision driving. However, the metabolic workload is increased for the same route because of the much longer travel times.

At the screen resolution and refresh rate used in this study, LCDs may induce motion sickness which in turn increases subjective stress. In addition to vestibular system conflicts attributable to differences between the visual scene and head movements, another source of motion sickness may be a loss of convergence accommodation. This loss may be induced by temporal motion blurring of the video display during rapid changes in the scene such as occur during road turns and passages over berms.

Associated with indirect vision is an increase in both the workload and the demand on SA. These increases are caused by an increase in mental and temporal demands on the cognitive facilities of the human driver. In turn, these may be attributable to the physical differences between the natural viewing and indirect vision with the decreased resolution of the displays, lack of stereooptics, and the change in apparent viewpoint with the camera array mounted over the center of the vehicle. Over time, the increase in workload can lead to fatigue and errors.

With indirect vision, the higher speeds and better lane-following accuracy are attained with a unity display when the display and camera have the same FOV. However, increasing the camera's FOV may facilitate the mental operations of spatial rotation and map imagery that are needed for course navigation. This is suggested by a trend in the cognitive ability for figure rotation and map planning to be higher after trials with a wider camera FOV.

7. Recommendations for Further Research

We recommend that unity vision be used for indirect vision driving; however, the ability to electronically change FOV may be of value in route navigation, and the advantages should be researched further. Although our study results with the near-unity FOV suggest that a view of the vehicle is not needed for route following, close steering around road obstacles may be best performed with the scene that includes a vehicle reference. This may be provided by a downward looking camera view that includes a view of the vehicle's sides and front. For this reason, research should be continued into optimal camera position for different steering regimens.

The use of subjective questionnaires to measure perceived workload, SA, and motion sickness has provided insight into the increases in mental workload incurred with indirect vision driving. We recommend the collection of subjective data in further experiments and the use of factorial analysis in data analysis of questionnaires for control of the Type I error. Motion sickness continues to be a concern for indirect vision driving, and techniques for controlling sickness without adversely affecting performance should be researched further.

We recommend investigating modeling task performance and the effects of mental workload on indirect vision driving. A point of particular concern is the inclusion of motion sickness (both the sources and symptoms) and their effect of performance.

Since future vehicle designs will include multi-tasking along with driving, we recommend research about multiple task performance that involves crew interaction and communications and navigation functions for indirect vision activities. The present study was limited to course driving and did not consider the higher cognitive functions that are required of future combat vehicle operators. A future study should include automated adaptive aiding for the performance of multiple tasks in future combat systems.

INTENTIONALLY LEFT BLANK

References

Allender, L., Salvi, L., & Promisel, D. (1998). Evaluation of human performance under diverse conditions via modeling technology. In Improved Performance Research Integration Tool (IMPRINT), User's Guide (Appendix A). Aberdeen Proving Ground, MD: U.S. Army Research Laboratory.

Baddeley, A. (1968). A 3-minute reasoning task based on grammatical transformation. Psychonomic Science, 10, 341-342.

Bailenson, J.N., Shum, M.S., & Uttal, D.H. (1998). Road climbing: Principles governing asymmetric route choices on maps. Journal of Environmental Psychology, 18, 237-249.

Baltzley, D.R., Kennedy, R.S., Berbaum, K.S., Lilienthal, M.G., & Gower D.W. (1989). The time course of post-flight simulator sickness symptoms. Aviation, Space, and Environmental Medicine, 60(11), 1043-1048.

Cooley, W.M., & Lohnes, P.R. (1971). Multivariate data analysis. New York: John Wiley & Sons, Inc.

Dixon, W.J. & Massey, F.J. Jr. (1969). Introduction to statistical analysis. New York: McGraw-Hill Book Company.

Ebenholtz, S.M. (1992). Motion sickness and oculomotor systems in virtual environments. Presence, 1(3), 302-305.

Endsley, M.R. (1993). Situation awareness and workload: Flip sides of the same coin. Proceedings of the 7th International Symposium on Aviation Psychology, April issue.

Fatkin, L.T., & Hudgens, G.A. (1994). Stress perceptions of soldiers participating in training at the chemical defense training facility: The mediating effects of motivation, experience, and confidence level (ARL-TR-365). Aberdeen Proving Ground, MD: U.S. Army Research Laboratory.

Fatkin, L.T., King, J.M., & Hudgens, G.A. (1990). Evaluation of stress experienced by Yellowstone Army fire fighters (Technical Memorandum 9-90). Aberdeen Proving Ground, MD: U.S. Army Human Engineering Laboratory.

Fatkin, L.T., & Mullins, L.L. (1995). Stress, overload and performance: High standards or high stakes. Proceedings of American Psychological Association-National Institute of Occupational Safety and Health (APA-NIOSH), February issue.

Glumm, M.M., A general formula for calculating camera positioning for remote driving (unpublished Technical Note). Aberdeen Proving Ground, MD: U.S. Army Research Laboratory.

Glumm, M.M., Marshak, W.P., Branscome, T.A., Wesler, M.M., Patton, D.J., & Mullins, L.L. (1997). A comparison of soldier performance using current land navigation equipment with information integrated on a helmet-mounted display (ARL-TR-1604). Aberdeen Proving Ground, MD: U.S. Army Research Laboratory.

Hart, S.G., & Staveland, L. (1988). Development of the NASA task load index (TLX): Results of empirical and theoretical research. In P.A. Hancock and N. Meshkati (Eds.) Human Mental Workload, pp. 139-183. Amsterdam: North-Holland.

Hendy, K.C., Hamilton, K.M. , & Landry, L.N. (1993). Measuring subjective workload: When is one scale better than many? Human Factors, 35(4), 579-601.

Kennedy, R.S., Fowlkes, J.E., & Hettinger, L.J. (4 September 1989). Review of simulator sickness literature. NTSC TR 89-024, p. 51, Orlando, FL.

Kennedy, R.S., Lane, N.E., Lilienthal, M.G., Berbaum, K.S., & Hettinger, L.J. (1992). Profile analysis of simulator sickness symptoms: Application to virtual environment systems. Presence, 1(3), 295-301.

Kennedy, R.S., Lilienthal, M.G., Berbaum, K.S., Baltzley, D.R., & McCauley, M.E. (1989). Simulator sickness in U.S. Navy flight simulators. Aviation, Space, and Environmental Medicine, 60, 10-16.

Keppel, G. (1982). Design and analysis: A researcher's handbook. Englewood Cliffs, NJ: Prentice-Hall, Inc.

Kerle, R.H., & Bialek, H.M. (1958). The construction, validation, and application of a subjective stress scale (Staff Memorandum Fighter IV, Study 23). Presidio of Monterey, CA: U.S. Army Leadership Research Unit.

Kroemer, K.H.E., Kroemer, H.J., & Kroemer-Elbert, K.E. (1997). Engineering physiology. New York: Van Nostrand Reinhold.

McCarley J.S., & Krebs, W.K. (2000). Visibility of road hazards in thermal, visible, and sensor-fused night-time imagery, Applied Ergonomics, 31(5), 523-530.

McCracken, J.H., & Aldrich, T.B. (1984). Analysis of selected LHX mission functions: Implications for operator workload and system automation goals. (Technical Note ASI 479-024-84). Fort Rucker, AL: Army Research Institute Aviation Research and Development Activity.

Mullins, L.L., & Fatkin, L.T. (1995). Personality traits and cognitive performance during sustained operations. Proceedings of American Psychological Association-National Institute of Occupational Safety and Health (APA-NIOSH), February issue.

Neter, J., Kutner, M.H., Nachtsheim, C.J., & Wasserman, W. (1996). Applied linear statistical models. New York: McGraw-Hill.

Pausch, R., Crea, T., & Conway, M. (1992). A literature survey for virtual environments: Military flight simulator visual systems and simulator sickness, Presence, 1(3), 344-362.

Pedhazur, E.J. (1982). Multiple regression in behavior research: Explanation and prediction. Chicago: Holt, Rinehart, and Winston, Inc.

Sanders, M.S., & McCormich, E.J. (1993). Human factors in engineering and design. New York: McGraw-Hill, Inc.

Scribner, D.R., & Gombash, J.W. (1998). The effect of stereoscopic and wide field of view conditions on teleoperator performance (ARL-TR-1598). Aberdeen Proving Ground, MD: U.S. Army Research Laboratory.

Schutz, R.W., & Gessaroli, M.E. (1987). The analysis of repeated measures designs involving multiple dependent variables. Research Quarterly for Exercise and Sport, 58(2), 132-149.

Selcon, S.J., Taylor, R.M., & Koritsas, E. (1991). Workload or SA?: TLX versus SART for aerospace systems design evaluation. Proceedings of the Human Factors Society, 35th Annual Meeting, pp. 62-66.

Shepherd, R.N. (1978). The mental image. American Psychologist, 33, 125-137.

Smyth, C.C. (2000). Cognitive workload and task performance for indirect vision driving with flat panel displays. Proceedings of the 23rd Army Science Conference, 10-13 December.

Smyth, C.C., & Whitaker, R.G. (1998). Indirect vision driving study. Proceedings of the 21st Army Science Conference, 15-17 June, pp. 497-502.

Taylor, R.M. (1988). Trust and awareness in human electronic crew teamwork. In T.J. Emerson, M. Reinecke, J.M. Reising, and R.M. Taylor (Eds.) The human–electronic crew: Can they work together? Proceedings of a joint GAF/USAF/RAF workshop, BSD-DR-G4, Dec. 1988, RAF Institute of Aviation Medicine, Farnborough, Hants, U.K.

Taylor, R.M. (1989). Situational awareness rating technique (SART): The development of a tool for aircrew systems design. In Proceedings of the AGARD AMP symposium on SA in aerospace operations, CP478, Seuilly-sur Seine: NATO AGARD.

Taylor, R.M., & Selcon, S.J. (1994). Situation in mind: Theory, applications, and measurement of SA. In R, D. Gilson, D. J. Garland, and J. M. Koonce (Eds.), Situational Awareness in Complex Systems, Embry-Riddle Aeronautical University Press.

Thorndike, E.L., & Lorge, I. (1944). The teacher's word book of 30,000 words. New York: Columbia University.

Tkacz, S. (1998). Learning map interpretation: Skill acquisition and underlying abilities. Journal of Environmental Psychology, 18, 237-249.

Vasey, M.W., & Thayer, J.F. (July 1987). The continuing problem of false positives in repeated measures ANOVA in psychophysiology: A multivariate solution. The Society for Psychophysiology Research, 479-486.

Velleman, P.F., & Payne, D.E. (1992). Applications, basics, and computing of exploratory data analysis. Boston, MA: Duxbury Press.

Wickens, C.D., Gordon, S.E., & Liu, Y. (1998). Introduction to human factors engineering. New York: Addison Wesley Longman, Inc.

Williams, H.L., Gieseking, C.F., & Lubin, A. (1966). Some effects of sleep loss on memory. Perceptual and Motor Skills, 23, 1287-1293.

Williams, H.L., & Lubin, A. (1967). Speeded addition and sleep loss. Journal of Experimental Psychology, 73(2), 313-317.

Yardley, L. (1992). Motion sickness and perception: A reappraisal of the sensory conflict approach. British Journal of Psychology, 83, 449-471.

Zuckerman, M., & Lubin, B. (1985). Manual for the multiple affect adjective check list--revised. San Diego, CA: Educational and Industrial Testing Service.

INTENTIONALLY LEFT BLANK

APPENDIX A

CAMERA FIELD OF VIEW

INTENTIONALLY LEFT BLANK

CAMERA FIELD OF VIEW

The amount of sky, ground, terrain features, including the "close-in" vision, and the body of the vehicle within the camera scene can influence the driving performance. The locations and angles of the cameras on the vehicle body, as well as the focal length of the camera lens, determines the portions of these features that are within view. Following a series of pilot studies that examined the effects of camera location and angle on teleoperational driving of a HMMWV, the investigators (Glumm, unpublished) concluded that the preferred camera settings were such that the conditions for sky-to-ground ratio, distance for close-in vision, and vehicle reference are as follow:

Sky-to-ground ratio: The ratio of sky to ground within the scene should be no less than 15% and no greater than 50%. The ratio is a measure of the amount of distant viewing that the driver has available for course selection and look-ahead planning.

Close-in vision: The driver of a HMMWV should be able to view the ground within 10 feet of the front of the vehicle and beyond (also see MIL-HDBK 759). Shorter distances improve obstacle avoidance.

Vehicle reference: The amount of vehicle hood within view should be at least 1 foot and no more than 5 feet back from the front. A visible hood gives a steering reference for obstacle avoidance.

Here, the sky-to-ground ratio, the close-in vision distance, and the amount of the vehicle hood that are within the central view are determined for the lens settings used in this experiment. We first derive expressions for the sky-to-ground ratio and the close-in vision distance. Consider Figure A-1, which shows a side view sketch of a vehicle with a roof-mounted, forward facing camera which is tilted downward at a boresight angle (θ_b) from the horizon. Given a vertical FOV (VFOV) as determined by the size of the CCD imager framer and the focal length of the camera lens, the bottom edge of the view is at an angle, $\theta_o = VFOV/2 + \theta_b$, from the horizon. The angle to the front of the hood from the horizon is $\theta_h = \arctan((\eta - \alpha)/\chi)$. Considering these expressions, the fraction of sky to ground in the scene is given by Ratio = $(VFOV/2 - \theta_b)/(VFOV/2 + \theta_b)$, assuming that some sky is in view, that is, $\theta_b > FOV/2$; otherwise Ratio = 0. Furthermore, considering the proportions of triangles, the viewing distance in front of the hood starts at $\nu = \chi^*\alpha / (\eta - \alpha)$, assuming that some hood is in view, that is, $\theta_o > \theta_h$; otherwise, the distance is $\nu = \eta/\tan(\theta_o) - \chi$.

While the above are derived from basic trigonometric relations, the HMMWV hood slopes downward to the front, and the amount of vehicle hood in the scene is computed by considering geometrically two intersecting planes, one for the bottom edge of the scene and the other for the hood. Letting the CCD imager be

located at position y_o, z_o in a coordinate system on the vehicle, the directional cosines of the midline to the bottom view are given by $b_o = \cos(\theta_o)$ and $c_o = -\sin(\theta_o)$. Here, the z-axis of the coordinate system is upward through the roof and the y-axis run forward longitudinal toward the front. Further, we let the midline to the hood be located at the end points y_1, z_1 at the cab and y_2, z_2 at the front. The total distance along the hood is r_m, the straight line between the points, the directional cosines of the midline are $b_1 = (y_2 - y_1)/r_m$, and $c_1 = (z_2 - z_1)/r_m$. Locating the origin of the coordinate system at the camera's CCD imager (y_o=0, z_o=0), the hood midline end points in terms of the dimensions on the diagram, are $y_1 = \chi - \mu$, and $z_1 = \beta - \eta$, and $y_2 = \chi$ and $z_2 = \alpha - \eta$. In terms of this notation, the straight line distance from the camera to the intersection point with the hood is $r_o = (c_1*(y_o - y_1) - b_1*(z_o - z_1))/(c_o*b_1 - b_o*c_1)$. Similarly, the distance from the cab to the intersection point is $r_1 = (y_o - y_1 + r_o*b_o)/b_1$. Finally, the portion of the hood in view is given by $r_v = r_m - r_1$.

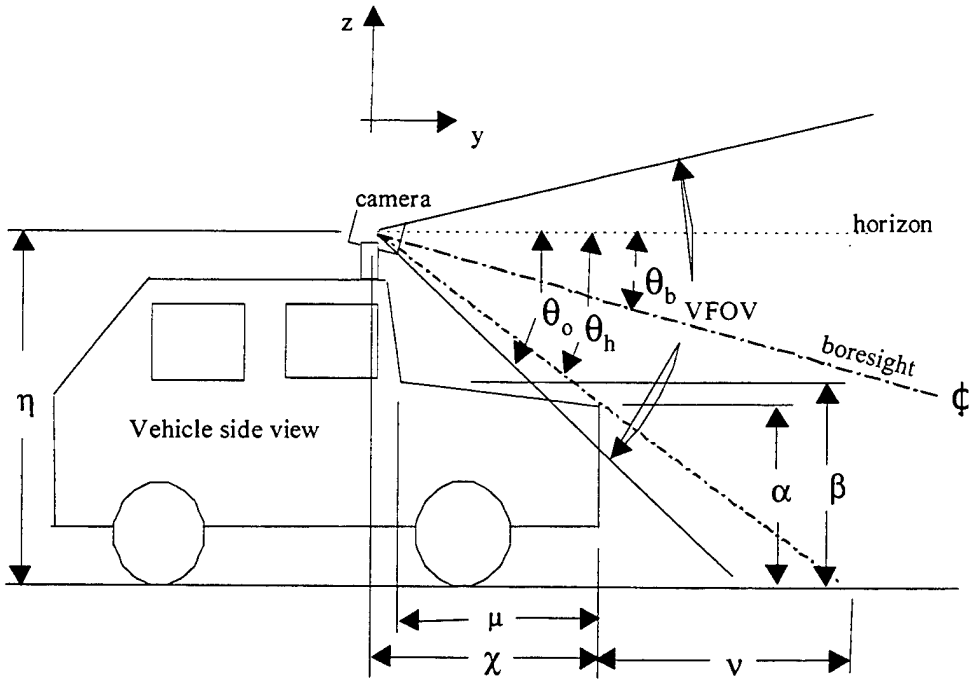

Figure A-1. Central Camera's Vertical FOV.

Equally important for obstacle avoidance is the distance from the vehicle at which lane markers move out of the field of view for the central camera. This is especially true for this experiment since the edges of the vehicle's front fenders were not visible. Considering Figure A-2 for the central camera's horizontal FOV (HFOV), the angle to the front fender is, $\theta_f = \arctan(\gamma/\chi)$, in which γ is the vehicle centerline to fender edge distance and χ is the distance between the CCD imager and the hood front along the y-axis. If this angle is greater than the HFOV of the camera, $\theta_f > HFOV/2$, then the fenders are in view. Otherwise, the portion of the

hood front that is in view is $\delta = \chi * \tan(HFOV/2)$, as measured from the centerline. Assuming for simplicity that the lane markers are points ($\alpha = 0$), the distance from the front of the vehicle to where the lane markers move out of view is $\sigma = \kappa/\tan(HFOV/2) - \chi$, in which κ is half the driving course width.

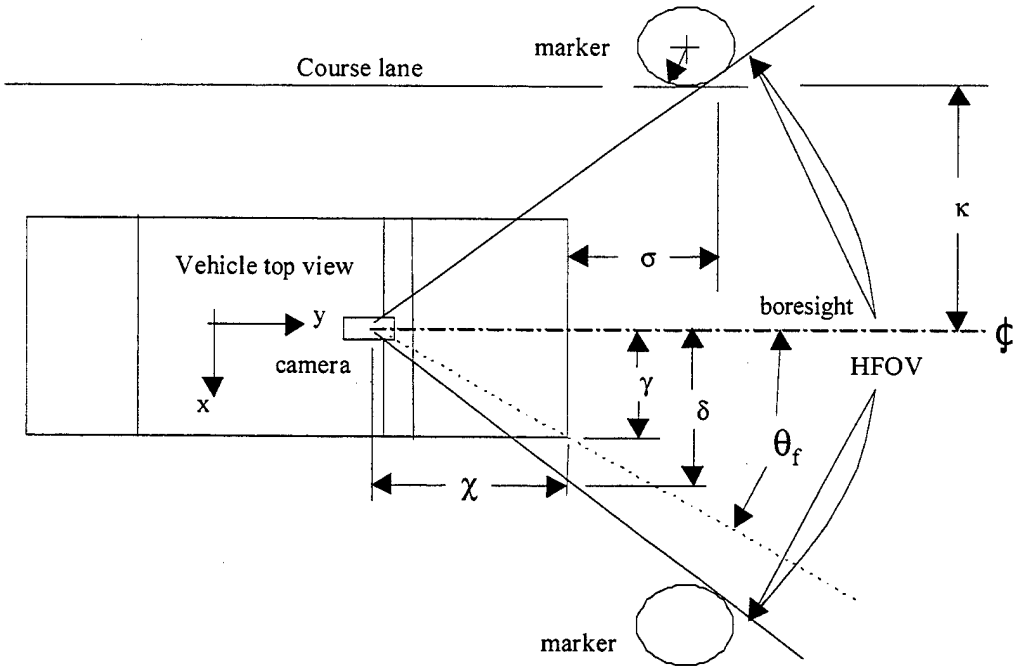

Figure A-2. Central Camera's Horizontal FOV.

Table A-1 lists the results of the calculations for the camera lens by focal length (mm). The horizontal and vertical field of views are for the 0.5-inch CCD imager of the camera. The table shows that while the near-unity FOV system has less than preferred sky-to-ground ratio and no hood in view, the close viewing distance is acceptable. Furthermore, the wide and extended FOV systems show reasonable amounts of the sky, hood and close ground for driving operations. While 50% of the scene in front of the hood is in view for the near-unity FOV, the wide FOV shows almost 3/4 of the hood front and the extended FOV—practically all. However, the lane markers moved out of view once they were beside the front fenders.

Table A-1. Viewing Parameters for the Lens Settings

FOV	Lens FL (mm)	HFOV (deg)	VFOV (deg)	θ_o (deg)	Sky (deg)	Ratio (%)	Front (%)	Hood (ft)	Distance Ground (ft)	Marker (ft)
Near unity	8.5	41.23	31.53	29.56	1.96	6.62	50.80	0.00	6.81	8.13
Wide	6.0	56.17	43.60	35.60	8.00	22.47	72.02	0.73	5.69	4.40
Extended	4.8	67.37	53.13	40.36	12.76	31.61	89.97	1.49	5.69	2.63

Notes: 0.5-inch CCD imager (6.4 mm H x 4.8 mm V).
Camera boresight angle, $\theta_b = 13.8°$.

APPENDIX B

EFFECTS OF DISPLAY COMPRESSION ON SCENE DYNAMICS

INTENTIONALLY LEFT BLANK

EFFECTS OF DISPLAY COMPRESSION ON SCENE DYNAMICS

The effects of the display compression on the viewed scene are discussed. A simple mathematical analysis provides the basis for generating functions for mapping the distortions in space and time of the actual scene to the display scene coordinates. Distortion plots are generated for the compression ratios used in this study.

Consider a real-world scene in a Cartesian coordinate system centered on the driver's display in a vehicle as shown in Figure B-1, with the longitudinal axis collinear with the forward looking y-axis of the display. Let the vehicle be moving forward in a straight line with a velocity υ and consider a known object located at a point (ξ_O,ζ_O) in the scene. Considering that this is a constant forward velocity along the y-axis with velocity components $\upsilon_\xi = 0$ and $\upsilon_\zeta = \upsilon$, the position of the object changes in the scene to $\xi = \xi_O$ and $\zeta = \zeta_O - \upsilon^*\tau$ over time, τ. From the driver's perspective, the object will appear in polar coordinates at a distance $\rho = \text{sqrt}(\xi^*\xi + \zeta^*\zeta)$ and bearing $\phi = \text{arctangent}(\xi/\zeta)$ moving with velocity $-\upsilon$. Since the direction of travel is along a straight line, the radial distance to the object as a function of bearing is $\rho = \xi_O^*\csc(\phi)$, and the corresponding radial angular velocity is $\omega_\rho = -(\upsilon/\xi_O)^*\cos(\phi)^*\sin(\phi)$ and the rotational angular velocity $\omega_\phi = -(\upsilon/\xi_O)^*\sin^2(\phi)$. Of course, the driver experiences no acceleration in this driving configuration.

Consider now a scene compressed by the display in angular FOV by the ratio of the scene FOV to that of the display, α. The object is compressed in linear dimensions by the same ratio along with the other elements in the scene. Because the object is identifiable with a known size by the driver, it appears perceptually at a greater range, $\rho_\alpha = \rho^*\alpha$, and a reduced angular bearing, $\phi_\alpha = \phi/\alpha$. The object appears to be located in the compressed display at the point $(\xi_\alpha,\zeta_\alpha)$, in which $\xi_\alpha = \rho_\alpha^*\sin(\phi_\alpha)$ and $\zeta_\alpha = \rho_\alpha^*\cos(\phi_\alpha)$. Again, considering a constant forward velocity along the y-axis, the apparent coordinates of the object's location reduce to $\xi_\alpha = \xi_O^*\alpha^*\csc(\phi)^*\sin(\phi_\alpha)$, and $\zeta_\alpha = \xi_O^*\alpha^*\csc(\phi)^*\cos(\phi_\alpha)$. The components of the apparent velocity of the object on the display are given by

$$\upsilon_{\xi\alpha} = -(\upsilon^*\alpha)^*[\cos(\phi_\alpha)/\alpha - \sin(\phi_\alpha)^*\cot(\phi)]^*\sin(\phi),$$

and

$$\upsilon_{\zeta\alpha} = -(\upsilon^*\alpha)^*[\sin(\phi_\alpha)/\alpha - \cos(\phi_\alpha)^*\cot(\phi)]^*\sin(\phi).$$

At a great distance, these velocities reduce to $\upsilon_{\xi\alpha} = 0$ and $\upsilon_{\zeta\alpha} = -(\upsilon^*\alpha)$, as the bearing approaches zero. The object appears to move toward the driver with an increased average speed $\upsilon_\alpha = -(\upsilon^*\alpha)^*(\cos(\phi_\alpha)/\cos(\phi))$, since the object appears smaller but takes the same time to be driven past. Now, although the driver experiences no acceleration, the velocity field appears to be accelerating as the object is approached. For these reasons, the display compression distorts the real-world scene in space and speed.

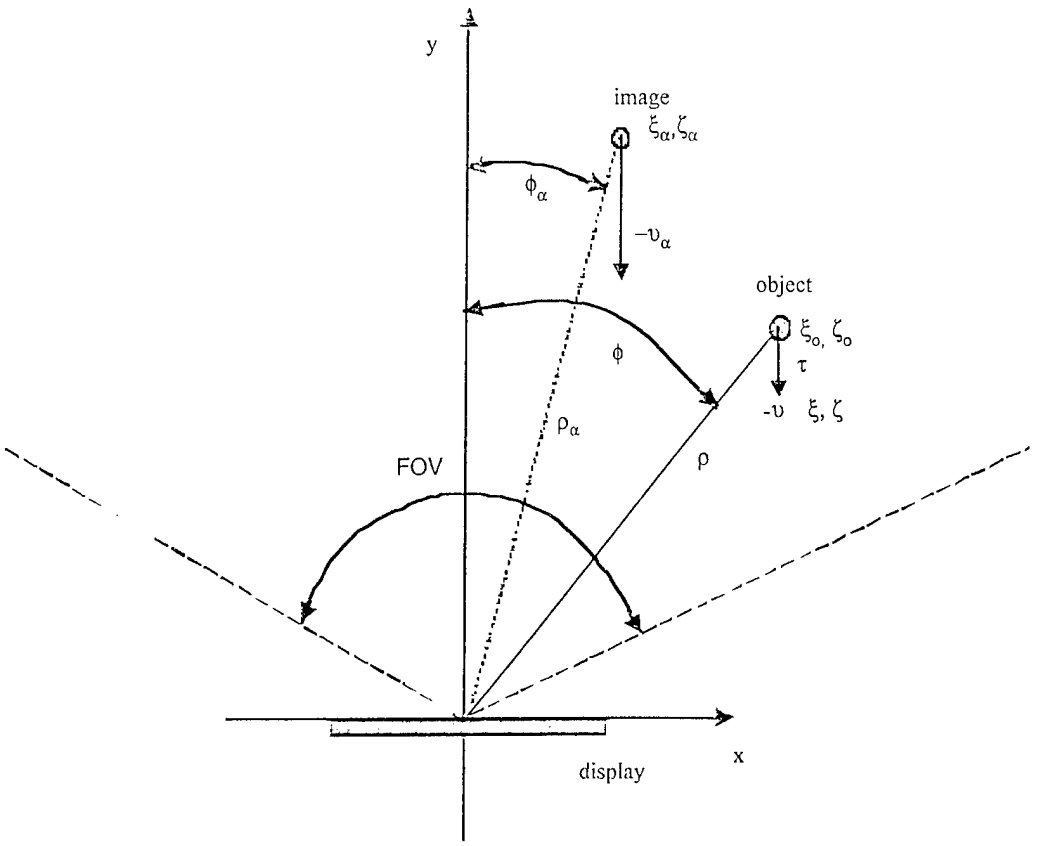

Figure B-1. Terrain Geometry.

Figures B-2 through B-4 are distortion plots of the real-world map plane overlaid onto the display world plane as derived from the previous expressions for the different compression ratios used in this study. Here, the display y-axis is aligned with the longitudinal axis of the vehicle and the x-axis is the pitch axis. The figures show a grid for the right side of the vehicle with the real scene ground surface mapped onto the Cartesian coordinates of the display ground scene. The grid is divided into relative values for the x and y coordinates with the coordinate system centered on the display. Relative approach speeds are shown as straight radial lines from the display viewing point as a function of the bearing. Superimposed on the figure are the angles subtended by the central and side displays that were used in this study. Considering a distant object being approached directly, the figures show from the mapping of the constant x-value lines, how the locus of locations of the object in the real world is distorted in the display world. The figures show that an object on such a constant x-value line appears more distant than it is while the path of approach bend outward with the mapping, and the apparent speed increases as the object approaches the vehicle. For this reason, as it is approached, the object appears to move farther laterally and faster on the display than it would in the real scene. Furthermore, since the real scene center of rotation for vehicle turns is a point on the x-axis (y = 0) with the turning radius determined by the steering wheel setting, the

turning point is visible in the side displays for the wide and extended compressed scenes.

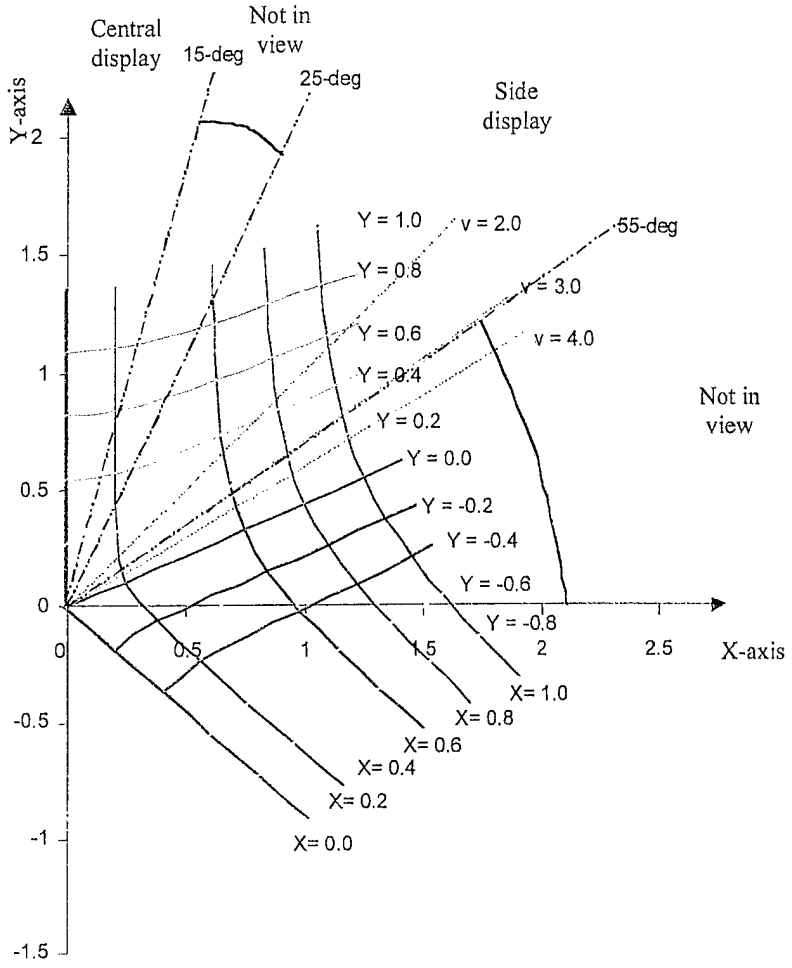

Figure B-2. Scene Compression Distortion Plot for the Near-unity FOV.

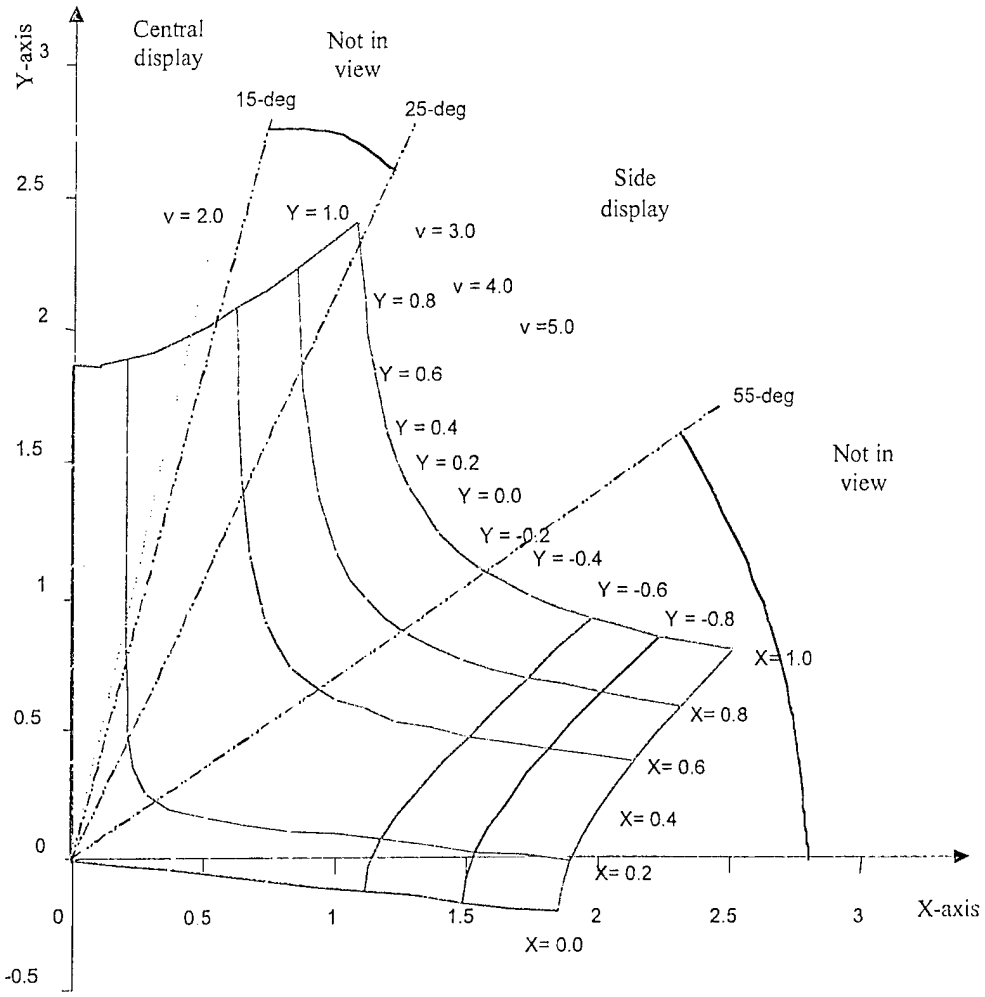

Figure B-3. Scene Compression Distortion Plot for the Wide FOV.

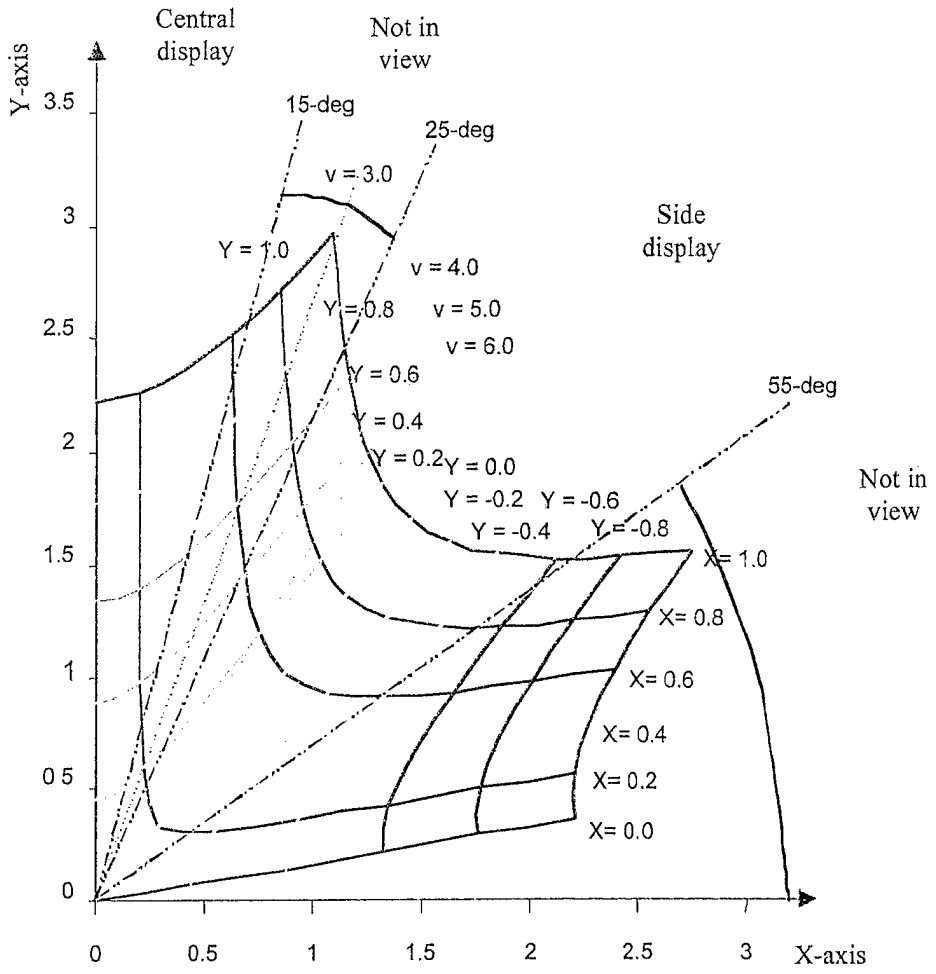

Figure B-4. Scene Compression Distortion Plot for the Extended FOV.

INTENTIONALLY LEFT BLANK

APPENDIX C

FORMS FOR INFORMED CONSENT BRIEFING AND FIRST AND FOURTH TEST SET QUESTIONNAIRES

INTENTIONALLY LEFT BLANK

SUBJECT CONSENT BRIEFING

Protocol: A comparison of direct vision driving with indirect vision driving using fixed flat-panel displays for unity, narrow and wide fields of camera view.

Investigator: Christopher Smyth
Army Research Laboratory
Human Research & Engineering Directorate
Soldier Systems Control Branch

INTRODUCTION: In support of TARDEC's development of the two-man tank concept vehicle, we are conducting a research study on the ability of soldiers to drive a moving vehicle with a camera system and panel mounted video displays. The test participant will drive a HMMWV with a forward viewing camera array attached to the front roof of the vehicle. The camera outputs are seen on three fixed flat-panel displays that are mounted in the cab area in front of the driver. The displays are mounted in front of the windshield and the driver's portion of the cab will be completely enclosed to prevent direct viewing. The displays are arranged with a central display directly in front of the driver, and left and right side displays. The video signal from the central camera feeds the central display and the two side cameras feed the corresponding side displays.

The participant will drive the vehicle over a test course as he normally would with direct viewing, and with the displays in place for three camera lens settings: 41-degrees, 56-degrees, and 67-degrees. The test course is about one-half mile in length and located on an open field enclosed by barriers to prevent other traffic and people from entering. An experimenter will ride with the participant to collect data and serve as a safety officer using an auxiliary brake to stop the vehicle if necessary. The participant will wear a safety helmet and a commercially available heart rate chest band and wrist recorder. Between test runs, the participant will be asked to fill out questionnaires on perceived workload and SA, on motion sickness, and the effects of the different camera settings upon his driving performance. These questionnaires will include an effective and cognitive battery of tests for stress level evaluation.

Risks: There are minimal risks associated with this experiment. The test is being conducted on a ground vehicle test site with concrete barriers to prevent traffic flow by others. The participant's vehicle will be the only one on the test course. A safety officer will ride with the participant throughout the test and he will have a vehicle safety brake for the participant's protection.

A potential risk concerns motion sickness which can occur in some people while riding in enclosed compartments. Symptoms of motion sickness are nausea, cold sweating, pallor, and possible vomiting. The participant will have the right to stop the experiment at any time by telling the safety officer of his condition. Motion sickness bags will be positioned near the driver's seat. For safety reasons,

the participant will wear a safety belt whenever the HMMWV is moving. In addition, the participant will receive an orientation and safety briefing before beginning the test.

Benefits: The participant will be helping in research on the usefulness of novel video display technology that is being considered by military designers for the design.

Estimating Workload Attention Allocation Questionnaire

Subject: Date: Time:

Test Condition:

Please check all workload elements performed during this test condition.

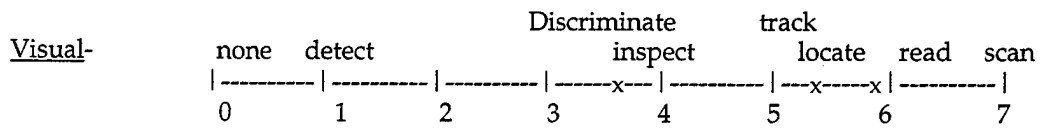

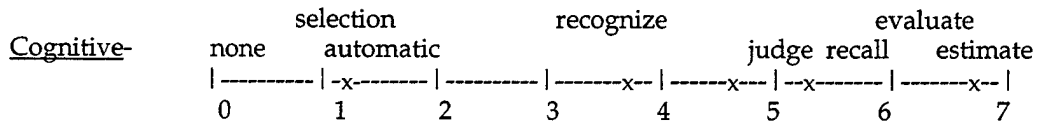

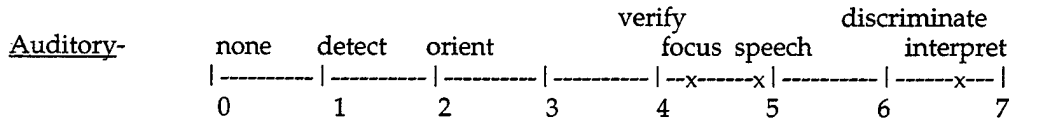

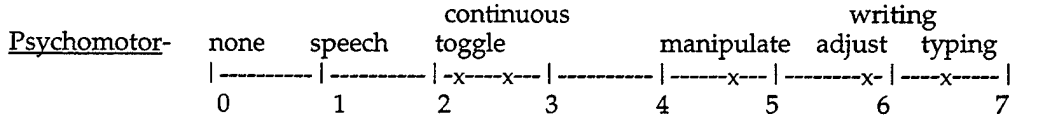

Estimating Workload Scales

1. Visual Loading-

Scale Value	*Descriptor*
0.0	No Visual Activity
1.0	Visual Register/Detect (detect occurrence of image)
3.7	Visual Discriminate (detect visual differences)
4.0	Visual Inspect/Check (discrete inspection/static condition)
5.0	Visual Locate/Align (selection orientation)
5.4	Visually Track/Follow (maintain orientation)
5.9	Visually Read (symbol)
7.0	Visually Scan/Search Monitor (continuous/serial inspection, multiple conditions)

2. Cognitive Loading-

Scale Value	*Descriptor*
0.0	No Cognitive Activity
1.0	Automatic (simple association)
1.2	Alternative Selection
3.7	Sign/Signal Recognition
4.6	Evaluation/Judgement (consider single aspect)
5.3	Encoding/Decoding, Recall
6.8	Evaluation/Judgement (consider several aspects)
7.0	Estimation, Calculation, Conversion.

3. Auditory Loading-

Scale Value	*Descriptor*
0.0	No Auditory Activity
1.0	Detect/register sound (detect occurrence of sound)
2.0	Orient to Sound (general orientation./attention)
4.2	Orient to Sound (selective orientation./attention)
4.3	Verify Auditory Feedback (detect occurrence of anticipated sound)
4.9	Interpret Semantic Content (speech)
6.6	Discriminate Sound Characteristics (detect auditory differences)
7.0	Interpret Sound Patterns (pulse rates, etc.)

4. Psychomotor Loading-

Scale Value	*Descriptor*
0.0	No Psychomotor Activity
1.0	Speech
2.2	Discrete Actuation (button, toggle, trigger)
2.6	Continuous Adjustment (movement control, sensor control)
4.6	Manipulative
5.8	Discrete Adjustive (rotary, vertical thumbwheel, level position)
6.5	Symbolic Production (writing)
7.0	Serial Discrete Manipulation (keyboard entries)

NASA Task Load Index (TLX) workload rating form.

Subject: Date: Time:

Test Condition:

Mental Demand: How much mental and perceptual activity was required (e.g. thinking, looking, searching, etc.)? Was the task easy or demanding, simple or complex, exacting or forgiving?

Low |----|----|----|----|----|----|----|----|----|----| high

Physical demand: How much physical activity was required (e.g. pushing, pulling, turning, controlling, activating, etc.)? Was the task easy or demanding, slow or brisk, slack or strenuous, restful or laborious?

Low |----|----|----|----|----|----|----|----|----|----| high

Temporal demand: How much time pressure did you feel due to the rate or pace at which the task or task elements occurred? Was the pace slow and leisurely or rapid and frantic?

Low |----|----|----|----|----|----|----|----|----|----| high

Effort: How hard did you have to work (mentally and physically) to accomplish your level of performance?

Low |----|----|----|----|----|----|----|----|----|----| high

Performance: How successful do you think you were in accomplishing the goals of the task set by the experimenter (or yourself)? How satisfied were you with your performance in accomplishing these goals?

Good |----|----|----|----|----|----|----|----|----|----| poor

Frustration: How insecure, discouraged, irritated, stressed and annoyed versus secure, gratified, content, relaxed and complacent did you feel during the task?

Low |----|----|----|----|----|----|----|----|----|----| high

Estimating Motion Sickness Questionnaire

Subject: Date: Time:

Test Condition:

Please rate the following measures of motion sickness:

General Discomfort	None	Slight	Moderate	Severe
Fatigue	None	Slight	Moderate	Severe
Headache	None	Slight	Moderate	Severe
Eyestrain	None	Slight	Moderate	Severe
Difficulty in Focusing	None	Slight	Moderate	Severe
Increased Salivation	None	Slight	Moderate	Severe
Sweating	None	Slight	Moderate	Severe
Nausea	None	Slight	Moderate	Severe
Difficulty in Concentrating	None	Slight	Moderate	Severe
Fullness of Head	None	Slight	Moderate	Severe
Blurred Vision	None	Slight	Moderate	Severe
Dizzy (eyes open)	None	Slight	Moderate	Severe
Dizzy (eyes closed)	None	Slight	Moderate	Severe
Vertigo *	None	Slight	Moderate	Severe
Stomach Awareness **	None	Slight	Moderate	Severe
Burping	None	Slight	Moderate	Severe

* Vertigo is experienced as loss of orientation with respect to vertical upright.
** Stomach awareness is usually used to indicate a feeling of discomfort which is just short of nausea.

Situation Awareness Rating Questionnaire

Subject: Date: Time:

Test Condition:

Please rate the following measures of situation awareness:

DEMAND			
Instability of situation:	low	1-------2-------3-------4-------5-------6-------7	high
Variability of situation:	low	1-------2-------3-------4-------5-------6-------7	high
Complexity of situation:	low	1-------2-------3-------4-------5-------6-------7	high
SUPPLY			
Arousal:	low	1-------2-------3-------4-------5-------6-------7	high
Spare Mental Capacity:	low	1-------2-------3-------4-------5-------6-------7	high
Concentration:	low	1-------2-------3-------4-------5-------6-------7	high
Division of attention:	low	1-------2-------3-------4-------5-------6-------7	high
UNDERSTANDING			
Information Quantity:	low	1-------2-------3-------4-------5-------6-------7	high
Information Quality:	low	1-------2-------3-------4-------5-------6-------7	high
Familiarity:	low	1-------2-------3-------4-------5-------6-------7	high

SUBJECTIVE STRESS SCALE

Circle one word that best describes how you feel right now.

Wonderful

Fine

Comfortable

Steady

Not Bothered

Indifferent

Timid

Unsteady

Nervous

Worried

Unsafe

Frightened

Terrible

In Agony

Scared Stiff

Route Selection Test

Subject: Date: Time:

Test Condition:

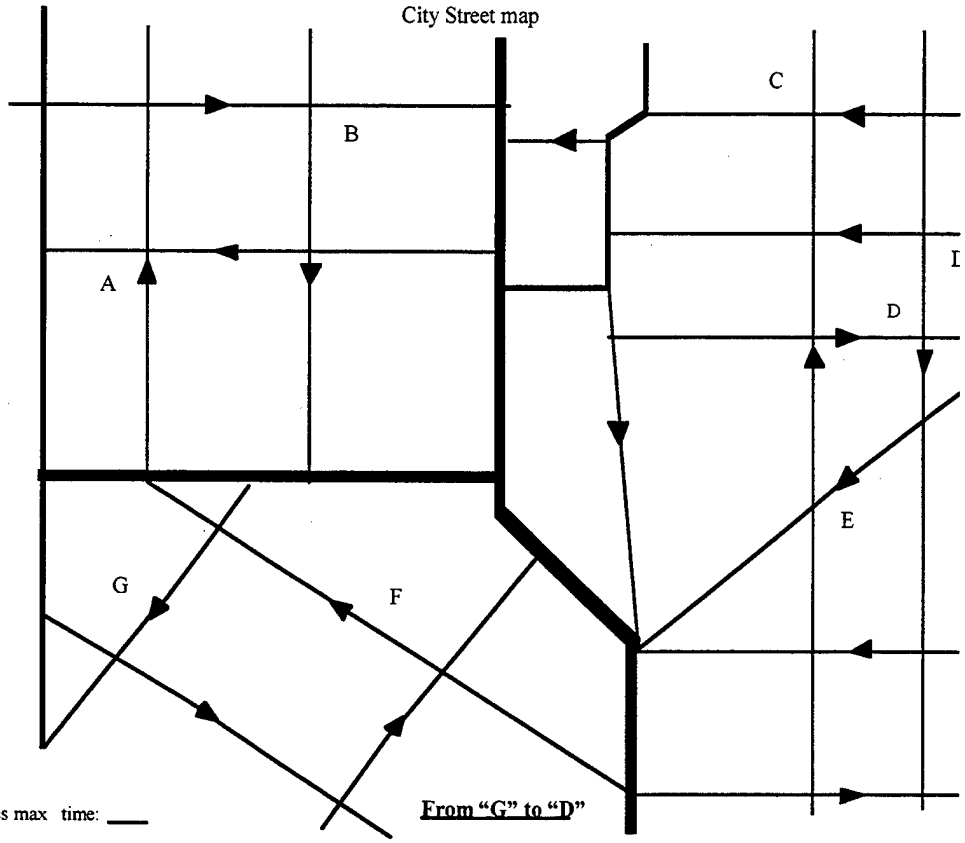

Exit evaluation of the display systems.

Subject: Date:

Please rate the display system on the following indices relative to what you feel is needed for good driving:

Display system: Direct Vision
Unity: 150 ° camera FOV
Wide: 205 ° camera FOV
Extended: 257 ° camera FOV

Image Quality :	low	1-------2-------3-------4-------5-------6-------7	high
Update rate :	low	1-------2-------3-------4-------5-------6-------7	high
Time delay :	low	1-------2-------3-------4-------5-------6-------7	high
Scene FOV :	low	1-------2-------3-------4-------5-------6-------7	high
Eye movements:	low	1-------2-------3-------4-------5-------6-------7	high
Head movements:	low	1-------2-------3-------4-------5-------6-------7	high
Steering activity:	low	1-------2-------3-------4-------5-------6-------7	high
Foot actions :	low	1-------2-------3-------4-------5-------6-------7	high
Workload :	low	1-------2-------3-------4-------5-------6-------7	high
Stress	low	1-------2-------3-------4-------5-------6-------7	high
Motion sickness :	low	1-------2-------3-------4-------5-------6-------7	high
Vehicle speed :	low	1-------2-------3-------4-------5-------6-------7	high
Road accuracy :	low	1-------2-------3-------4-------5-------6-------7	high
Overall Performance:	low	1-------2-------3-------4-------5-------6-------7	high

Comments:

APPENDIX D

BOX PLOTS FOR ATTENTION ALLOCATIONS

INTENTIONALLY LEFT BLANK

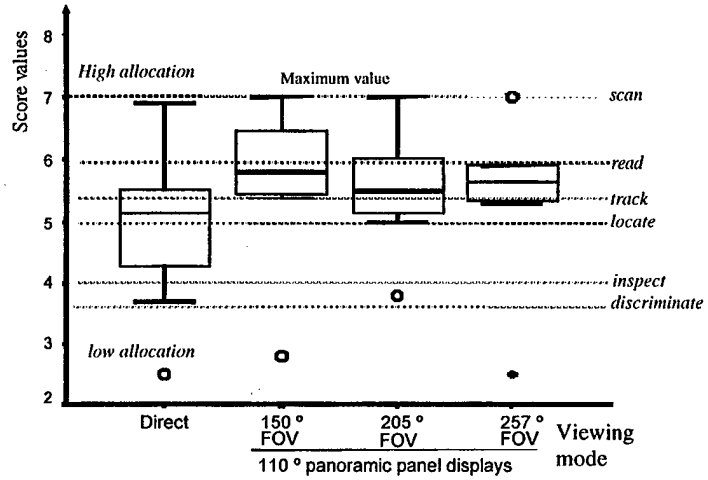

Figure D-1. Visual Channel Allocation.

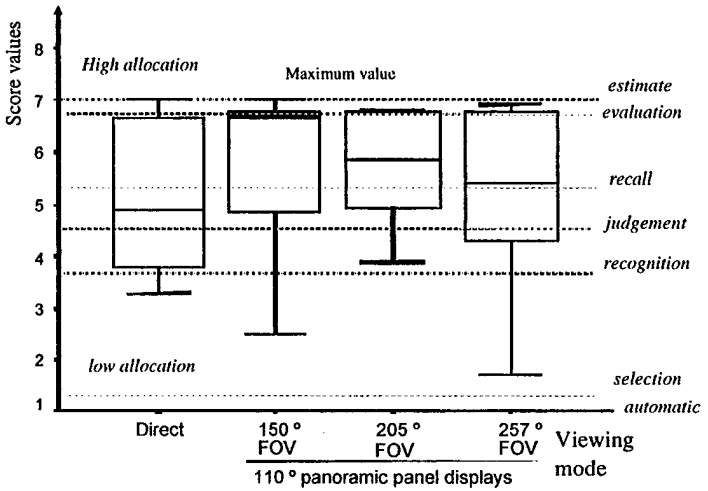

Figure D-2. Cognitive Channel Allocation.

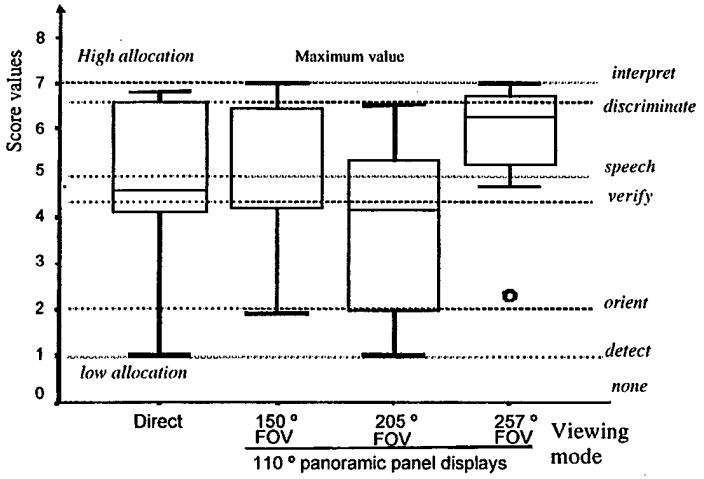

Figure D-3. Auditory Channel Allocation.

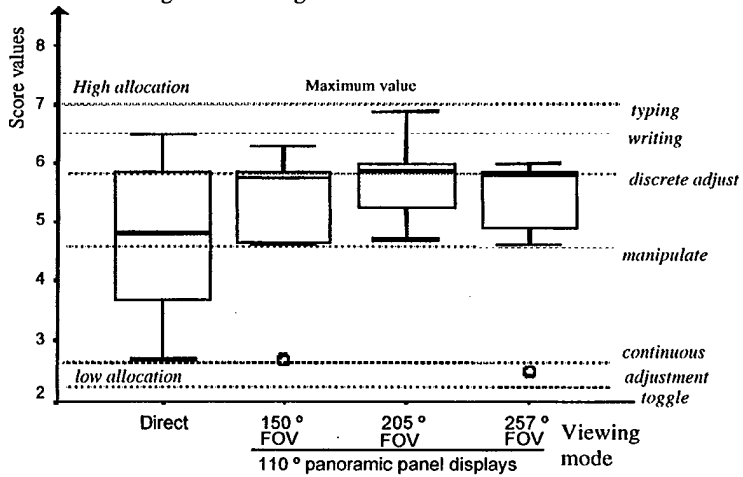

Figure D-4. Psychomotor Channel Allocation.

INTENTIONALLY LEFT BLANK

APPENDIX E

BOX PLOTS FOR PERCEIVED WORKLOAD QUESTIONNAIRE SCORES

INTENTIONALLY LEFT BLANK

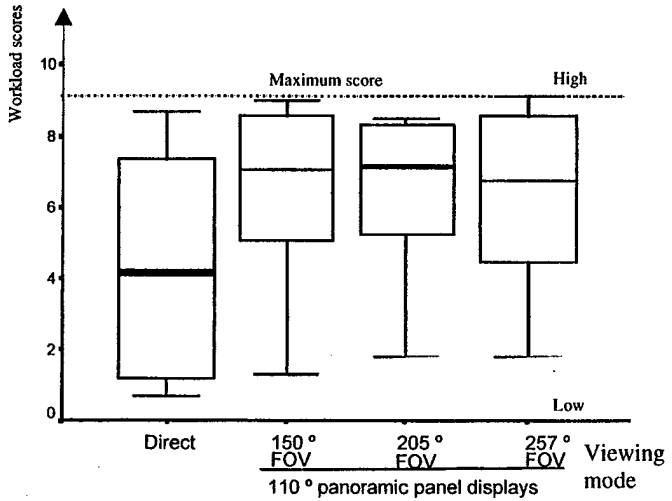

Figure E-1. TLX Mental Demand.

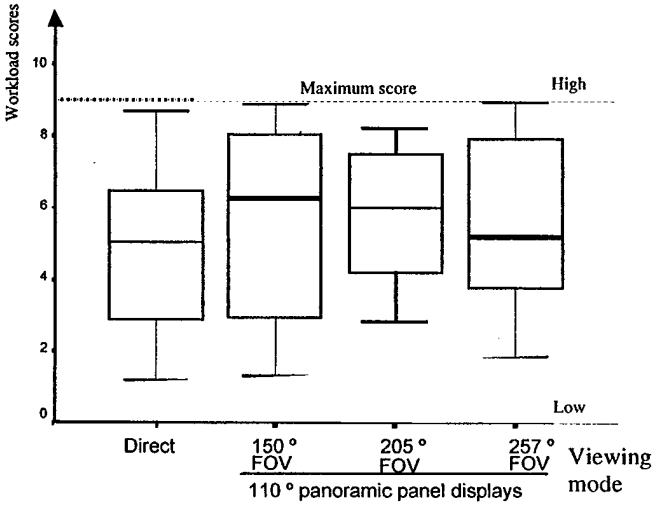

Figure E-2. TLX Physical Demand.

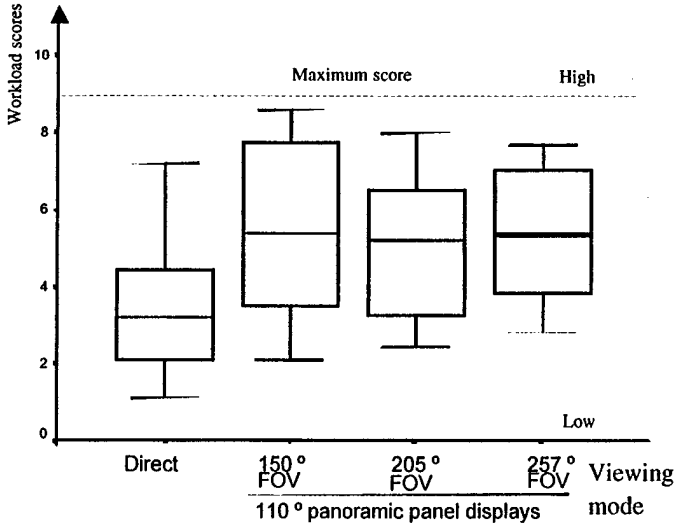

Figure E-3. TLX Temporal Demand.

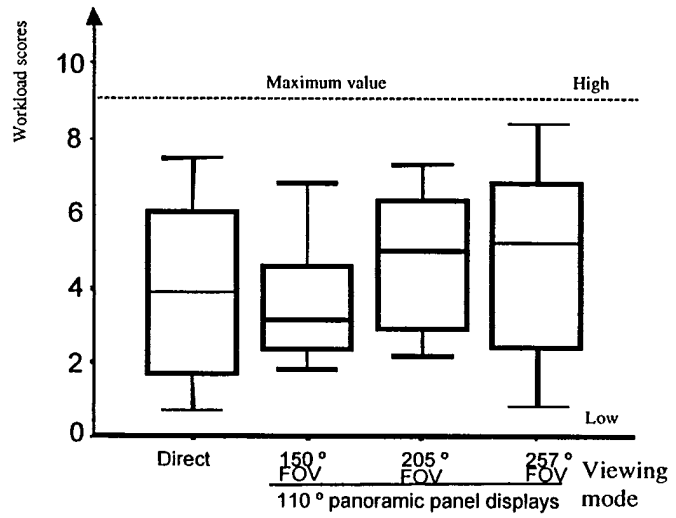

Figure E-4. TLX Interactive Effort.

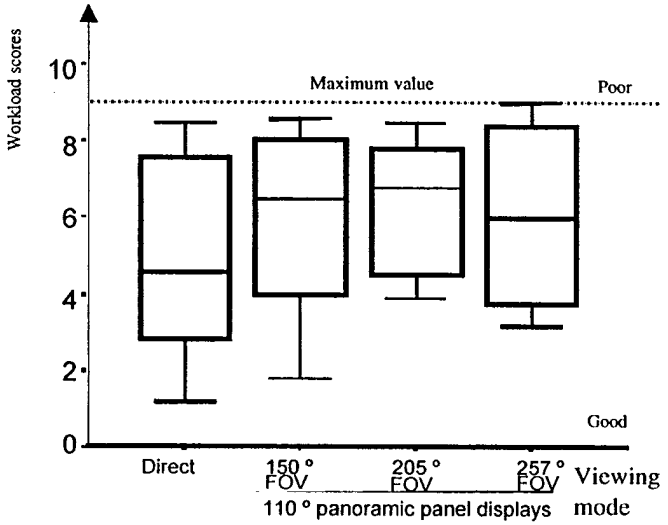

Figure E-5. TLX Interactive Performance.

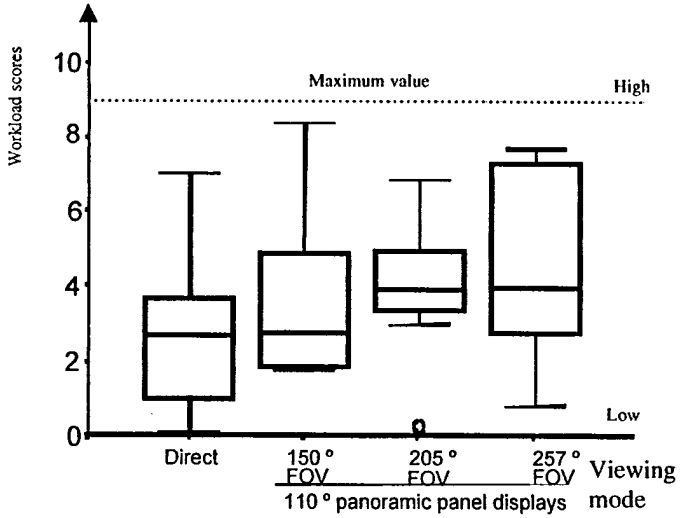

Figure E-6. TLX Interactive Frustration.

APPENDIX F

BOX PLOTS FOR SA QUESTIONNAIRE SCORES

INTENTIONALLY LEFT BLANK

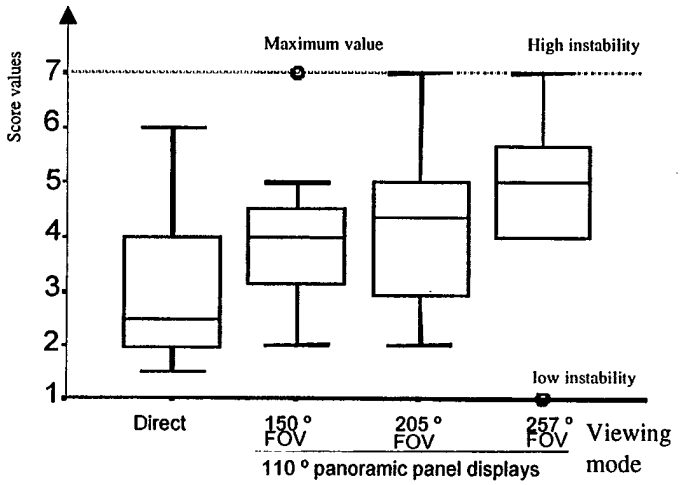

Figure F-1. SART Instability Demand.

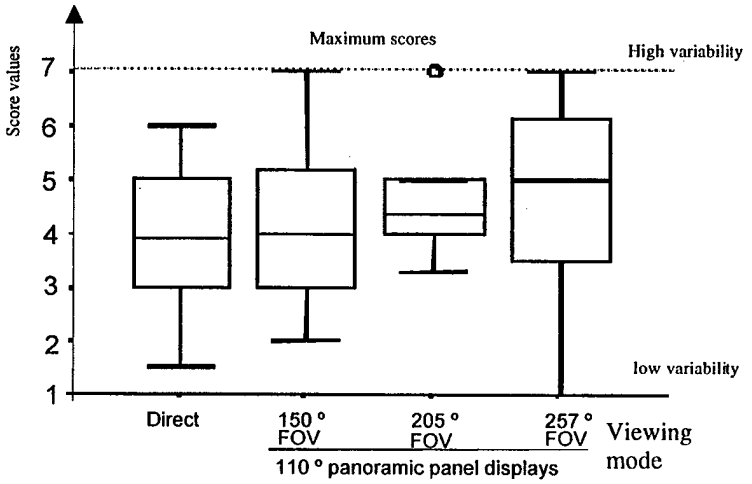

Figure F-2. SART Variability Demand.

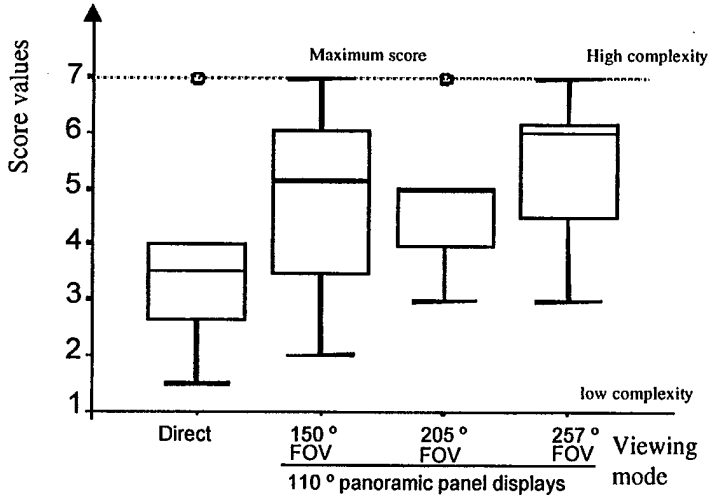

Figure F-3. SART Complexity Demand.

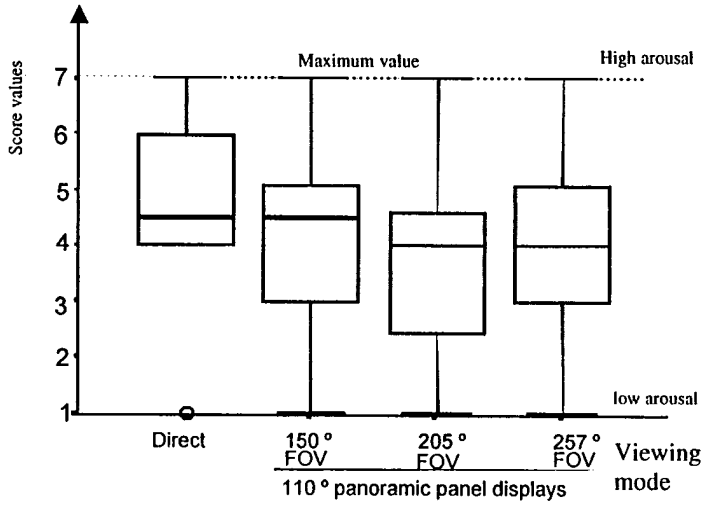

Figure F-4. SART Arousal Supply.

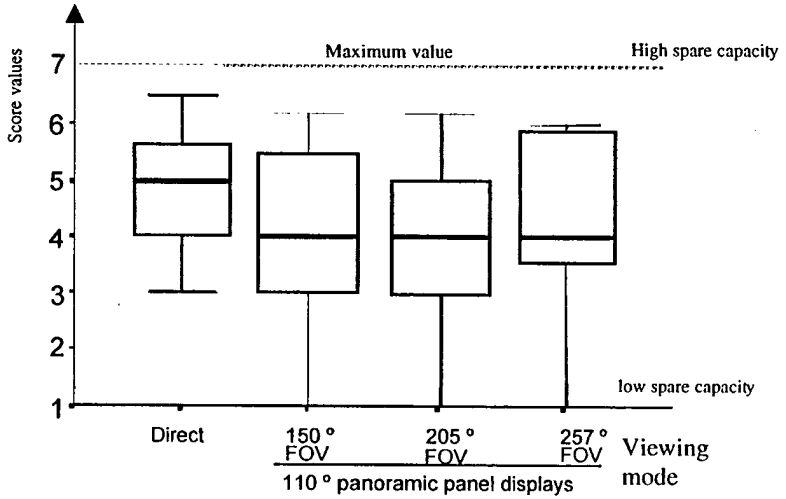

Figure F-5. SART Spare Mental Capacity Supply.

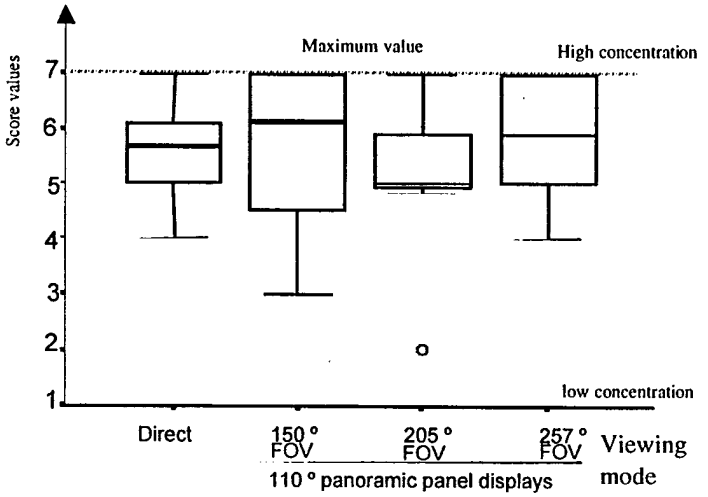

Figure F-6. SART Concentration Supply.

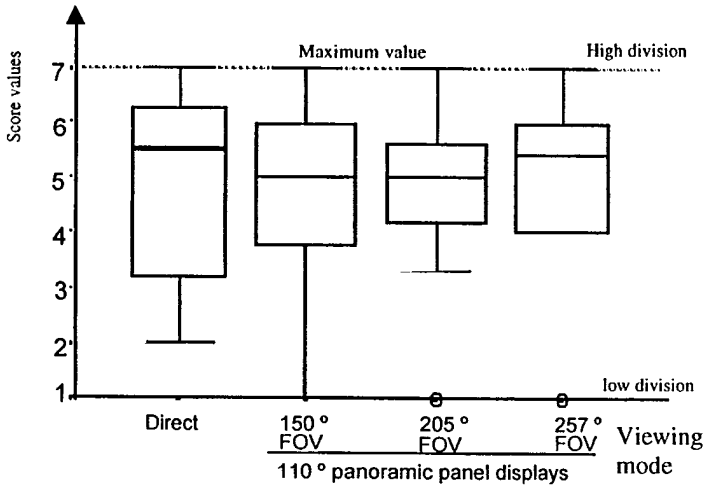

Figure F-7. SART Division of Attention Supply.

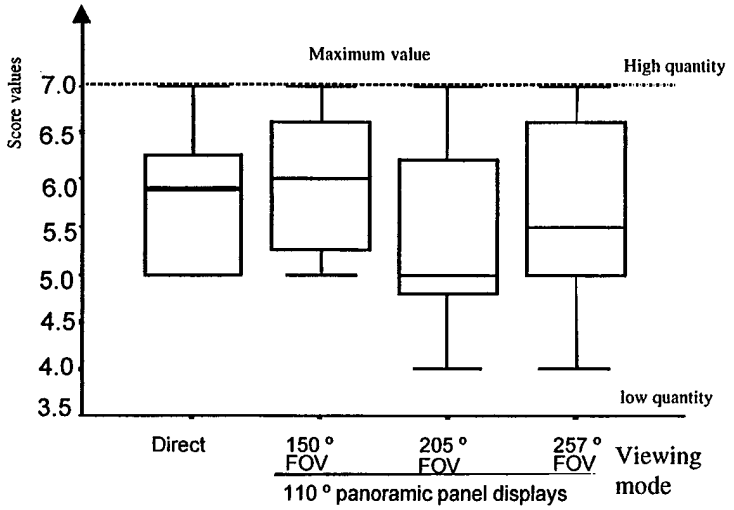

Figure F-8. SART Information Quantity for Understanding.

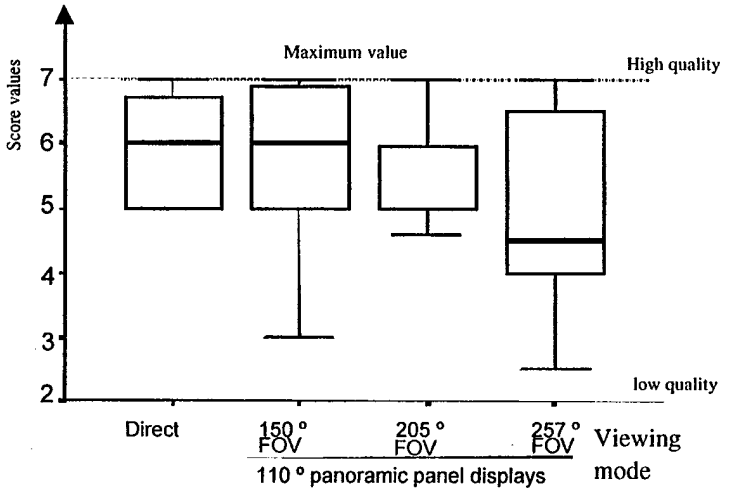

Figure F-9. SART Information Quality for Understanding.

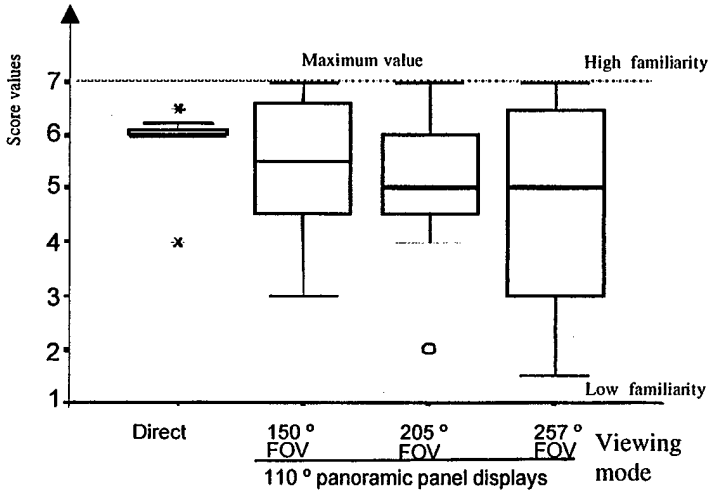

Figure F-10. SART Familiarity for Understanding.

INTENTIONALLY LEFT BLANK

APPENDIX G

BOX PLOTS FOR MOTION SICKNESS QUESTIONNAIRE SCORES

INTENTIONALLY LEFT BLANK

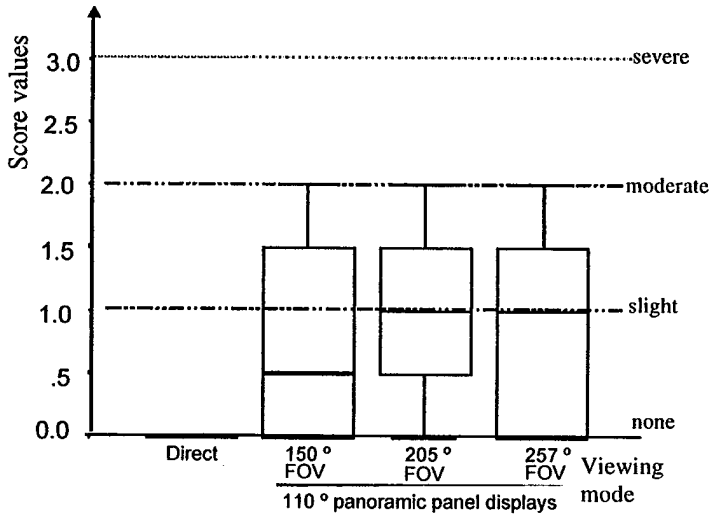

Figure G-1. General Discomfort.

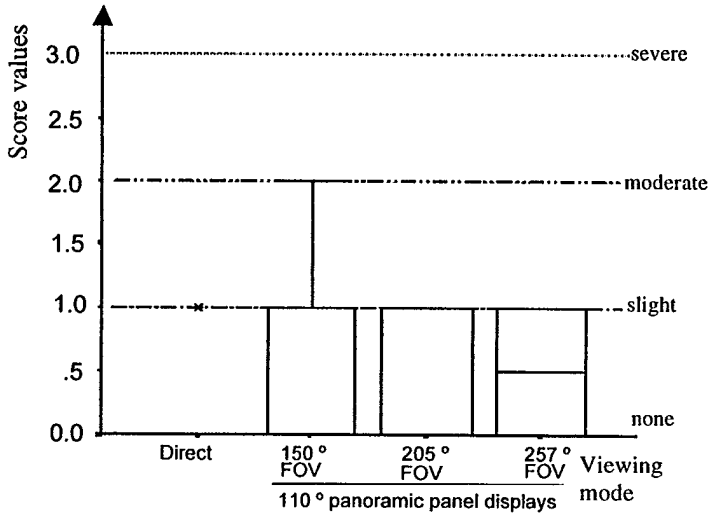

Figure G-2. Fatigue.

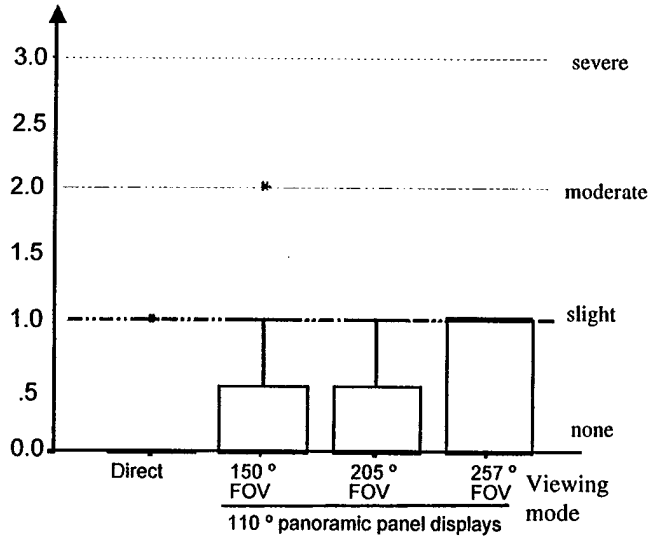

Figure G-3. Headache.

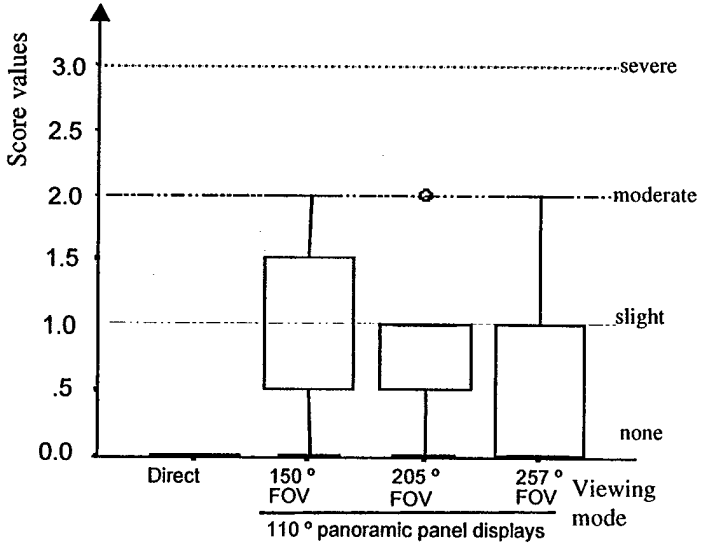

Figure G-4. Eyestrain.

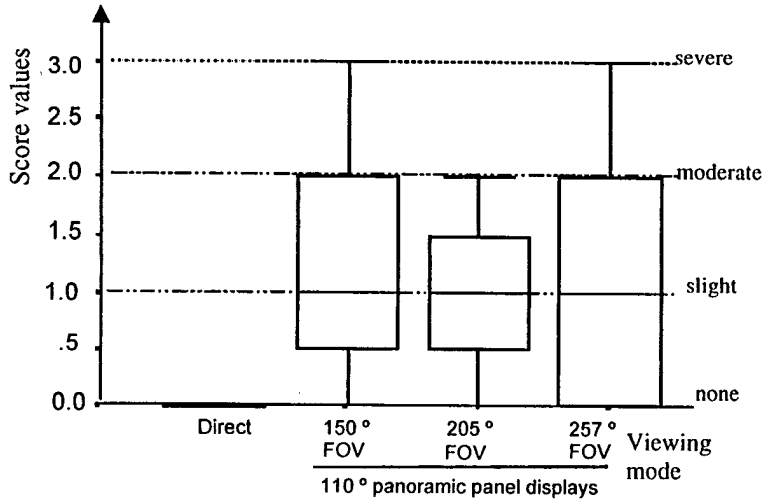

Figure G-5. Difficulty in Focusing.

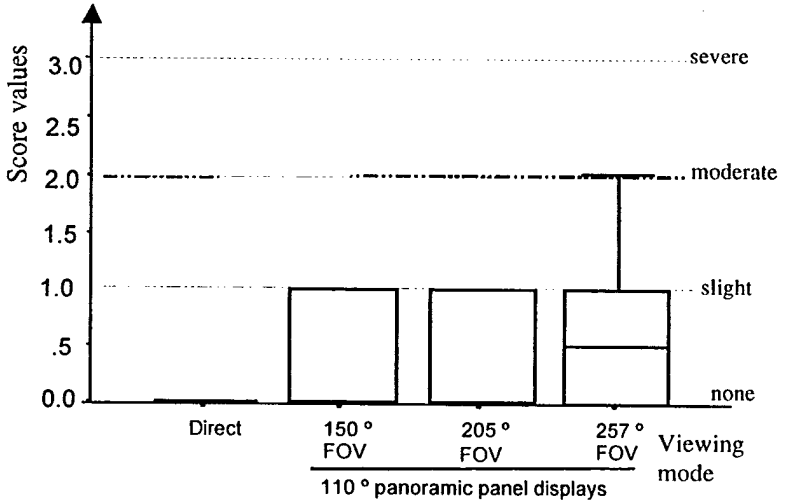

Figure G-6. Increased Salivation.

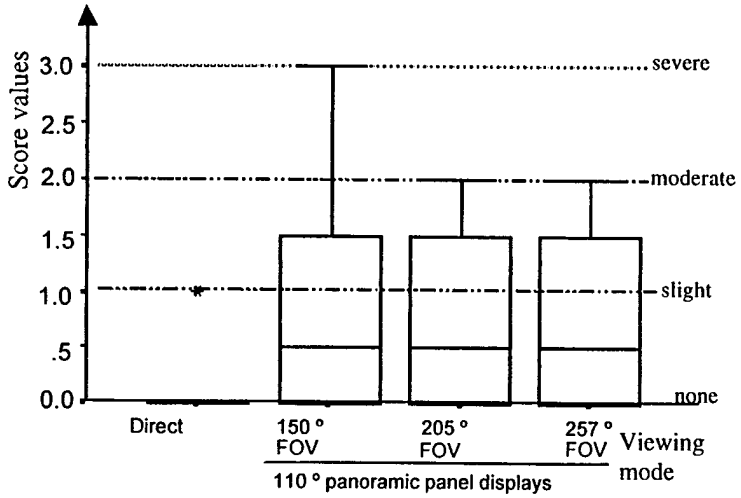

Figure G-7. Sweating.

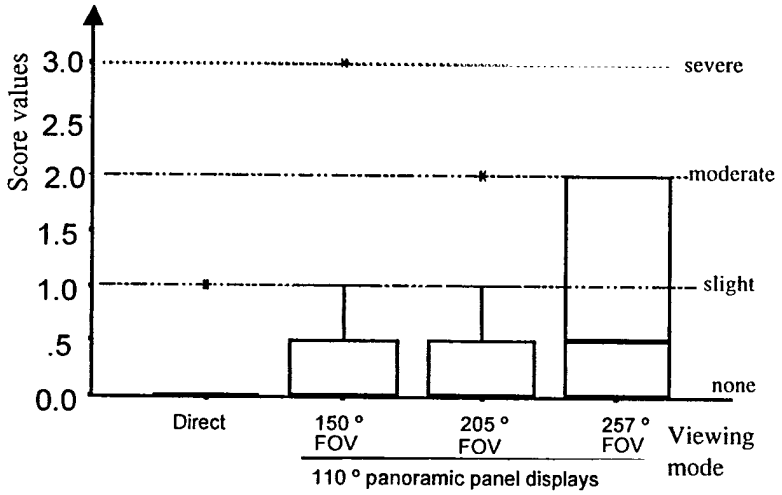

Figure G-8. Nausea.

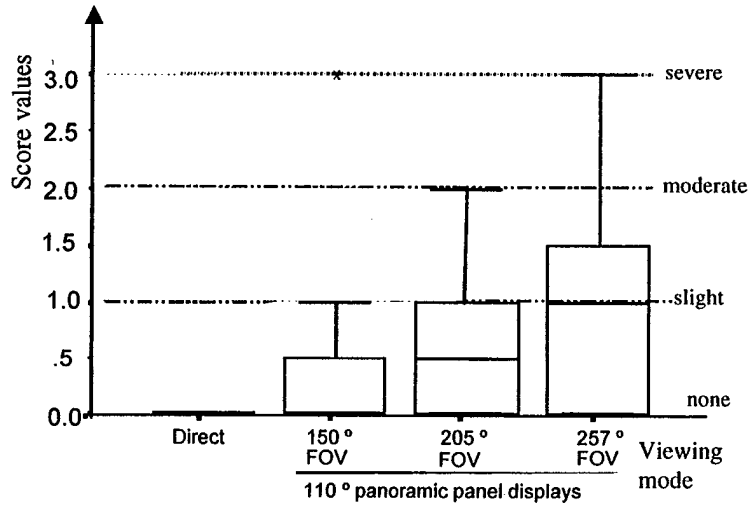

Figure G-9. Difficulty in Concentrating.

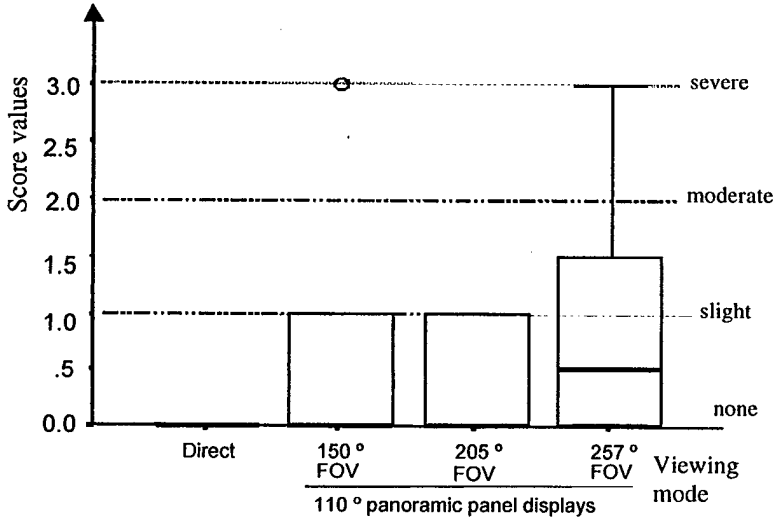

Figure G-10. Fullness of Head.

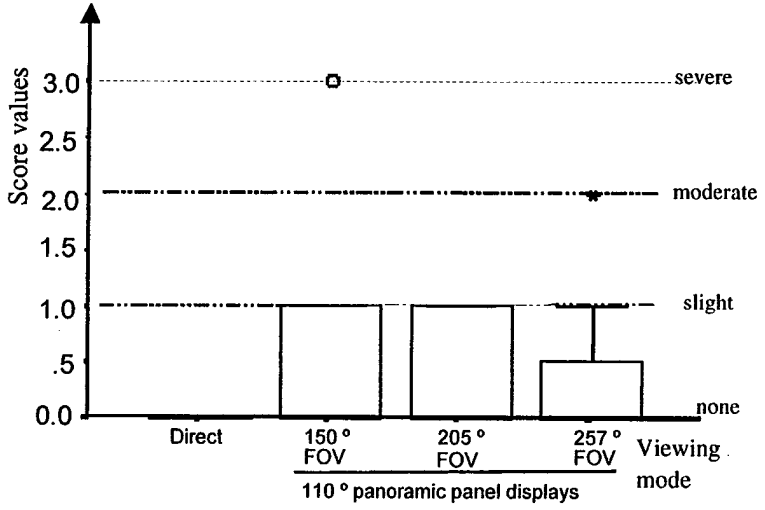

Figure G-11. Blurred Vision.

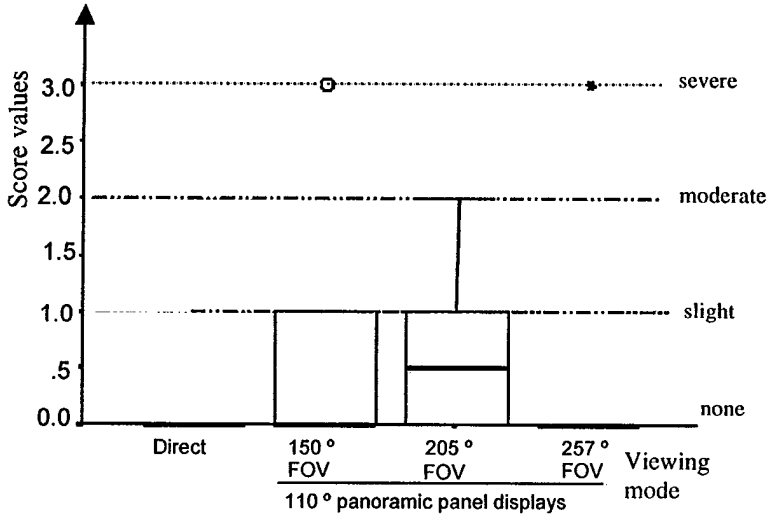

Figure G-12. Dizzy (eyes open).

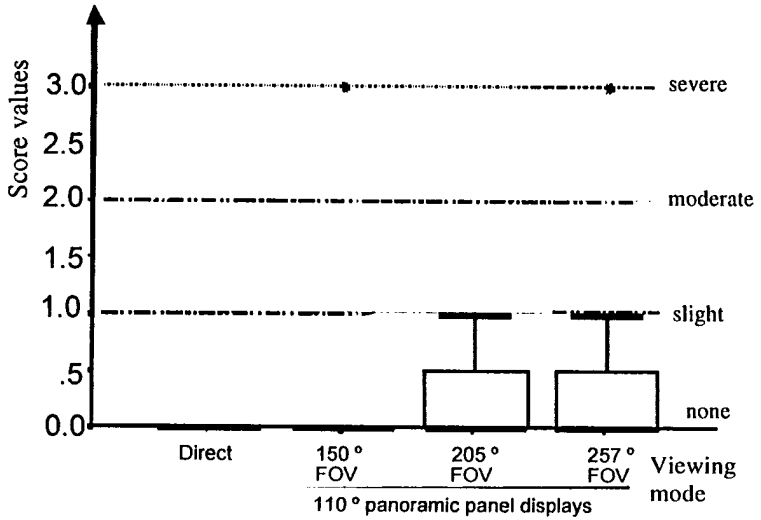

Figure G-13. Dizzy (eyes closed).

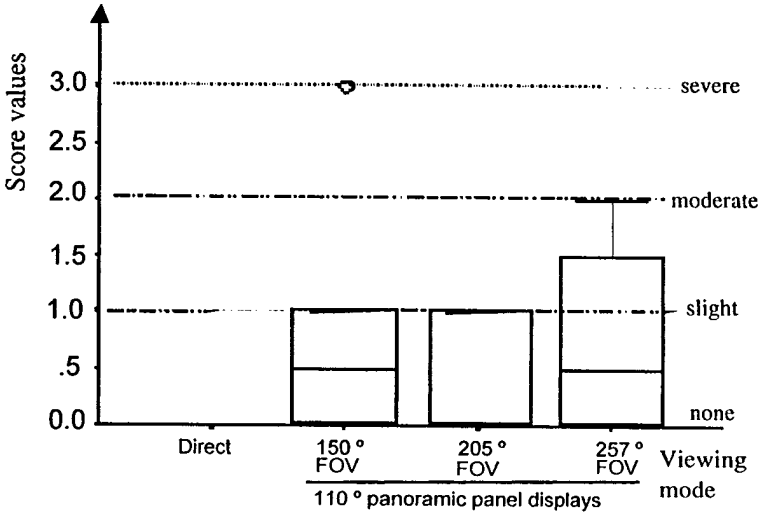

Figure G-14. Vertigo.

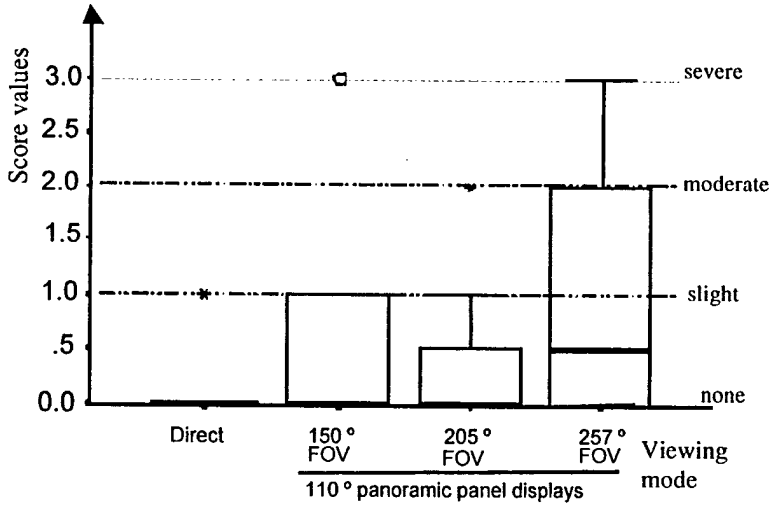

Figure G-15. Stomach Awareness.

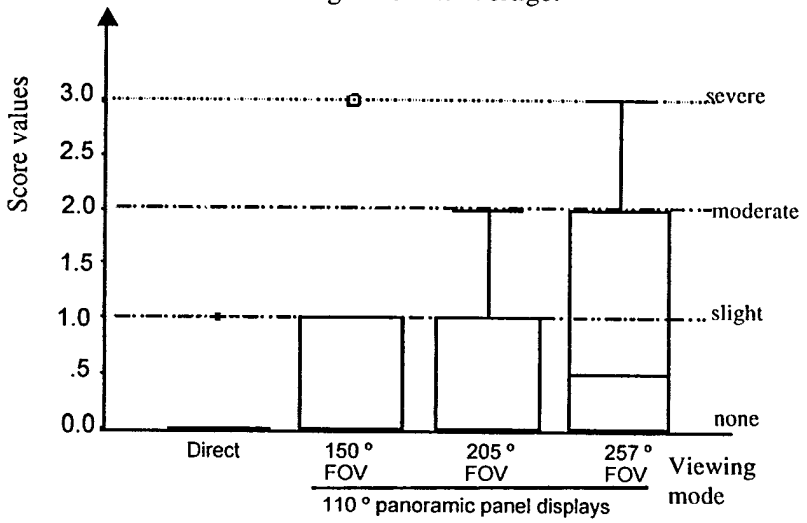

Figure G-16. Burping.

APPENDIX H

BOX PLOTS FOR COGNITIVE TESTS

INTENTIONALLY LEFT BLANK

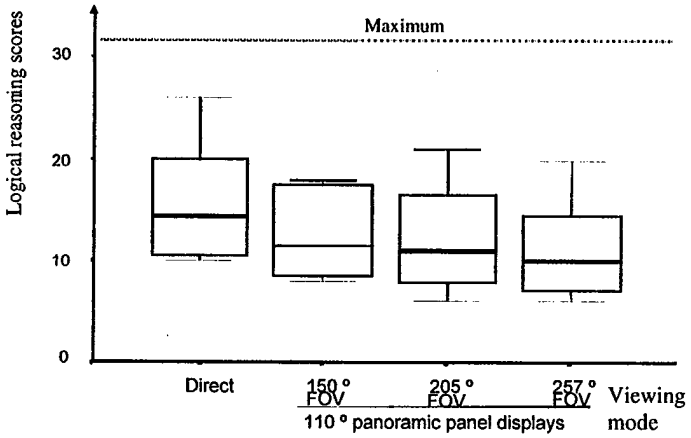

Figure H-1. Logical Reasoning.

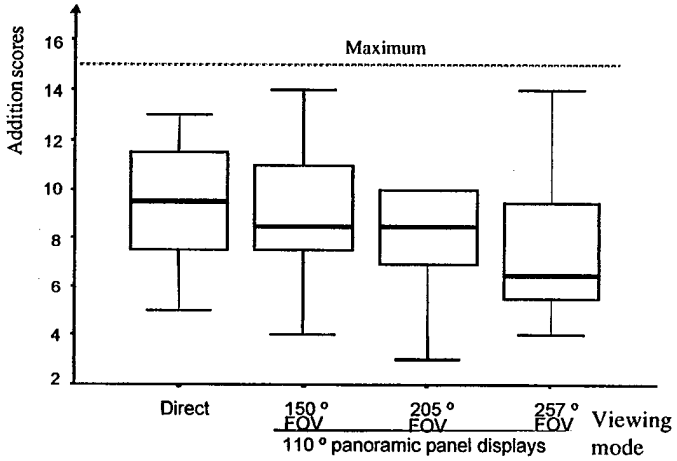

Figure H-2. Addition.

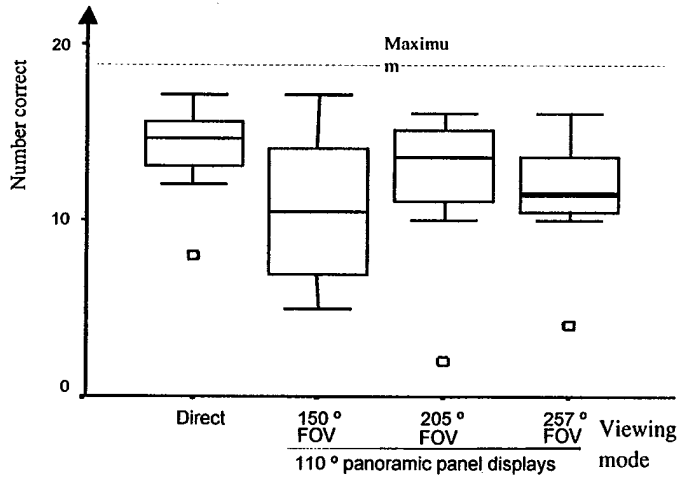

Figure H-3. Spatial Rotation.

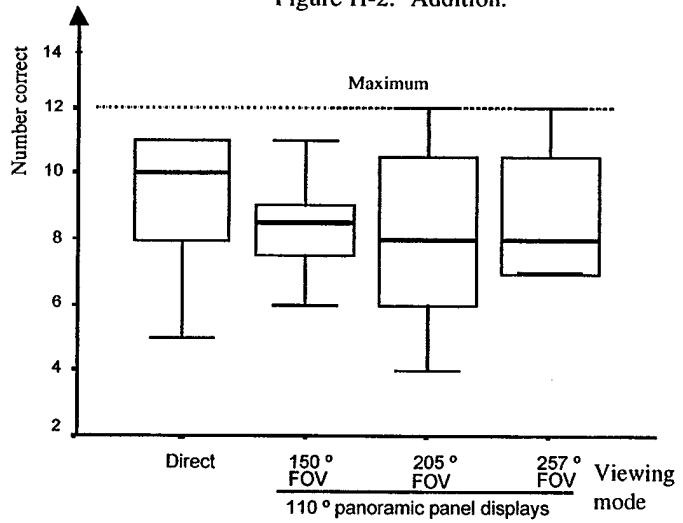

Figure H-4. Word Recall.

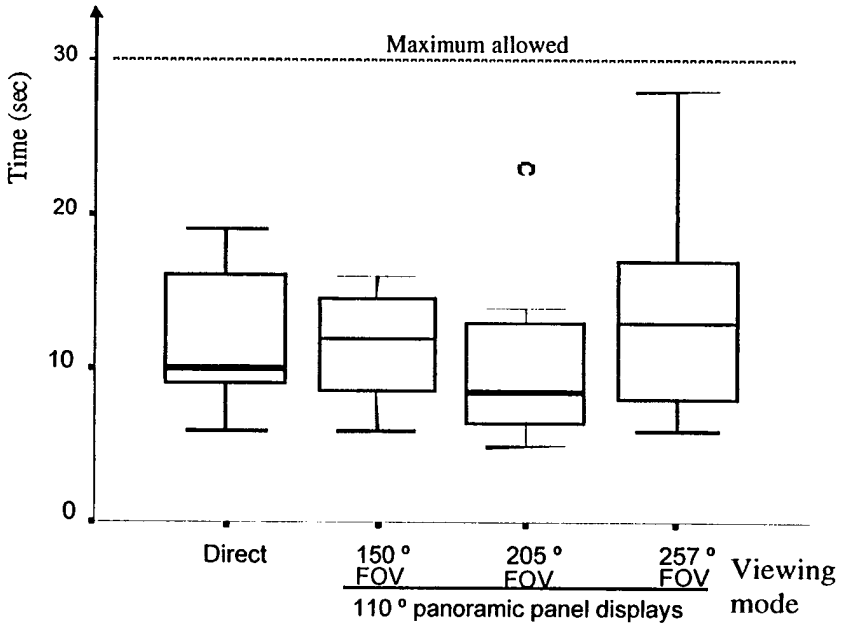

Figure H-5. Map Route Selection Time.

APPENDIX I

BOX PLOTS FOR EXIT EVALUATION QUESTIONNAIRE SCORES

INTENTIONALLY LEFT BLANK

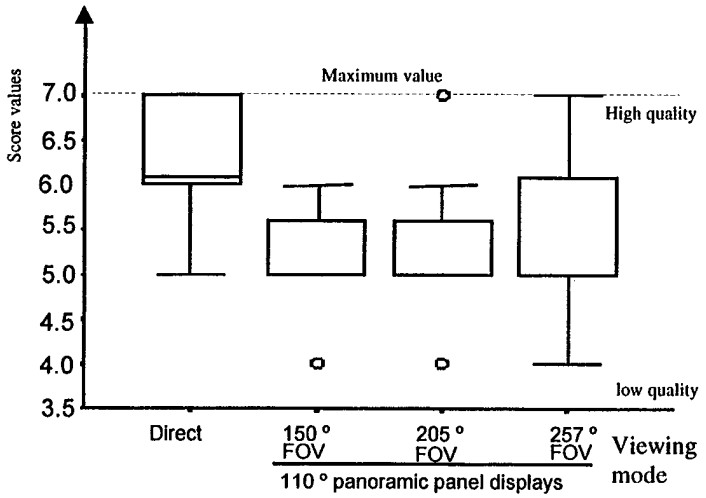

Figure I-1. Display Image Quality.

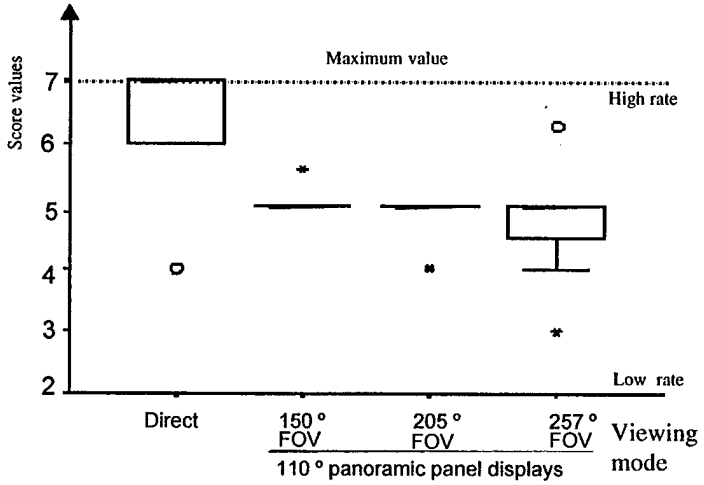

Figure I-2. Display Refresh Rate.

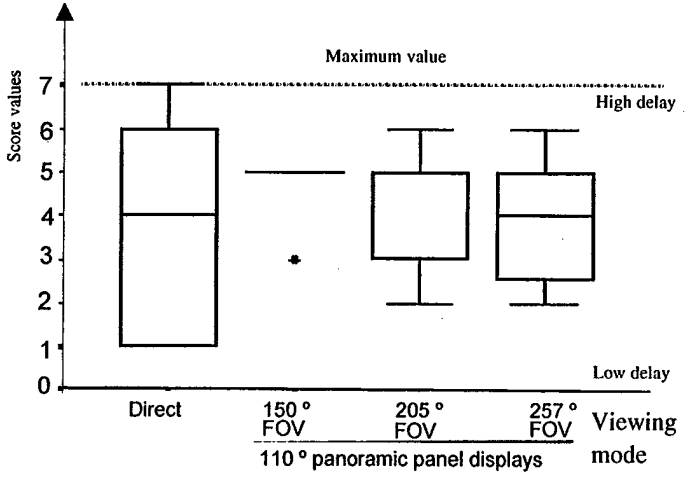

Figure I-3. Display Time Delay.

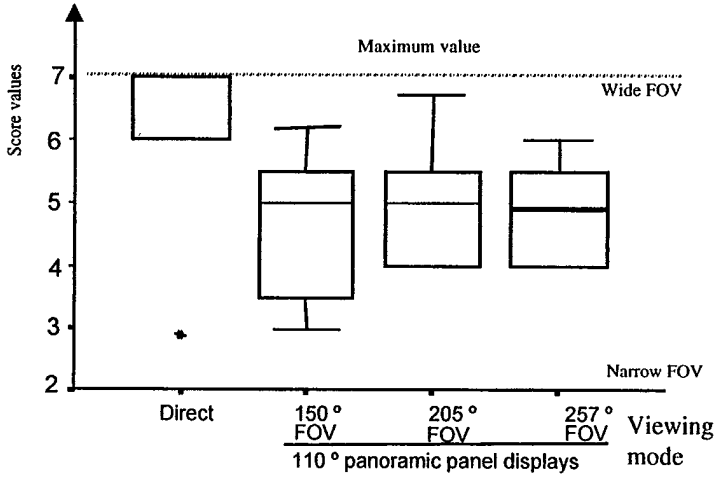

Figure I-4. Display FOV.

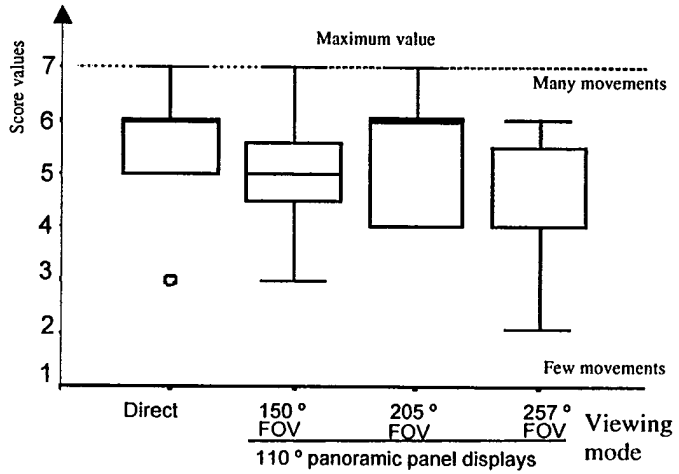

Figure I-5. Eye Movement Activity.

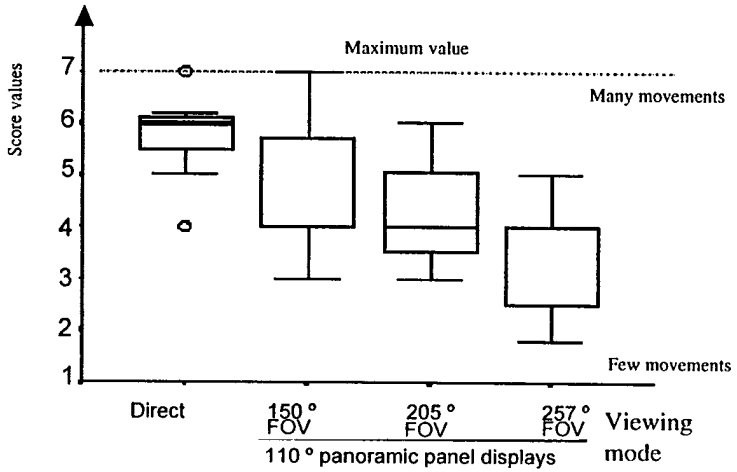

Figure I-6. Head Movement Activity.

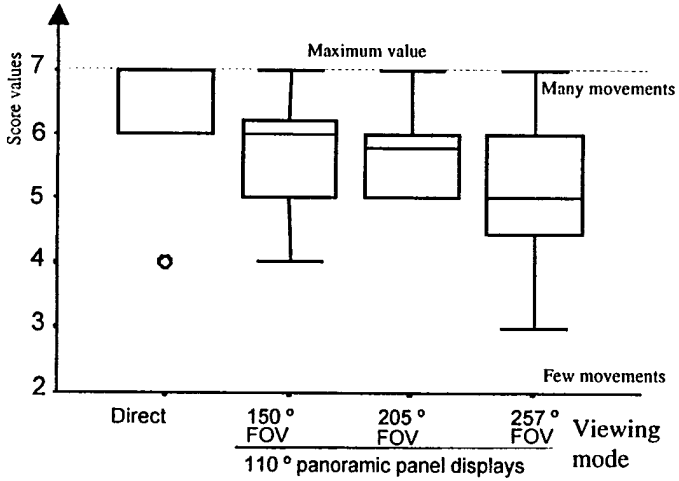

Figure I-7. Steering Activity.

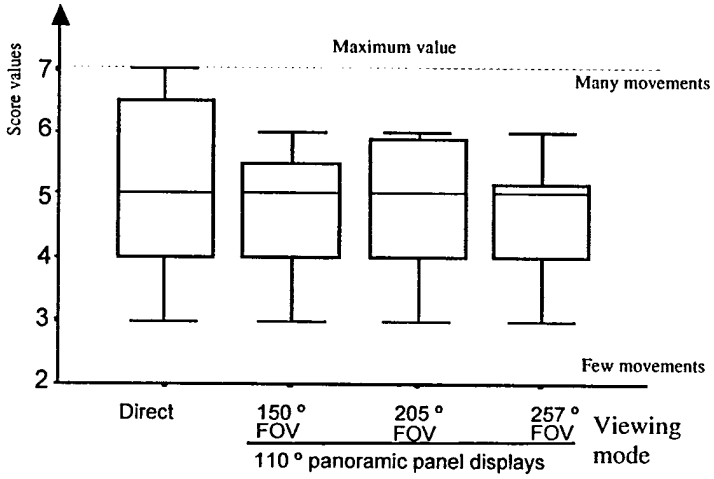

Figure I-8. Feet Activity.

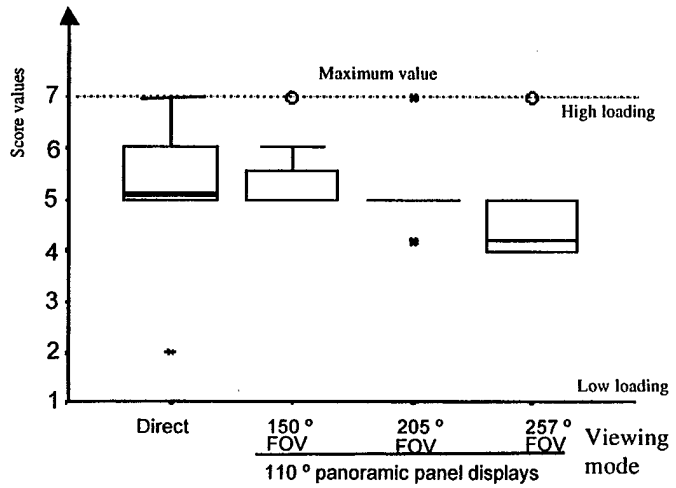

Figure I-9. Workload.

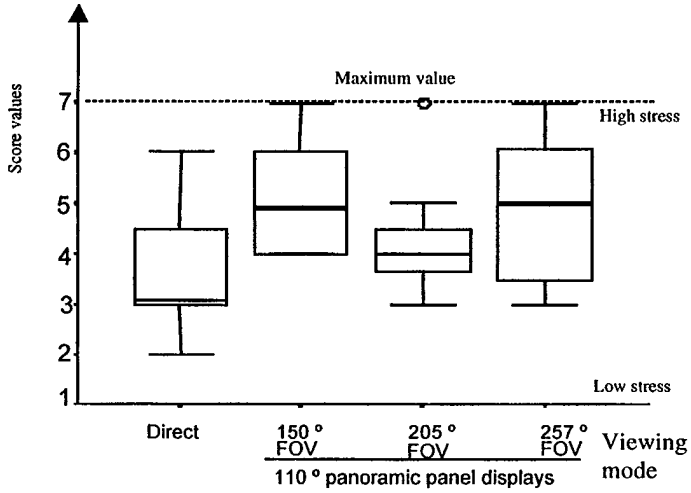

Figure I-10. Stress.

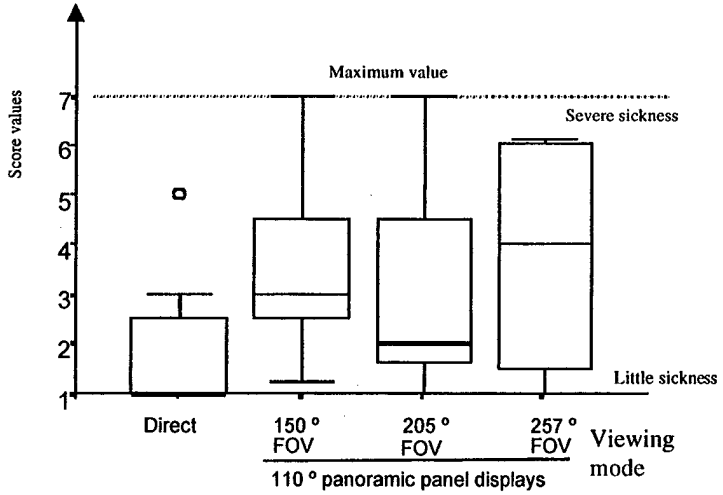

Figure I-11. Motion Sickness.

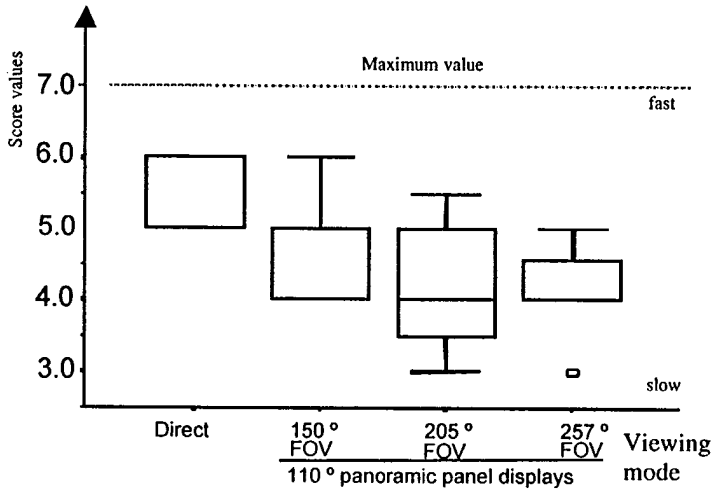

Figure I-12. Vehicle Speed.

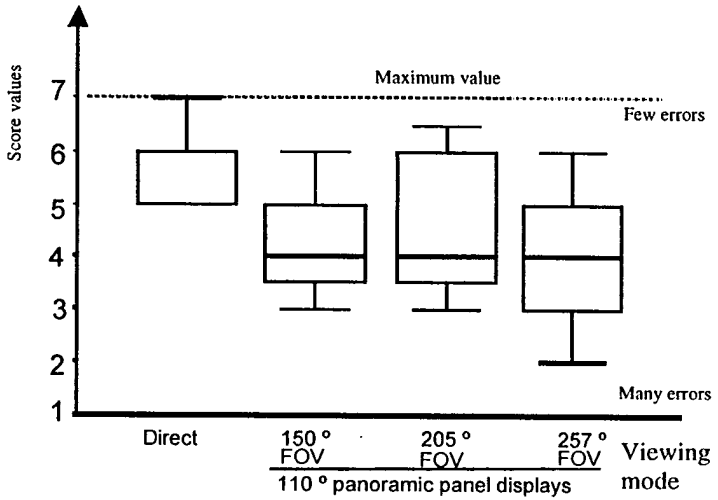

Figure I-13. Lane-Following Accuracy.

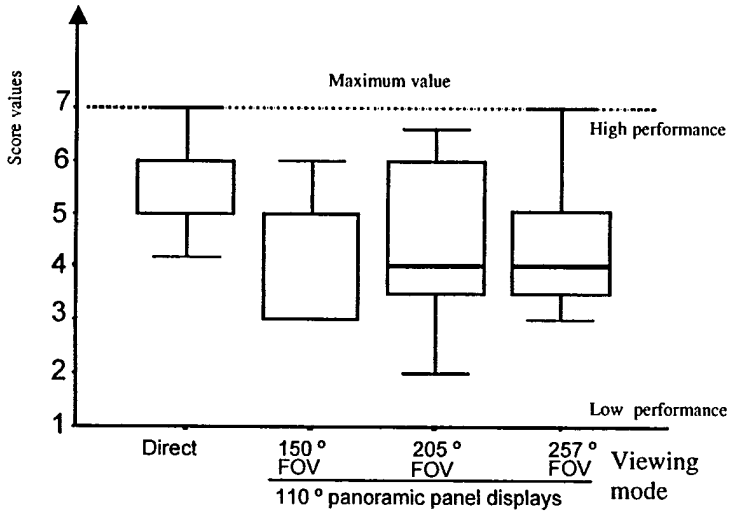

Figure I-14. Overall Performance.

NO. OF COPIES ORGANIZATION

1 ADMINISTRATOR
DEFENSE TECHNICAL INFO CTR
ATTN DTIC OCA
8725 JOHN J KINGMAN RD STE 0944
FT BELVOIR VA 22060-6218

1 DIRECTOR
US ARMY RSCH LABORATORY
ATTN AMSRL CI AI R REC MGMT
2800 POWDER MILL RD
ADELPHI MD 20783-1197

1 DIRECTOR
US ARMY RSCH LABORATORY
ATTN AMSRL CI LL TECH LIB
2800 POWDER MILL RD
ADELPHI MD 20783-1197

1 DIRECTOR
US ARMY RSCH LABORATORY
ATTN AMSRL D D SMITH
2800 POWDER MILL RD
ADELPHI MD 20783-1197

1 DIR FOR PERS TECHNOLOGIES
DPY CHIEF OF STAFF PERS
300 ARMY PENTAGON 2C733
WASHINGTON DC 20310-0300

1 OUSD(A)/DDDR&E(R&A)/E&LS
PENTAGON ROOM 3D129
WASHINGTON DC 20301-3080

1 CODE 1142PS
OFC OF NAVAL RSCH
800 N QUINCY STREET
ARLINGTON VA 22217-5000

1 WALTER REED INST OF RSCH
ATTN SGRD UWI C
COL REDMOND
WASHINGTON DC 20307-5100

1 DR ARTHUR RUBIN
NATL INST OF STDS & TECH
BLDG 226 ROOM A313
GAITHERSBURG MD 20899

NO. OF COPIES ORGANIZATION

1 CDR
US ARMY RSCH INST
ATTN PERI ZT DR E M JOHNSON)
5001 EISENHOWER AVENUE
ALEXANDRIA VA 22333-5600

1 DEF LOGISTICS STUDIES
INFORMATION EXCHANGE
ATTN DIR DLSIE ATSZ DL
BLDG 12500
2401 QUARTERS ROAD
FORT LEE VA 23801-1705

1 HEADQUARTERS USATRADOC
ATTN ATCD SP
FORT MONROE VA 23651

1 CDR
USATRADOC
COMMAND SAFETY OFC
ATTN ATOS MR PESSAGNO/MR LYNE
FORT MONROE VA 23651-5000

1 DIRECTOR TDAD DCST
ATTN ATTG C
BLDG 161
FORT MONROE VA 23651-5000

1 HQ USAMRDC
ATTN SGRD PLC
FORT DETRICK MD 21701

1 CDR
USA AEROMEDICAL RSCH LAB
ATTN LIBRARY
FORT RUCKER AL 36362-5292

1 US ARMY SAFETY CTR
ATTN CSSC SE
FORT RUCKER AL 36362

1 CHIEF
ARMY RSCH INST
AVIATION R&D ACTIVITY
ATTN PERI IR
FORT RUCKER AL 36362-5354

1 AF FLIGHT DYNAMICS LAB
ATTN AFWAL/FIES/SURVIAC
WRIGHT PATTERSON AFB OH
45433

NO. OF COPIES ORGANIZATION

1 US ARMY NATICK RD&E CTR
ATTN STRNC YBA
NATICK MA 01760-5020

1 US ARMY TROOP SUPPORT CMD
NATICK RD&E CTR
ATTN BEHAVIORAL SCI DIV SSD
NATICK MA 01760-5020

1 US ARMY TROOP SUPPORT CMD
NATICK RD&E CTR
ATTN TECH LIB (STRNC MIL)
NATICK MA 01760-5040

1 DR RICHARD JOHNSON
HEALTH & PERFORMANCE DIV
US ARIEM
NATICK MA 01760-5007

1 NAVAL SUB MED RSCH LAB
MEDICAL LIB BLDG 148
BOX 900 SUBMARINE BASE
NEW LONDON
GROTON CT 06340

1 USAF ARMSTRONG LAB/CFTO
ATTN DR F W BAUMGARDNER
SUSTAINED OPERATIONS BR
BROOKS AFB TX 78235-5000

1 CDR
USAMC LOGISTICS SUP ACTIVITY
ATTN AMXLS AE
REDSTONE ARSENAL AL
35898-7466

1 ARI FIELD UNIT FT KNOX
BLDG 2423 PERI IK
FORT KNOX KY 40121-5620

1 CDR
WHITE SANDS MISSILE RANGE
ATTN STEWS TE RE
WSMR NM 88002

1 USA TRADOC ANALYSIS CMD
ATTN ATRC WSR D ANGUIANO
WSMR NM 88002-5502

1 STRICOM
12350 RSCH PARKWAY
ORLANDO FL 32826-3276

NO. OF COPIES ORGANIZATION

1 CDR
USA COLD REGIONS TEST CTR
ATTN STECR TS A
APO AP 96508-7850

1 GOVT PUBLICATIONS LIB
409 WILSON M
UNIVERSITY OF MINNESOTA
MINNEAPOLIS MN 55455

1 DR RICHARD PEW
BBN SYSTEMS &TECH CORP
10 MOULTON STREET
CAMBRIDGE MA 02138

1 DR ANTHONY DEBONS
IDIS UNIV OF PITTSBURGH
PITTSBURGH PA 15260

1 MR R BEGGS
BOEING-HELICOPTER CO
P30-18
PO BOX 16858
PHILADELPHIA PA 19142

1 DR ROBERT KENNEDY
ESSEX CORPORATION STE 227
1040 WOODCOCK ROAD
ORLANDO FL 32803

1 DR NANCY ANDERSON
DEPT OF PSYCHOLOGY
UNIVERSITY OF MARYLAND
COLLEGE PARK MD 20742

1 DR BEN B MORGAN
DEPT OF PSYCHOLOGY
UNIV OF CENTRAL FLORIDA
PO BOX 25000
ORLANDO FL 32816

1 LAWRENCE C PERLMUTER PHD
UNIV OF HEALTH SCIENCES
THE CHICAGO MEDICAL SCHOOL
DEPT OF PSYCHOLOGY
3333 GREEN BAY ROAD
NORTH CHICAGO IL 60064

1 GENERAL DYNAMICS
LAND SYSTEMS DIV LIBRARY
PO BOX 1901
WARREN MI 48090

NO. OF COPIES ORGANIZATION

1 GMC N AMER OPERATIONS
PORTFOLIO ENGINEERING CTR
HUMAN FACTORS ENGINEERING
ATTN A J ARNOLD STAFF
PROJ ENG
ENGINEERING BLDG
30200 MOUND RD BOX 9010
WARREN MI 48090-9010

1 DR LLOYD A AVANT
DEPT OF PSYCHOLOGY
IOWA STATE UNIVERSITY
AMES IA 50010

1 DR MM AYOUB DIRECTOR
INST FOR ERGONOMICS RSCH
TEXAS TECH UNIVERSITY
LUBBOCK TX 79409

1 DELCO DEF SYS OPERATIONS
ATTN RACHEL GONZALES B204
7410 HOLLISTER AVE
GOLETA CA 93117-2583

1 MR WALT TRUSZKOWSKI
NASA/GODDARD SPACE
FLIGHT CTR
CODE 588.0
GREENBELT MD 20771

1 US ARMY
ATTN AVA GEDDES
MS YA:219-1
MOFFETT FIELD CA 94035-1000

1 CDR
US ARMY RSCH INST OF
ENVIRONMNTL MEDICINE
NATICK MA 01760-5007

1 HQDA (DAPE ZXO)
ATTN DR FISCHL
WASHINGTON DC 20310-0300

1 HUMAN FACTORS ENG PROGRAM
DEPT OF BIOMEDICAL ENGNG
COLLEGE OF ENGINEERING &
COMPUTER SCIENCE
WRIGHT STATE UNIVERSITY
DAYTON OH 45435

NO. OF COPIES ORGANIZATION

1 CDR
USA MEDICAL R&D COMMAND
ATTN SGRD PLC LTC K FRIEDL
FORT DETRICK MD 21701-5012

1 PEO ARMORED SYS MODERNIZATION
US ARMY TANK-AUTOMOTIVE CMD
ATTN SFAE ASM S
WARREN MI 48397-5000

1 PEO COMMUNICATIONS
ATTN SFAE CM RE
FT MONMOUTH NJ 07703-5000

1 PEO AIR DEF
ATTN SFAE AD S
US ARMY MISSILE COMMAND
REDSTONE ARSENAL AL
35898-5750

1 PEO STRATEGIC DEF
PO BOX 15280 ATTN DASD ZA
US ARMY STRATEGIC DEF CMD
ARLINGTON VA 22215-0280

1 PROGRAM MANAGER RAH-66
ATTN SFAE AV
BLDG 5300 SPARKMAN CTR
REDSTONE ARSENAL AL 35898

1 JON TATRO
HUMAN FACTORS SYS DESIGN
BELL HELICOPTER TEXTRON INC
PO BOX 482 MAIL STOP 6
FT WORTH TX 76101

1 CHIEF CREW SYS INTEGRATION
SIKORSKY AIRCRAFT M/S S3258
NORTH MAIN STREET
STRATFORD CT 06602

1 GENERAL ELECTRIC COMPANY
ARMAMENT SYS DEPT RM 1309
ATTN HF/MANPRINT R C MCLANE
LAKESIDE AVENUE
BURLINGTON VT 05401-4985

1 JOHN B SHAFER
250 MAIN STREET
OWEGO NY 13827

NO. OF
COPIES ORGANIZATION

1 OASD (FM&P)
WASHINGTON DC 20301-4000

1 COMMANDANT
US ARMY ARMOR SCHOOL
ATTN ATSB CDS
FT KNOX KY 40121-5215

1 CDR
US ARMY AVIATION CTR
ATTN ATZQ CDM S
FT RUCKER AL 36362-5163

1 CDR
US ARMY SIGNAL CTR &
FT GORDON
ATTN ATZH CDM
FT GORDON GA 30905-5090

1 DIRECTOR
US ARMY AEROFLIGHT
DYNAMICS DIR
MAIL STOP 239-9
NASA AMES RSCH CTR
MOFFETT FIELD CA 94035-1000

1 CDR
MARINE CORPS SYSTEMS CMD
ATTN CBGT
QUANTICO VA 22134-5080

1 DIR AMC-FIELD ASSIST IN
SCIENCE & TECHNOLOGY
ATTN AMC-FAST
FT BELVOIR VA 22060-5606

1 CDR
US ARMY FORCES CMD
ATTN FCDJ SA BLDG 600
AMC FAST SCIENCE ADVISER
FT MCPHERSON GA 30330-6000

1 CDR
I CORPS AND FORT LEWIS
AMC FAST SCIENCE ADVISER
ATTN AFZH CSS
FORT LEWIS WA 98433-5000

1 HQ III CORPS & FORT HOOD
OFC OF THE SCIENCE ADVISER
ATTN AFZF CS SA
FORT HOOD TX 76544-5056

NO. OF
COPIES ORGANIZATION

1 CDR
HQ XVIII ABN CORPS & FT BRAGG
OFC OF THE SCI ADV BLDG 1-1621
ATTN AFZA GD FAST
FORT BRAGG NC 28307-5000

1 SOUTHCOM WASHINGTON
FIELD OFC
1919 SOUTH EADS ST STE L09
AMC FAST SCIENCE ADVISER
ARLINGTON VA 22202

1 HQ US SPECIAL OPERATIONS CMD
AMC FAST SCIENCE ADVISER
ATTN SOSD
MACDILL AIR FORCE BASE
TAMPA FL 33608-0442

1 HQ US ARMY EUROPE AND
7TH ARMY
ATTN AEAGX SA
OFC OF THE SCIENCE ADVISER
APO AE 09014

1 CDR
HQ 21ST THEATER ARMY AREA CMD
AMC FAST SCIENCE ADVISER
ATTN AERSA
APO AE 09263

1 CDR
HEADQUARTERS USEUCOM
AMC FAST SCIENCE ADVISER
UNIT 30400 BOX 138
APO AE 09128

1 HQ 7TH ARMY TRAINING CMD
UNIT #28130
AMC FAST SCIENCE ADVISER
ATTN AETT SA
APO AE 09114

1 CDR
HHC SOUTHERN EUROPEAN
TASK FORCE
ATTN AESE SA BLDG 98
AMC FAST SCIENCE ADVISER
APO AE 09630

1 CDR US ARMY PACIFIC
AMC FAST SCIENCE ADVISER
ATTN APSA
FT SHAFTER HI 96858-5L00

NO. OF COPIES ORGANIZATION

1 AMC FAST SCIENCE ADVISERS
PCS #303 BOX 45 CS-SO
APO AP 96204-0045

1 ENGINEERING PSYCH LAB
DEPT OF BEHAVIORAL
SCIENCES & LEADERSHIP
BLDG 601 ROOM 281
US MILITARY ACADEMY
WEST POINT NY 10996-1784

1 DIR
SANDIA NATL LAB
ENGNRNG MECHANICS DEPT
MS 9042 ATTN J HANDROCK
Y R KAN J LAUFFER
PO BOX 969
LIVERMORE CA 94551-0969

1 DR SEHCHANG HAH
WM J HUGHES TECH CTR FAA
NAS HUMAN FACTORS BR
ACT-530 BLDG 28
ATLANTIC CITY INTNATL
AIRPORT NJ 08405

1 US ARMY RSCH INST
ATTN PERI IK D L FINLEY
2423 MORANDE STREET
FORT KNOX KY 40121-5620

1 US MILITARY ACADEMY
MATHEMATICAL SCIENCES CTR
OF EXCELLENCE
DEPT OF MATH SCIENCES
ATTN MDN A MAJ HUBER
THAYER HALL
WEST POINT NY 10996-1786

1 NAIC/DXLA
4180 WATSON WAY
WRIGHT PATTERSON AFB OH
45433-5648

1 CDR USA TACOM
ATTN TECH LIBRARY
WARREN MI 48397

1 CDR US ARMY ARMOR SCHOOL
ATTN TECH LIBRARY
FT KNOX KY 40121

NO. OF COPIES ORGANIZATION

5 CDR USA TACOM
ATTN AMSTA TR R (MS264 BRENDLE)
WARREN MI 48397-5000

1 ARL HRED AVNC FLD ELMT
ATTN AMSRL HR MJ
R ARMSTRONG
PO BOX 620716 BLDG 4506 (DCD)
RM 107
FT RUCKER AL 36362-5000

1 ARL HRED AMCOM FLD ELMT
ATTN AMSRL HR MI D FRANCIS
BLDG 5464 RM 202
REDSTONE ARSENAL AL
35898-5000

1 ARL HRED AMCOM FLD ELMT
ATTN ATTN AMSRL HR MO
T COOK
BLDG 5400 RM C242
REDSTONE ARS AL 35898-7290

1 ARL HRED USAADASCH FLD ELMT
ATTN AMSRL HR ME
K REYNOLDS
ATTN ATSA CD
5800 CARTER ROAD
FORT BLISS TX 79916-3802

1 ARL HRED ARDEC FLD ELMT
ATTN AMSRL HR MG R SPINE
BUILDING 333
PICATINNY ARSENAL NJ
07806-5000

1 ARL HRED ARMC FLD ELMT
ATTN AMSRL HR MH C BIRD
BLDG 1002 ROOM 206B
1ST CAVALRY REGIMENT RD
FT KNOX KY 40121

1 ARL HRED CECOM FLD ELMT
ATTN AMSRL HR ML J MARTIN
MYER CENTER RM 2D311
FT MONMOUTH NJ 07703-5630

1 ARL HRED FT BELVOIR FLD ELMT
ATTN AMSRL HR MK P SCHOOL
10170 BEACH RD
FORT BELVOIR VA 22060-5800

NO. OF COPIES ORGANIZATION

1 ARL HRED FT HOOD FLD ELMT
ATTN AMSRL HR MV HQ USAOTC
E SMOOTZ
91012 STATION AVE ROOM 111
FT HOOD TX 76544-5073

1 ARL HRED FT HUACHUCA
FIELD ELEMENT
ATTN AMSRL HR MY B KNAPP
GREELY HALL BLDG 61801 RM 2631
FT HUACHUCA AZ 85613-5000

1 ARL HRED FLW FLD ELMT
ATTN AMSRL HR MZ A DAVISON
3200 ENGINEER LOOP STE 166
FT LEONARD WOOD MO 65473-8929

1 ARL HRED NATICK FLD ELMT
ATTN AMSRL HR MQ M R FLETCHER
NATICK SOLDIER CTR BLDG 3
RM 341 AMSSB RSS E
NATICK MA 01760-5020

1 ARL HRED OPTEC FLD ELMT
ATTN AMSRL HR MR H DENNY
ATEC CSTE PM ARL
4501 FORD AVE RM 860
ALEXANDRIA VA 22302-1458

1 ARL HRED SC&FG FLD ELMT
ATTN AMSRL HR MS R ANDERS
SIGNAL TOWERS RM 303A
FORT GORDON GA 30905-5233

1 ARL HRED STRICOM FLD ELMT
ATTN AMSRL HR MT A GALBAVY
12350 RESEARCH PARKWAY
ORLANDO FL 32826-3276

1 ARL HRED TACOM FLD ELMT
ATTN AMSRL HR MU
M SINGAPORE
6501 E 11 MILE ROAD
WARREN MI 48397-5000

1 ARL HRED USAFAS FLD ELMT
ATTN AMSRL HR MF L PIERCE
BLDG 3040 RM 220
FORT SILL OK 73503-5600

NO. OF COPIES ORGANIZATION

1 ARL HRED USAIC FLD ELMT
ATTN AMSRL HR MW E REDDEN
BLDG 4 ROOM 332
FT BENNING GA 31905-5400

1 ARL HRED USASOC FLD ELMT
ATTN AMSRL HR MN F MALKIN
HQ USASOC BLDG E2929
FORT BRAGG NC 28310-5000

1 ARL HRED HFID FLD ELMT
ATTN AMSRL HR MP
D UNGVARSKY
BATTLE CMD BATTLE LAB
415 SHERMAN AVE UNIT 3
FT LEAVENWORTH KS 66027-2326

1 CDR AMC - FAST
JRTC & FORT POLK
ATTN AFZX GT DR J AINSWORTH
CMD SCIENCE ADVISOR G3
FORT POLK LA 71459-5355

1 CPT ANGUS RUPERT
MC US NAVY
51 HOVEY RD
PENSACOLA FL 32508-1046

1 RSK ASSESSMENTS INC
ATTN ROBERT KENNEDY
1040 WOODCOCK RD STE 227
ORLANDO FL 32803

ABERDEEN PROVING GROUND

2 DIRECTOR
US ARMY RSCH LABORATORY
ATTN AMSRL CI LP (TECH LIB)
BLDG 305 APG AA

1 LIBRARY
ARL BLDG 459
APG-AA

1 ARL HRED ECBC FLD ELMT
ATTN AMSRL HR M
BLDG 459

1 ARL HRED
ATTN AMSRL HR MB
F PARAGALLO
BLDG 459

NO. OF
COPIES ORGANIZATION

1 US ATEC
RYAN BLDG
APG-AA

1 CDR
CHEMICAL BIOLOGICAL &
DEF CMD
ATTN AMSCB CI
APG-EA

1 CDN ARMY LO TO ATEC
ATTN AMSTE CL
RYAN BLDG

ABSTRACT ONLY

1 DIRECTOR
US ARMY RSCH LABORATORY
ATTN AMSRL CI AP TECH PUB BR
2800 POWDER MILL RD
ADELPHI MD 20783-1197

INTENTIONALLY LEFT BLANK

REPORT DOCUMENTATION PAGE

Form Approved OMB No. 0704-0188

1. AGENCY USE ONLY *(Leave blank)*	2. REPORT DATE	3. REPORT TYPE AND DATES COVERED
	June 2001	Final

4. TITLE AND SUBTITLE

Indirect Vision Driving With Fixed Flat Panel Displays for Near-Unity, Wide, and Extended Fields of Camera View

5. FUNDING NUMBERS

AMS Code 622716
PR: AH70

6. AUTHOR(S)

Smyth, C.C.; Gombash, J.W.; Burcham, P.M. (all of ARL)

7. PERFORMING ORGANIZATION NAME(S) AND ADDRESS(ES)

U.S. Army Research Laboratory
Human Research & Engineering Directorate
Aberdeen Proving Ground, MD 21005-5425

8. PERFORMING ORGANIZATION REPORT NUMBER

9. SPONSORING/MONITORING AGENCY NAME(S) AND ADDRESS(ES)

U.S. Army Research Laboratory
Human Research & Engineering Directorate
Aberdeen Proving Ground, MD 21005-5425

10. SPONSORING/MONITORING AGENCY REPORT NUMBER

ARL-TR-2511

11. SUPPLEMENTARY NOTES

12a. DISTRIBUTION/AVAILABILITY STATEMENT

Approved for public release; distribution is unlimited.

12b. DISTRIBUTION CODE

13. ABSTRACT *(Maximum 200 words)*

Of interest to designers of future combat vehicles is the effect of indirect vision upon vehicle driving, particularly the effect of the camera lens field of view (FOV). In a field study with eight participants negotiating a road course in a military vehicle, the driving performance was measured for natural and indirect vision. The indirect vision system was driven with fixed panoramic flat panel, liquid crystal displays in the cab and a forward viewing monocular camera array mounted on the front roof of the vehicle and tilted slightly downward.

The results are that for benign driving conditions (a well-marked course, good visibility, and essentially flat terrain), the participants successfully drove the vehicle with indirect vision for the different camera FOVs: near unity, wide, and extended. However, with natural vision, they drove the course 26.5% faster and made a nominal 0.5% fewer lane-marker strikes than they did with the indirect vision systems. Further, the course speed significantly decreased with increased camera FOV, while the number of lane marker strikes increased slightly. While the course speed decreased with increasing FOV, the speed of travel was perceived as increased because of the scene compression. Although the heart rate increased significantly with course speed because of the increased exertion, the estimated metabolic work output was least for the natural vision and increased with the indirect FOV because of the longer course times.

Workload ratings show a significant increase in perceived workload with indirect vision, while an investigation of situational awareness shows an increase in the demand component. Most participants reported discomfort associated with motion sickness while in the moving vehicle with the displays. The estimated subjective stress rating of the drivers was least for natural vision and increased with indirect FOV.

When the camera's FOVs were compared, the driving performance was fastest with the near-unity FOV. However, cognitive processing experiments show a trend for improved spatial rotation and map planning following the wide FOV trial. The wide FOV was intentionally selected by the researchers to provide a balance of the resolution needed for obstacle avoidance and scene perspective for course following. Finally, the participants rated the near unity as more useful for steering; however, the wider FOVs were preferred for navigation since they allow the driver to see farther for path selection.

14. SUBJECT TERMS

driving
indirect vision driving
mental workload
motion sickness

15. NUMBER OF PAGES
160

16. PRICE CODE

17. SECURITY CLASSIFICATION OF REPORT	18. SECURITY CLASSIFICATION OF THIS PAGE	19. SECURITY CLASSIFICATION OF ABSTRACT	20. LIMITATION OF ABSTRACT
Unclassified	Unclassified	Unclassified	